

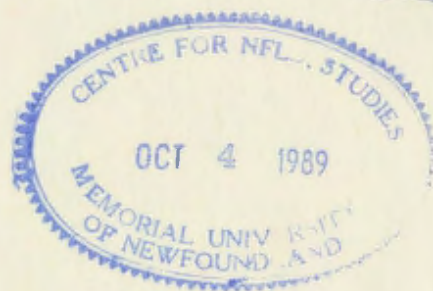
THE STRATIGRAPHY, STRUCTURE,
GEOCHEMISTRY, AND METALLOGENY OF THE
MORAN LAKE GROUP CENTRAL MINERAL
BELT, LABRADOR

CENTRE FOR NEWFOUNDLAND STUDIES

**TOTAL OF 10 PAGES ONLY
MAY BE XEROXED**

(Without Author's Permission)

JON W. NORTH





National Library
of Canada

Bibliothèque nationale
du Canada

Canadian Theses Service *Service des thèses canadiennes

Ottawa, Canada
K1A 0N4

NOTICE

The quality of this microform is heavily dependent upon the quality of the original thesis submitted for microfilming. Every effort has been made to ensure the highest quality of reproduction possible.

If pages are missing, contact the university which granted the degree.

Some pages may have indistinct print, especially if the original pages were typed with a poor typewriter ribbon or if the university sent us an inferior photocopy.

Previously copyrighted materials (journal articles, published tests, etc.) are not filmed.

Reproduction in full or in part of this microform is governed by the Canadian Copyright Act, R.S.C. 1970, c. C-30.

AVIS

La qualité de cette microforme dépend grandement de la qualité de la thèse soumise au microfilmage. Nous avons tout fait pour assurer une qualité supérieure de reproduction.

S'il manque des pages, veuillez communiquer avec l'université qui a conféré le grade.

La qualité d'impression de certaines pages peut laisser à désirer, surtout si les pages originales ont été dactylographiées à l'aide d'un ruban usé ou si l'université nous a fait parvenir une photocopie de qualité inférieure.

Les documents qui font déjà l'objet d'un droit d'auteur (articles de revue, tests publiés, etc.) ne sont pas microfilmés.

La reproduction, même partielle, de cette microforme est soumise à la Loi canadienne sur le droit d'auteur, S.L.C. 1970, c. C-30.

The Stratigraphy, Structure, Geochemistry, and Metallogeny
of the Moran Lake Group
Central Mineral Belt, Labrador

by

Ⓒ Jon W. North, B.Sc.

A thesis submitted in partial fulfillment of the
requirements for the degree of
Master of Science

Department of Earth Sciences
Memorial University of Newfoundland

1988

Permission has been granted to the National Library of Canada to microfilm this thesis and to lend or sell copies of the film.

The author (copyright owner) has reserved other publication rights, and neither the thesis nor extensive extracts from it may be printed or otherwise reproduced without his/her written permission.

L'autorisation a été accordée à la Bibliothèque nationale du Canada de microfilmer cette thèse et de prêter ou de vendre des exemplaires du film.

L'auteur (titulaire du droit d'auteur) se réserve les autres droits de publication; ni la thèse ni de longs extraits de celle-ci ne doivent être imprimés ou autrement reproduits sans son autorisation écrite.

ISBN 0-315-45068-1

ABSTRACT

The lower Proterozoic (Aphebian) Moran Lake Group was deposited in a marine shelf environment unconformably on granitoid rocks of the Archean Nain province. The Moran Lake Group is unconformably overlain by the continental (Helikian) Bruce River Group. The Moran Lake Group consists of two provisional formations viz.: the Warren Creek Formation which has been informally subdivided here, into a Lower Member composed of siltstone, sandstone, and shale, with occasional red beds and calcareous beds, and an Upper Member consisting of pyritic black shale, and siltstone, with minor vesicular basalt, arkose, and banded ironstone; and the Joe Pond Formation consisting of pillowed and massive basalt. The Moran Lake Group underwent polyphase deformation during the Makkovikian-Ketilidian event ca. 1810-1790 Ma, prior to the deposition of the overlying Helikian Bruce River Group which was affected by Grenvillian deformation ca. 1000 Ma.

The geology and geochemistry of Fe-Zn-Cu-bearing sulphide beds in the Upper Member of the Warren Creek Formation indicate that basinal heat flow was low to moderate during the deposition of the Lower Member of the Warren Creek Formation, and high during the late stages of Upper Member deposition. Circulation of metal chloride-bearing formation brines occurred by slow seepage and upward advective flow along pressure gradients and normal

faults in the lower part of the Upper Member. These brines were expelled, depositing pyritic Fe-Zn-Cu-rich sulphide beds in stable, reduced brine pools downslope from their discharge vents. An increase in the geothermal gradient near the end of Upper Member deposition, caused uplift and downward penetration of seawater in shallow ephemeral convection cells which ultimately deposited stratabound Zn-rich, Cu-poor, disseminated sulphide mineralization in a porous host lithology. The change in geothermal gradient and character of sulphide mineralization, reflects the development of a stable magma chamber below the basin, from which the Joe Pond Formation basalts were ultimately derived. The paucity of Pb and Ag and overall low base metal content of both the Fe-Cu-Zn sulphide beds and the Zn-rich, Cu-poor stratabound sulphide mineralization, indicate that the Moran Lake Group has limited to nil potential for economic sedimentary exhalative Zn-Pb-Cu (Ag) deposits. The mechanisms by which the mineral occurrences in the Warren Creek Formation were formed however, may represent incipient stages of classic "sedex" mineralization which did not reach maturity.

ACKNOWLEDGEMENTS

This thesis was initiated by Dr. Derek Wilton, who provided a great deal of encouragement, advice, and enthusiasm for the project. Dr. Wilton executed the financial logistics for this project which were in the form of an NSTP grant to the author, and funding from the Geological Survey of Canada through ERDA (MDA) Agreement II-2, Metallogeny of the Central Mineral Belt. Thanks also to the NDME for logistical support from Goose Bay, and discussions concerning this project with Bruce Ryan and Dick Wardle, in St. John's. The help of the technical staff (D. Press, C. Emeryson, G. Andrews, S. Jackson, to name a few) at M.U.N. is gratefully acknowledged, without which, the geochemical analyses could not have been carried out. Special thanks to my field assistant in 1986, Kevin Staples, who was energetic and supportive throughout the field work, and to my associates and now good friends, Craig MacDougall, Len MacKenzie, and Derek Wilton whose boozy, hazy and often ridiculous discussions have helped me plan my kick at the can.

TABLE OF CONTENTS

Page

ABSTRACT.....	ii
ACKNOWLEDGEMENTS.....	iv
LIST OF TABLES.....	ix
LIST OF FIGURES.....	x

CHAPTER 1

INTRODUCTION

1.1 Purpose.....	1
1.2 Location and access.....	1
1.3 Previous work.....	2
1.4 Physiography, glacial history, and vegetation.....	9
1.5 Methods.....	12

CHAPTER 2

GEOLOGICAL SETTING

2.1 Regional geology.....	14
2.2 Geology and stratigraphy of study area.....	16
2.2.1 Map unit 1: Archean basement.....	16
2.2.2 Map units 2 & 3: Warren Creek Formation.....	22
2.2.2.1 General description.....	22
2.2.2.2 Map unit 2: Lower Member.....	25
2.2.2.3 Map unit 3: Upper Member.....	30
2.2.2.3.1 Middle dolostone.....	32
2.2.2.3.2 Vesicular basalt.....	33

	Page
2.2.2.3.3 Arkose bed.....	33
2.2.2.3.4 Banded ironstone.....	39
2.2.3 Map unit 4: Joe Pond Formation.....	41
2.2.4 Map unit 5: Bruce River Group.....	43
2.2.5 Map unit 6: Gabbro.....	44
2.3 Structural geology.....	48
2.3.1 D ₁	50
2.3.2 D ₂	53
2.3.3 D ₃	53
2.3.4 Summary.....	53
2.4 Archean-Aphebian unconformity.....	55
2.5 Aphebian-Helikian unconformity.....	58
2.6 Summary.....	59

CHAPTER 3

GEOCHEMISTRY

3.1 Archean basement.....	61
3.2 Warren Creek Formation.....	65
3.2.1 Upper Member.....	65
3.2.1.1 Typical shale, showings, Teuva showing....	66
3.2.1.2 Extended REE plots (spider diagrams).....	87
3.2.1.3 Summary.....	92
3.2.2 Lower Member.....	94
3.3 Basalt geochemistry.....	97
3.3.1 Joe Pond Formation.....	97

	Page
3.3.2 Upper Member basalt.....	101
3.3.3 Extended REE plots (spider diagrams).....	106
3.3.4 Summary.....	109
3.4 Gabbro.....	110

CHAPTER 4

ECONOMIC MINERALIZATION

4.1 General introduction.....	115
4.2 Geology of mineral occurrences.....	120
4.2.1 Date Grid showing.....	120
4.2.2 Warren Grid showing.....	122
4.2.3 Fault Creek showing.....	126
4.2.4 Three Ponds showing.....	126
4.2.5 Teuva showing.....	128
4.2.6 Summary.....	134
4.3 Geochemistry.....	138
4.4 Summary.....	141

CHAPTER 5

BASIN EVOLUTION AND METALLOGENY

5.1 Introduction.....	143
5.2 Model for basin evolution: evidence from sulphide deposition.....	143
5.3 Discussion and metallogenic model.....	159
5.4 Conclusions and recommendations.....	164

	Page
BIBLIOGRAPHY.....	166
APPENDIX 1 - Analytical methods.....	178
APPENDIX 2 - Chemical analyses.....	185

LIST OF TABLES

Table	Page
3.1 Normative mineral compositions of Archean basement.....	62
A3.2 Trace element abundances of average shales.....	86
3.3 Chemical screen for basalts.....	103
4.1 Base metal abundances in average shale.....	118
4.2 Metal contents of mineral occurrences.....	119

x

LIST OF FIGURES

Figure	Page
1.1 Location of study area.....	3
1.2 Topography of Warren Creek Formation.....	10
1.3 Topography of Bruce River Group.....	10
2.1 Moran Lake Group stratigraphic column.....	17
2.2 Archean basement slab.....	19
2.3 TiO_2 in Archean basement.....	19
2.4 Zircon in Archean basement.....	20
2.5 Monazite in Archean basement.....	20
2.6 Intergrown anatase & monazite, Archean basement...	21
2.7 Barite in Archean basement.....	21
2.8 Regolith below basal Moran Lake Group.....	23
2.9 Regolith in Archean basement.....	23
2.10 Red bed in Lower Member.....	27
2.11 Lower Member silty dolostone bed.....	27
2.12 Lower Member silt and dolostone outcrop.....	28
2.13 Upper Member, typical rusty gossan.....	28
2.14 Upper Member massive pyrite bed.....	31
2.15 Upper Member dolostone bed.....	31
2.16 Upper Member vesicular basalt flow.....	34
2.17 Upper Member vesicular basalt flow.....	34
2.18 Upper Member arkose bed.....	36
2.19 Structural cross section, Moran Lake Group.....	36
2.20 Upper Member shale-lithic conglomerate.....	37

Figure	Page
2.21 Upper Member banded ironstone.....	37
2.22 Joe Pond pillow basalt.....	42
2.23 Carbonatized Joe Pond basalt.....	42
2.24 Bruce River Group boulder conglomerate.....	45
2.25 Bruce River Group felsic volcanic.....	45
2.26 Bruce River Group felsic volcanic.....	46
2.27 Bruce River Group volcanoclastic sandstone.....	46
2.28 Gabbro dike.....	47
2.29 Moran Lake/Bruce River Group stereonets.....	49
2.30 D ₁ fold, Moran Lake Group.....	51
2.31 D ₁ buckle fold, Moran Lake Group.....	51
2.32 D ₂ crenulations, Moran Lake Group.....	54
2.33 Stratigraphy of Archean-Aphebian unconformity....	56
2.34 Archean-Aphebian unconformity.....	56
3.1 Ternary feldspar plot, Archean basement.....	63
3.2 Ternary FeO-Na ₂ O-K ₂ O plot, Archean basement.....	63
3.3 Monazite in pyritic Upper Member shale.....	67
3.4 Monazite enclosed in pyrite grain.....	67
3.5 Rutile in Upper Member shale.....	68
3.6 Amorphous diagenetic TiO ₂ overgrowth in shale.....	68
3.7a TiO ₂ -Al ₂ O ₃ -Zr plot, basement vs detritus.....	70
3.7b TiO ₂ vs P ₂ O ₅ , basement vs shale.....	70
3.8a Zn vs Cu variation diagram for shales.....	72
3.8b Zn vs Cu variation diagram for showings.....	72
3.9 Pb vs Zn, Cu variation diagram for shales.....	73

Figure	Page
3.10 Pb vs Zn, Cu variation diagrams for showings.....	74
3.11 Ba vs Pb, Zn, Cu variation diagrams for shales....	76
3.12 Ba vs Pb, Zn, Cu variation diagrams for showings.....	77
3.13 Comparison of Pb, Zn, Cu ratios in basement, shales, and showings.....	78
3.14 Ternary (Co+Ni+Cu)x10-Fe-Mn plot, Warren Creek Formation.....	81
3.15 SiO ₂ vs Al ₂ O ₃ , Warren Creek Formation.....	83
3.16 Ternary Al-Fe-Mn plot, Warren Creek Formation....	83
3.17 Comparison of Warren Creek Formation base metal ratios with established sedex/volcanogenic fields.....	84
3.18 Spider diagrams, Archean, shales, showings, Teuva.....	88
3.19 Lower Member Pb-Zn-Cu ratios.....	95
3.20 Lower Member, Upper Member TiO ₂ vs P ₂ O ₅	95
3.21 Lower Member TiO ₂ -Al ₂ O ₃ -Zr ternary plot.....	96
3.22 Joe Pond SiO ₂ -Na ₂ O + K ₂ O.....	98
3.23 Joe Pond AFM diagram.....	98
3.24 Joe Pond Ti vs Zr.....	99
3.25 Joe Pond log Ti vs log Cr.....	99
3.26 Joe Pond, Upper Member TiO ₂ vs Al ₂ O ₃ /TiO ₂	100
3.27 Upper Member basalt AFM diagram.....	104
3.28 Upper Member basalt log Ti vs log Cr.....	104

Figure	Page
3.29 Upper Member basalt ternary Zr-Ti/100-Sr/2.....	105
3.30 Upper Member basalt spider diagram.....	107
3.31 Joe Pond spider diagram.....	107
3.32 Gabbro $\text{SiO}_2\text{-Na}_2\text{O} + \text{K}_2\text{O}$	112
3.33 Gabbro AFM diagram.....	112
3.34 Gabbro TiO_2 vs CaO/TiO_2	113
3.35 Gabbro TiO_2 vs $\text{Al}_2\text{O}_3/\text{TiO}_2$	113
4.1 Moran Lake Group geology and mineral occurrences..	116
4.2 Sphalerite in Date Grid.....	121
4.3 Brecciated siltstone, Date Grid.....	121
4.4 Warren Grid massive sulphide bed.....	123
4.5 Warren Grid massive sulphide bed.....	123
4.6 Chalcopyrite in Warren Grid.....	124
4.7 Sphalerite in Warren Grid.....	124
4.8 Finely bedded pyrite, Warren Grid.....	125
4.9 Sphalerite in Fault Creek showing.....	127
4.10 Sphalerite in Three Ponds showing.....	127
4.11 Galena in Three Ponds showing.....	129
4.12 Three Ponds fractured massive sulphide bed.....	129
4.13 Rutile in Teuva showing.....	132
4.14 Disseminated and stringer shalerite, Teuva showing.....	132
4.15 Intergrown sphalerite-pyrite, Teuva showing.....	133
4.16 Teuva showing sample location sketch.....	133
4.17 Location of showings vs depth to basement.....	136

Figure	Page
5.1 Stage 1 of basin evolution.....	144
5.2 Stage 2 of basin evolution.....	146
5.3 Oxidized Lower Member detritus.....	147
5.4 Fe-oxide coating on sandstone clast, Lower Member.....	147
5.5 Fluid temperature vs density.....	150
5.6 Stage 3 of basin evolution.....	153
5.7 Stage 4 of basin evolution.....	153
5.8 Stage 5 of basin evolution.....	155
5.9 Stage 6 of basin evolution.....	158

CHAPTER 1

INTRODUCTION

1.1 Purpose

Prospectors and mining companies have directed exploration efforts in the Moran Lake Group since 1929, for a variety of mineral deposits including precious and base metals, uranium, and iron ore. The purpose of this research is to quantify the stratiform sedimentary exhalative (sedex) Pb-Zn-Cu (Ag) deposit potential of the Moran Lake Group. The earliest explorationists working the area recognized a thick sequence of mineralized black shales north of Pocket Knife Lake. This sequence of rocks, which was later defined as part of the Moran Lake Group (Smyth et al., 1975), and tentatively named the Warren Creek Formation (Ryan, 1984), is the main focus of the present study due to the similarities with other well known base metal producing areas such as the Sullivan mine (Hamilton, et al., 1983) in Canada, the McArthur River (Murray, 1975) orebody in northern Australia, and the Rammelsberg (Hannak, 1981) deposit in West Germany.

1.2 Location and Access

The study area is located in the Labrador Central Mineral Belt (CMB), and comprises approximately 70 square kilometres in the vicinity of Croteau and Pocket Knife

Lakes ($54^{\circ} 27'N$, $61^{\circ} 10' W$). Access to this remote area must be accomplished by float-equipped fixed-wing aircraft or helicopter from Goose Bay, 135 km to the south-southeast (Fig. 1.1).

The community of Happy Valley-Goose Bay has a population of approximately 7,300, and serves as a transportation, service, and military centre for coastal Labrador. Goose Bay is serviced by daily jet service from St. John's, Newfoundland. CN Marine coastal boats, providing inexpensive passenger and freight service, depart Lewisporte, Newfoundland for Happy Valley-Goose Bay twice a week from June 13 to September 12, and depart St. John's for Goose Bay during the summer shipping season. Electricity is supplied to Happy Valley-Goose Bay from the Churchill Falls hydroelectric generating station which is located 240 km west of Goose Bay and 200 km southwest of the study area. The powerline follows a gravel road to Churchill Falls. The road ends at Esker, on the Labrador-Quebec border and the North Shore and Labrador Railway, 400 km west of Goose Bay.

1.3 Previous Work

There is a long history of exploration in the Moran Lake Group, however most of the effort in the immediate area has been of a reconnaissance nature due to a number of factors, not the least of which are the remoteness of

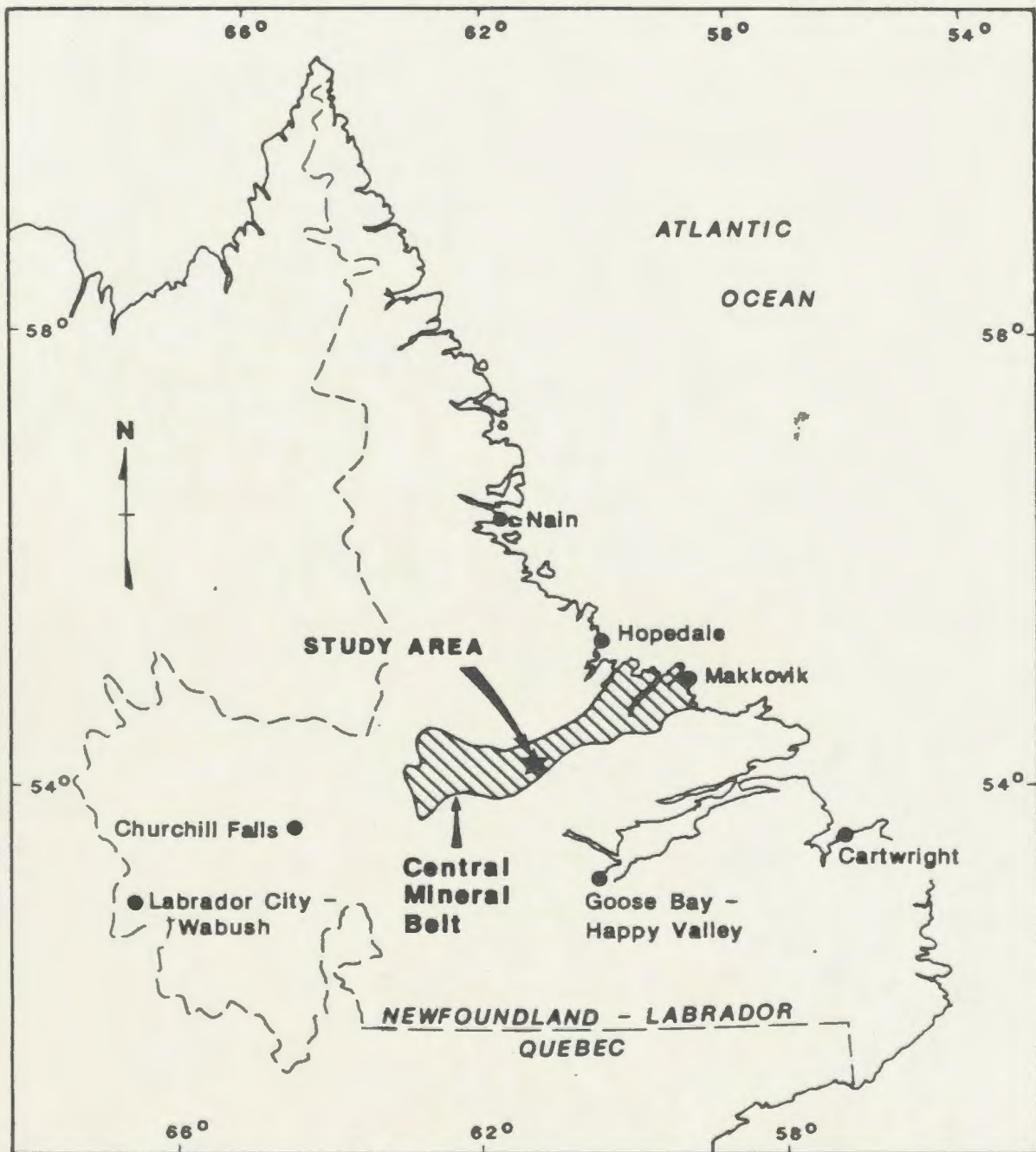


Fig. 1.1. Location of study area.

the area with respect to many of the major Canadian mining camps, the sheer immensity of the Central Mineral Belt, and the inherent difficulties of early exploration in an area as far inland as this, and the outdated concession system of mining land distribution which was replaced in 1974. British Newfoundland Exploration Ltd. (Brinex) and Frobisher Ltd. carried out most of the exploration in this study area on several mining land concessions which were periodically renewed but have since expired. The following paragraphs give a detailed account of that history.

In 1929 Paul and Wilfred Croteau discovered banded ironstones in the Seal and Pocket Knife Lakes area while on a prospecting expedition for iron deposits similar to the giant iron ore deposits of western Labrador. Presumably their discoveries included the ironstones north of the east arm of Pocket Knife Lake, and north of Croteau Lake. The discovery of these ironstones was confirmed by later workers (Smyth et al., 1975; Ryan, 1984), and these are listed in the Newfoundland Department of Mines (NDM) Mineral Occurrence Data System as Files 13K/6 Fe001, and Fe002.

In 1946 Dome Exploration (Canada) Ltd. commissioned a prospecting field party, led by R.A. Halet, to search for iron ore northeast of the Seal Lake basin. Pyritic shales were discovered northeast of Pocket Knife Lake and several pits were blasted. Trench samples were taken and analyzed

for gold and copper with negative results. Halet (1946) described the Croteau Series with a lower marine shale sequence (later defined as the the Moran Lake Group by Smyth et al., 1975; 1978) which was disconformably overlain by a continental red quartzite and volcanic succession (later defined as the Bruce River Group by Smyth et al., 1975; 1978).

In 1950 Frobisher Ltd. obtained a 22,000 square mile mineral concession to prospect the late Precambrian rocks of the Seal Lake area, and to investigate earlier reports of sulphide mineralization in black shales east of Pocket Knife Lake. Prospecting (Evans, 1950) was directed south of Seal Lake and east of Pocket Knife Lake. Showings of sulphide mineralization were confirmed in a belt of black shales described as at least one half of a mile wide, outcropping from Pocket Knife Lake to Moran Lake. The mineralization was described as consisting of pyrite and pyrrhotite with traces of chalcopyrite. Two pits were blasted north of Pocket Knife Lake, however no economic concentrations of copper or any other commodity were discovered. No stratigraphic revisions were made to Halet's definition of the Croteau Series.

In 1951 Frobisher Ltd. obtained a 3,600 square mile mineral concession for three years which included the Croteau Lake area. A smaller 500 square mile portion of this concession was renewed in 1954 which included the

Croteau Lake area.

Under a joint venture agreement between Frobisher Ltd. and Brinex Ltd. in 1957, Brinex completed a geochemical silt survey in the Croteau Lake area. The survey was located in "Block A" of the Frobisher concession. Several total heavy metal anomalies were delineated north of Croteau Lake and a limited program of follow-up work was carried out. This work is described in separate company reports by C.R. Corriveau (1958) and J.A. Hansuld (1958) which include the first detailed geology maps of the area (Brinex Maps G-F-3 and G-F-5). This work is the most extensive to date in the immediate study area, consisting of 6,600 m of line cutting, soil geochemistry, reconnaissance geological mapping, and 43.35 m of X-ray diamond drilling. Numerous beds of "massive sedimentary pyrite" were reported from argillaceous sediments north of Croteau Lake and although traces of chalcopyrite, nickeliferous pyrrhotite, and sphalerite were reported, all assays from drill core samples contained only trace amounts of copper, nickel, and zinc.

A Brinex exploration party headed by S.G. Ellingwood was also camped in the area, at Moran Lake, in 1958 to investigate the Montague Nos. 1 and 2 uranium showings (approximately 5 km northeast of the study area). A significant number of lead-zinc bearing veins were

discovered in lower Croteau Group (Fahrig, 1959) volcanics and argillite north of Moran Lake. These epigenetic showings consist of sphalerite-galena-pyrite mineralization in quartz-carbonate (+/- barite) veins. The best assays reported from various trench samples include: 56.6 g/t Ag, 20.51% Pb, 28.19% Zn, and 0.04% Cu (Piloski, 1958).

Fahrig (1959) published a geological map of the western part of the Croteau Series, and re-defined the Croteau Series as the Croteau Group. Fahrig's Croteau Group consisted of a lower succession of pyritic black shales, greywacke, quartzite, dolostone, and basalt, and an upper succession of conglomerate, sandstone, and porphyritic volcanics. No mention was made of a possible unconformity between the upper and lower successions of the Croteau Group.

Brinex Ltd. commissioned a 1:20,000 geological mapping survey of the Pocket Knife Lake area in 1969. DeGrace (1969) described the unconformable relationship between the lower marine and upper continental successions of the Croteau Group. The unconformity was described as being marked by a conglomerate bed at the base of the continental sequence. DeGrace subdivided the Croteau Group into three subgroups on the basis of the unconformity, and on the basis of a transition within the continental succession from predominantly sedimentary to predominantly volcanic rocks. DeGrace's provisional nomenclature was not used in

later literature. DeGrace also described the contact between the basal Croteau Group and the "underlying" granite as an intrusive contact.

Sander Geophysics Ltd. conducted an extensive airborne geophysical survey in the Ten Mile Lake, Seal Lake and Moran Lake areas on behalf of Brinex Ltd. in 1970 (Sander, 1971). Total field magnetics, gamma ray spectrometry, and EM were flown over the Croteau Lake area on 1/4 mile line spacings. All anomalies were moderate in intensity and no follow-up prospecting was done in the area.

In 1974 the Newfoundland Department of Mines and Energy (NDME) conducted a geological mapping survey of the Croteau Group. Smyth et al. (1975; 1978) subdivided the Croteau Group into the Aphebian Moran Lake and Helikian Bruce River Groups on the basis of an observed angular unconformity between the lower marine and upper continental successions. The Archean-Aphebian unconformity, between the basal of the Moran Lake Group sediments and underlying granite was described as a depositional contact.

In 1978 the NDME published a 1:50,000 geology map of the Pocket Knife Lake area (NDM Map 78171; Smyth and Ryan, 1978).

Ryan (1984) summarized the geology and economic mineralization of the Moran Lake Group in a memoir on the regional geology of the central part of the Central Mineral Belt. Ryan subdivided the Moran Lake Group into two

provisional formations viz.: the Warren Creek Formation, consisting mainly of slate, mudstone, and siltstone, and the Joe Pond Formation, consisting of massive and pillowed mafic volcanic rocks.

1.4 Physiography, Glacial History, and Vegetation

The Moran Lake Group occupies a low, poorly drained area in the northeast corner of a triple junction between the Moran Lake, Bruce River, and Seal Lake Groups. The triple point is formed by the juxtaposition of the Moran Lake and overlying Bruce River Groups against the younger Seal Lake Group along the north-south trending Pocket Knife Lake Fault Zone. In contrast to the recessively weathered pyritic shales, carbonates, and sandstones which dominate the stratigraphy of the Moran Lake Group (Fig. 1.2), the overlying Bruce River and Seal Lake Groups are well exposed along rugged step-like parallel ridges which reflect the stratigraphy of their interlayered volcanic and siliciclastic members (Fig. 1.3).

In the northern part of the study area, within the varied clastic and chemical sediments of the Warren Creek Formation, the topography is low and rolling with elongate mounds of glacial cover forming the areas of highest relief in the northern and western parts of the Warren Creek Formation. Elevations seldom exceed 320 m above sea level. The more resistant volcanics of the Joe Pond



Fig. 1.2 Topography of Warren Creek Formation looking west from south shore of Meathook Lake.



Fig. 1.3 Topography of Bruce River Group looking south from north shore of Croteau Lake.

Formation form distinct east-west trending ridges rising to heights of up to 380 m above sea level. The rugged high relief areas directly north of Croteau Lake are underlain exclusively by Joe Pond volcanics. The study area drains northeast to the Atlantic Ocean via Warren Creek which flows into the KaipokoK River.

The thick glacial mantle which obscures most of the Warren Creek Formation was deposited in two periods of Pleistocene glaciation (Fulton et al., 1970). The ice direction in the early episode was northeast, and was followed by an east-northeast advance (Thompson and Klassen, 1986). The glacial cover over the Moran Lake Group thickens to the north and west and largely conceals the bedrock in the western part of the study area. Sinuous narrow east-west trending esker ridges, rolling ground moraine, and broad open boulder fields form dissected bogs and a pervasive mantle on exposed outcrop ridges. The stratigraphic trend of the Moran Lake Group in this area is approximately parallel to the ice direction making lithological contact determinations by boulder examination impractical, except where frost heave from subcrop under thin till sheets is recognizeable.

Outcrop is exposed over approximately 10% of the Moran Lake Group, largely due to the incompetency of the Warren Creek Formation shales to weathering. The best exposures crop out along discontinuous east-west trending ridges and

bald hilltops. A number of northwest to northeast-trending faults create some excellent exposures in the southern parts of the map area.

Black spruce forest interspersed with an occasional stand of hardwood covers most of the area. The timber grows evenly and widely spaced on the sandy till making ground travel quite easy, however dense alder thickets thrive on many hillsides, creek beds, and bogs impeding ground travel at times. Tundra-like vegetation consisting of Labrador tea and antler moss grows on all hilltops and bogs.

1.5 Methods

This research consists of both field and laboratory investigations. The field investigation took place over a five week period, and consisted of reconnaissance bedrock mapping and outcrop sampling. Reconnaissance bedrock mapping simply involves traversing across the stratigraphy, describing exposures of bedrock, and selecting samples for laboratory investigations. The location of each outcrop was plotted on a 1:20,000 scale air photo, and lithologic and structural descriptions were transferred from field notes to the final geology map.

Rock samples, of approximately 2 kilograms each, were collected from all mineralized gossans (containing greater than 2% sulphide) within Upper Member shales of the Warren Creek Formation. Samples of unmineralized rock from all

lithologies were collected at random for later petrographic and geochemical study, and for comparison with mineralized rock of the same lithology (in particular Upper Member shales).

The rock samples were shipped to Memorial University for petrographic and geochemical analyses. Representative suites of sedimentary, volcanic, and igneous rocks from the area were analyzed for major, trace, and rare earth elements.

These data were then combined with field structural and stratigraphic relations, petrographic examinations using both conventional microscopy and scanning electron microscopy, and comparisons with published literature from similar geological environments to arrive at a model for basin evolution based on the geochemistry of sulphide-bearing gossans in the Upper Member of the Warren Creek Formation, and to infer from this, the potential of the Moran Lake Group for economic concentrations of sediment hosted base-metal sulphide mineralization.

CHAPTER 2

GEOLOGICAL SETTING

2.1 Regional Geology

The Moran Lake Group (Smyth et al., 1978) is a 3 to 5 km wide, 85 km long belt of Aphebian supracrustal strata which extends from Pocket Knife Lake ($54^{\circ} 25' N$, $61^{\circ} 20' W$) to the Kanairiktok River ($54^{\circ} 55' N$, $60^{\circ} 27' W$). These rocks are part of the Makkovik structural province of the Canadian Shield (Wardle et al., 1986) which has a regional northeast-southwest structural trend and lies along the northeast-southwest trending boundary of the Grenville tectonic province to the south, and the Archean Nain province to the north. Wardle et al. (1986) extend the limit of Grenvillian deformation north of the Makkovik-Nain boundary into the study area.

The rocks of the Archean Nain province form part of the North Atlantic Craton (ibid.) which extends along the northeast coast of Labrador to Greenland. These rocks have yielded Rb-Sr dates of up to 3100 Ma (Grant et al., 1983) in the southern part of the Nain province.

The Aphebian Moran Lake Group is unconformably overlain by the Paleohelikian Bruce River Group for which a U-Pb zircon age of 1649 Ma has been determined (Scharer et al., in prep.). The Bruce River Group is also part of the Makkovik province and was affected by Grenvillian

deformation ca. 1000 Ma (Wardle et al., 1986). The Moran Lake Group underwent polyphase deformation during the Makkovikian-Ketilidian event (1810 to 1790 Ma (ibid.) prior to the deposition of the Bruce River Group.

The Aphebian-Helikian unconformity separates two metallogenic provinces (Smyth et al., 1975) viz.: the Moran Lake Group which is characterized by black shale-hosted, stratiform, disseminated and massive sulphide mineralization, and the Bruce River Group which is characterized by epigenetic uranium and copper mineralization and forms part of the Labrador Uranium Area, a metallogenic province first described by Beavan (1958). The Paleohelikian Bruce River Group is in turn unconformably overlain by the Neohelikian (Smyth et al., 1978) Seal Lake Group which is unconformably juxtaposed against the Moran Lake Group along the north-south trending Pocket Knife Lake Fault Zone.

The supracrustal rocks of the Lower Proterozoic Lower Aillik Group in the coastal area of the CMB, have been inferred (Gower et al., 1982; Ryan, 1984; Wilton and North, 1987) to be regionally correlative with the Moran Lake Group. These rocks were also affected by Makkovikian-Ketilidian deformation, however a number of outstanding structural, stratigraphic, and metallogenic differences (Wilton and North, 1987; Wilton et al., 1987) suggest that they are not directly laterally

equivalent with the Moran Lake Group.

The stratigraphy of the Moran Lake Group is dominated by a marine shelf sequence of sandstones, black pyritic shales and pillowed mafic flows attesting to the development of a stable continental margin on the Nain craton prior to the Makkovikian-Ketilidian orogeny (1810 to 1790 Ma.)

2.2 Geology and stratigraphy of study area

The stratigraphy of the Moran Lake Group is shown in Figure 2.1. Since the stratigraphy of the group is structurally thickened in the Croteau-Pocket Knife Lakes area (see Section 2.3), the indicated stratigraphic thicknesses given in Figure 2.1 represent an estimation of actual thicknesses without accurate structural balancing to compensate for tectonic redistribution. The wide range of stratigraphic thicknesses listed in this section also serve to illustrate the intensity of tectonism and concomitant thickening of the Group in this area.

2.2.1 Map unit 1: Archean basement

Massive to foliated, medium-grained, beige to pink granitoid basement rocks, of the Kanairiktok Valley Complex (Ermanovics and Raudsepp, 1979a) part of the Nain Structural Province, underlie the basal Moran Lake Group and crop out in the northern map area. In the field, these

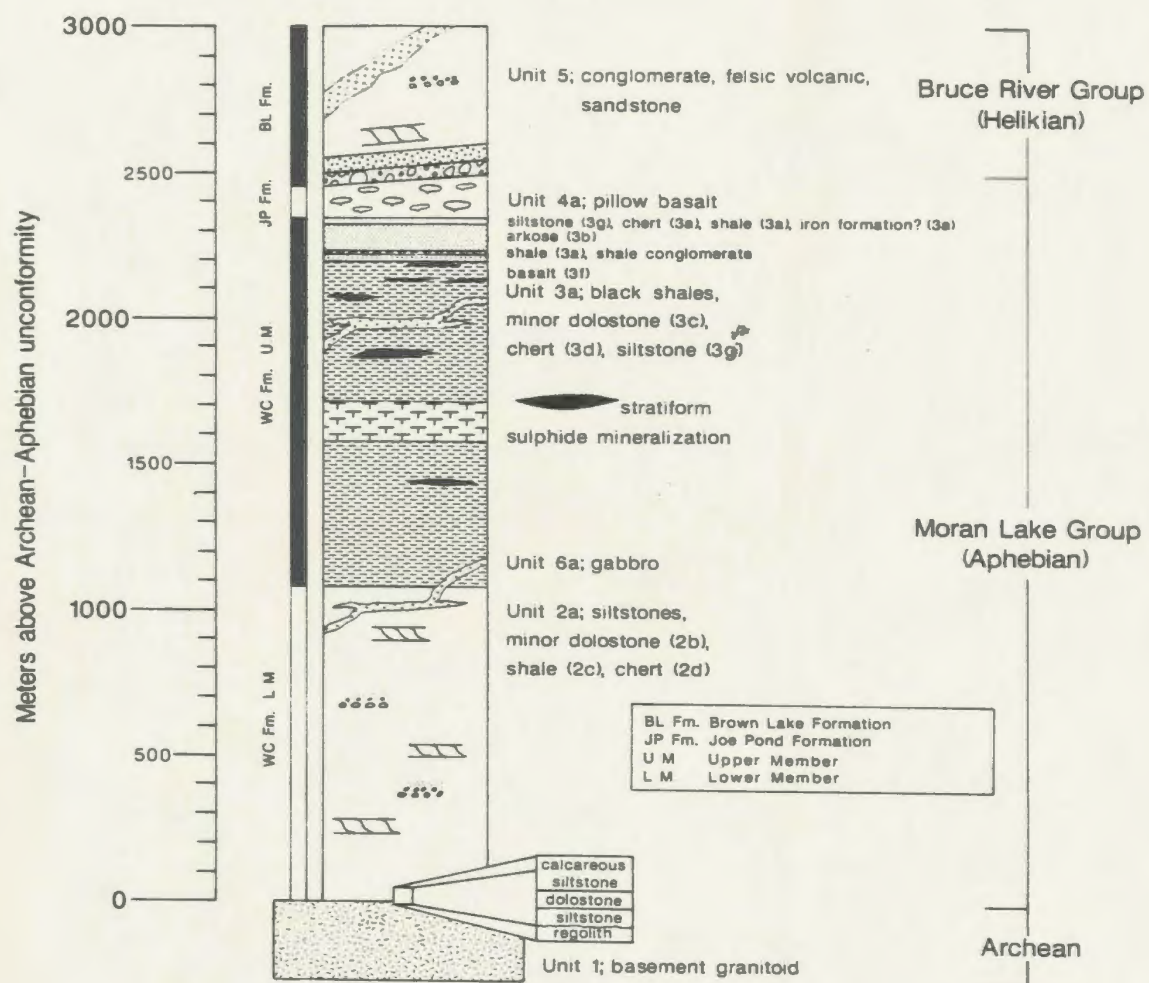


Fig. 2.1 Moran Lake Group stratigraphic column.

phaneritic rocks consist of anhedral to subhedral interlocking medium-grained quartz and feldspar, mottled with fine to medium-grained interstitial muscovite and biotite (Fig. 2.2). Sulphides, consisting mainly of pyrite, occur as accessory minerals, and as secondary mineralization within quartz-carbonate-filled fractures.

Accessory minerals identified by scanning electron microscopy include very fine-grained, subhedral to euhedral rutile (and anatase after rutile) and zircon, and subhedral to anhedral monazite and barite (Figs. 2.3 - 2.7).

In thin section these rocks are allotriomorphic granular, and consist of approximately 40-45% plagioclase, 10% orthoclase, 20-30% quartz, 5-7% biotite, 3-5% muscovite, and 2-3% fine-grained opaque minerals. Minor sericite and ankerite occur as very fine rims along feldspar-quartz grain boundaries.

These rocks vary from massive to foliated, and in places are gneissic. The structural fabric is defined by the alignment of interstitial biotite flakes, and to a lesser extent muscovite. Quartz and feldspar grains are always undulose, and serrated quartz grain boundaries rimmed by recrystallized fine-grained polygonal quartz are common.

Outcrops of the basement proximal to the Archean-Aphebian unconformity are very limonitic. In the field it appears as though the feldspar has altered to



Fig. 2.2 Archean granitoid, scale in cm.



Fig. 2.3 TiO_2 (anatase after rutile) in basement granitoid



Fig. 2.4 Zircon in basement granitoid.



Fig. 2.5 Accessory monazite in basement granitoid.

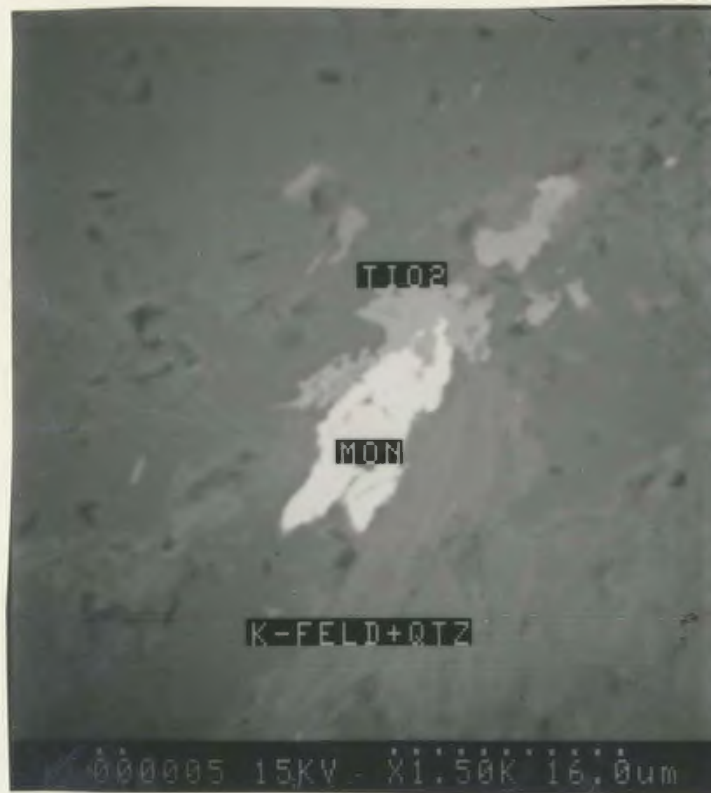


Fig. 2.6 Accessory monazite (white) intergrown with anatase (light grey) in basement granitoid.

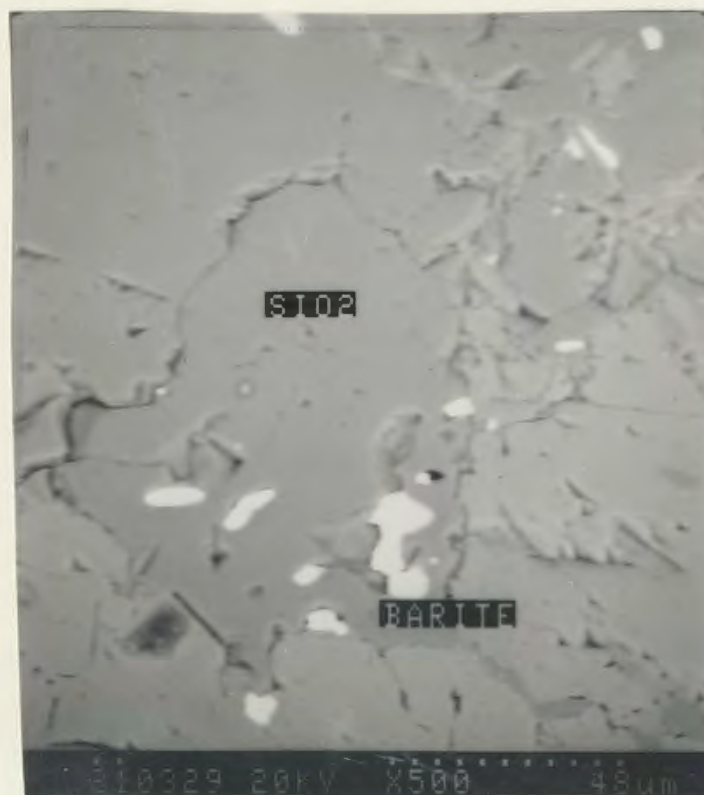


Fig. 2.7 Accessory barite in basement granitoid.

clay and rusty weathering carbonate, which gives the rock a rotten saprolitic appearance (Figs. 2.8, 2.9). This alteration increases with proximity to the Archean-Aphebian unconformity indicating the development of a regolith in the basement rock by Aphebian weathering, prior to deposition of the Moran Lake Group. Thin sections from basement trondjhemite directly below the unconformity south of Moon Pond indicate that regolith development caused 50-60% replacement of albite to calcite by corrosion of grain boundaries, and alteration by fluid percolation along cleavage lamellae and microfractures. Equant, fine-grained secondary pyrite and minor galena were introduced into the basement regolith along with, in decreasing order of abundance, fine-grained quartz, carbonate, and sericite. Subsequent recent surface weathering has oxidized the carbonate and sulphide minerals in the regolith to the distinctive rusty colour observed in the field.

2.2.2 Map units 2 and 3: Warren Creek Formation

2.2.2.1 General description

The Warren Creek Formation (Ryan, 1984) is a 1200 to 4600 m thick sequence of clastic and chemical metasedimentary rocks, and minor basalt, which was deposited in a marine shelf environment unconformably on the Archean basement granitoids. The apparent thickness of



Fig. 2.8 Regolith below basal Moran Lake Group.

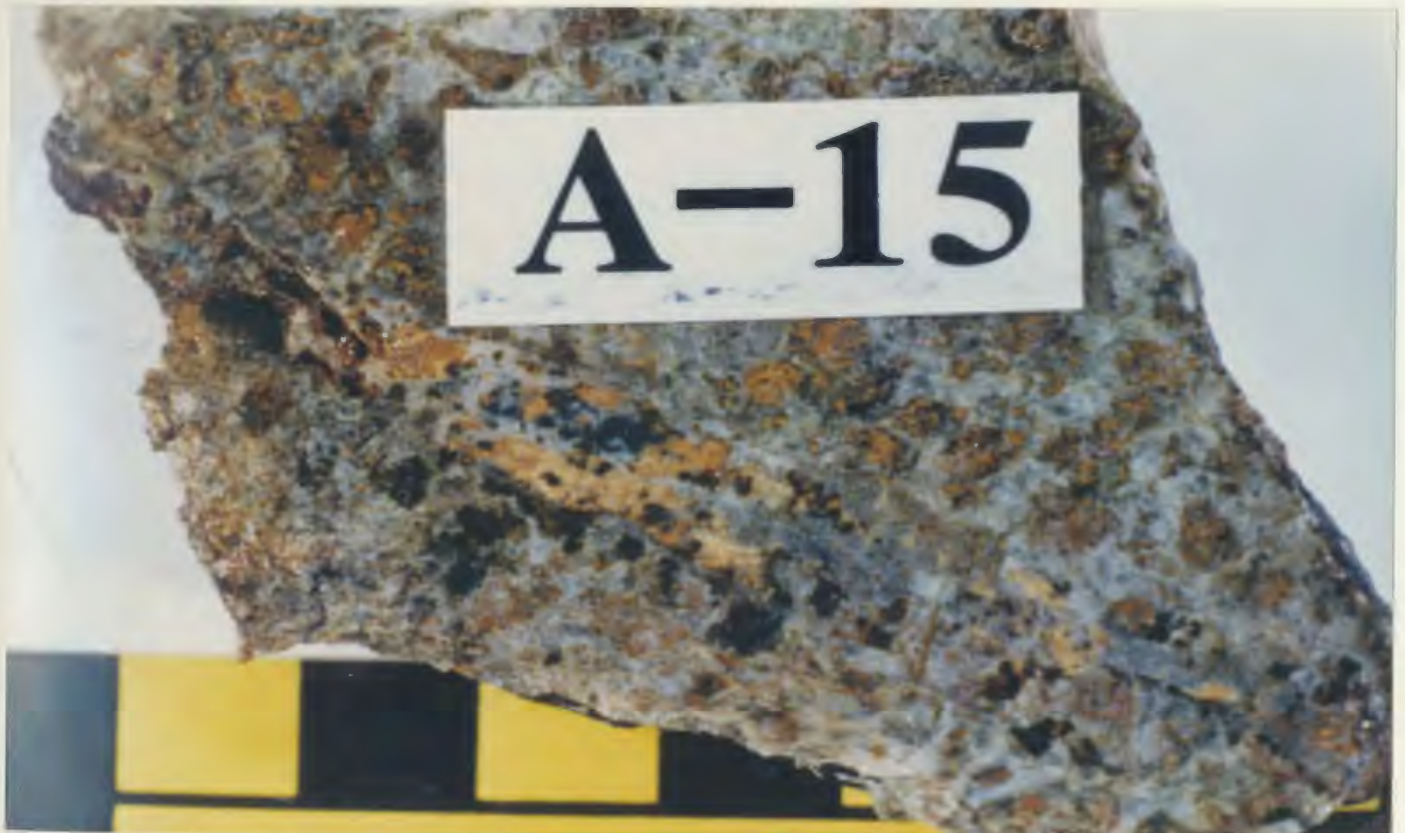


Fig. 2.9 Regolith in Archean basement, scale in cm.

the Warren Creek Formation is probably exaggerated by as much as 50% in many areas, due to structural thickening by east-west trending isoclinal D_1 folding. D_1 buckle folds in chert, carbonate, and siltstone interbeds in the heterogeneous black shale sequence, also indicate that structural thickening of the less viscous shales by layer parallel shortening (Ramberg, 1963b; Dieterich, 1969; Ramsay, 1976) has occurred.

The definition of the Warren Creek Formation by Ryan (1984), is an accurate provisional subdivision whereby the pillowed mafic volcanic rocks of the upper Moran Lake Group, Joe Pond Formation, are distinguished in lithological and tectonic style from the basal Moran Lake Group marine sedimentary rocks. Ryan's description of the Warren Creek Formation is as follows:

"On the basis of field and petrographic studies, a tentative four-fold subdivision of the [Warren Creek Formation] is proposed. In ascending stratigraphic order these are: (a) a basal grey feldspathic quartz arenite, (b) a dominantly shale (slate) ~ arkosic siltstone member, (c) a brown dolostone, and (d) a dominantly shale (slate) ~ greywacke member." (Ryan, 1984, pg. 32).

These subdivisions within the Warren Creek Formation were alluded to by previous workers in the area including Smyth et al. (1975; 1978), and Halet (1946), however,

factors including the general paucity of outcrop, the highly tectonized nature of the Moran Lake Group, and lack of detailed exploration in the area by mining companies have precluded more definitive control on the stratigraphy of the formation and interpretation of the evolution of the lithologic sequence. Therefore, no further formal formational subdivisions, or subdivisions requiring member status, were proposed for the Warren Creek Formation.

The present mapping indicates that the Warren Creek Formation can be subdivided into two Members viz.: the Lower Member, consisting primarily of laminated siltstone, calcareous siltstone, and arkosic sandstone, with a narrow dolostone bed proximal to the Archean-Aphebian unconformity; and the Upper Member consisting of pyritiferous black shale, slate, and argillite, which are intimately interbedded with grey siltstone and chert and a thick dolostone bed in the middle of the sequence, and an arkose bed and banded ironstone bed at the top of the sequence. The exact location of the ironstone bed in the section is not known as it only crops out twice in the study area, and is obscured by the overlying Bruce River Group. However it appears to be discontinuous and overlies the arkose bed.

2.2.2.2 Map unit 2: Lower Member

The Lower Member varies in thickness from 180 to 1300

m. This variation is largely due to structural thickening, but also due to the paleotopography of the basin. The member consists mainly of beige to light green, laminated, fine-grained siltstone and feldspathic sandstone with minor red to mauve varieties (Unit 2a), calcareous siltstone and dolostone (Unit 2b), minor shales and slate (Unit 2c), intercalated chert (Unit 2d), and feldspathic quartz arenite (Unit 2e) (Figs. 2.10 - 2.12). The stratigraphy strikes roughly east-northeast and dips 60° to 80° south. Normal graded bedding and cross bedding on a 1 to 5 cm scale are common throughout the sequence, and indicate that the sequence faces south.

In thin section these rocks consist of poorly sorted, angular to subrounded quartz/feldspar silt and grit with variable amounts of fine-grained interstitial idiomorphic carbonate rhombs, and amorphous masses of matrix carbonate which may comprise 10 to 20% of the rock. Much of the finer silt and clay-rich (shale) beds are altered to ultrafine sericite with minor (exsolved?) iron oxide and fine-grained interstitial hematite. Minute hair-like stringers of recrystallized vein quartz +/- carbonate fill discordant fractures.

The member seems to thin to the east where as little as 180 m of arkose and siltstone overlie Archean granitoids along Warren Creek, but to the west, the member is up to 1300 m thick and more varied in texture and grain size from

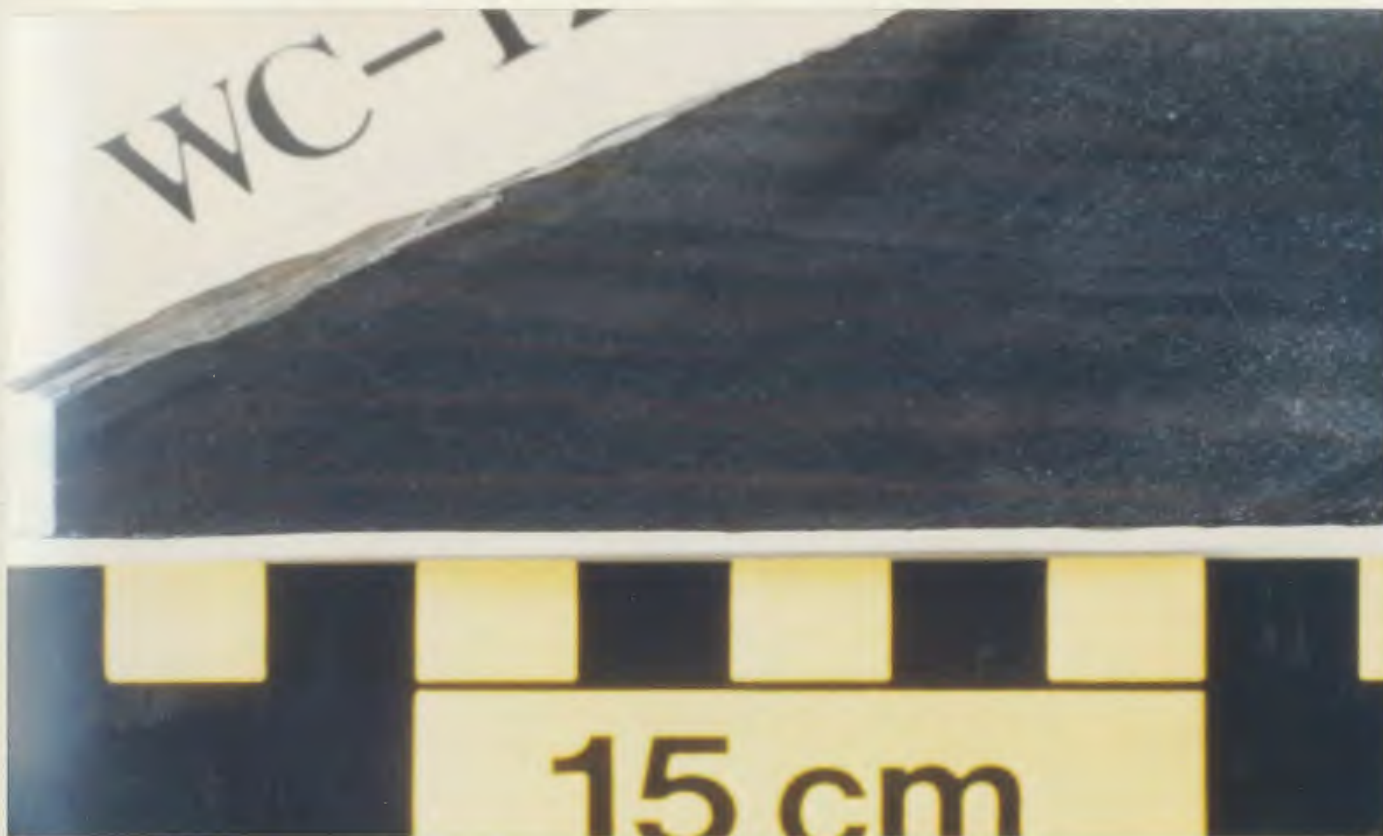


Fig. 2.10 Red bed in Lower Member, scale in cm.

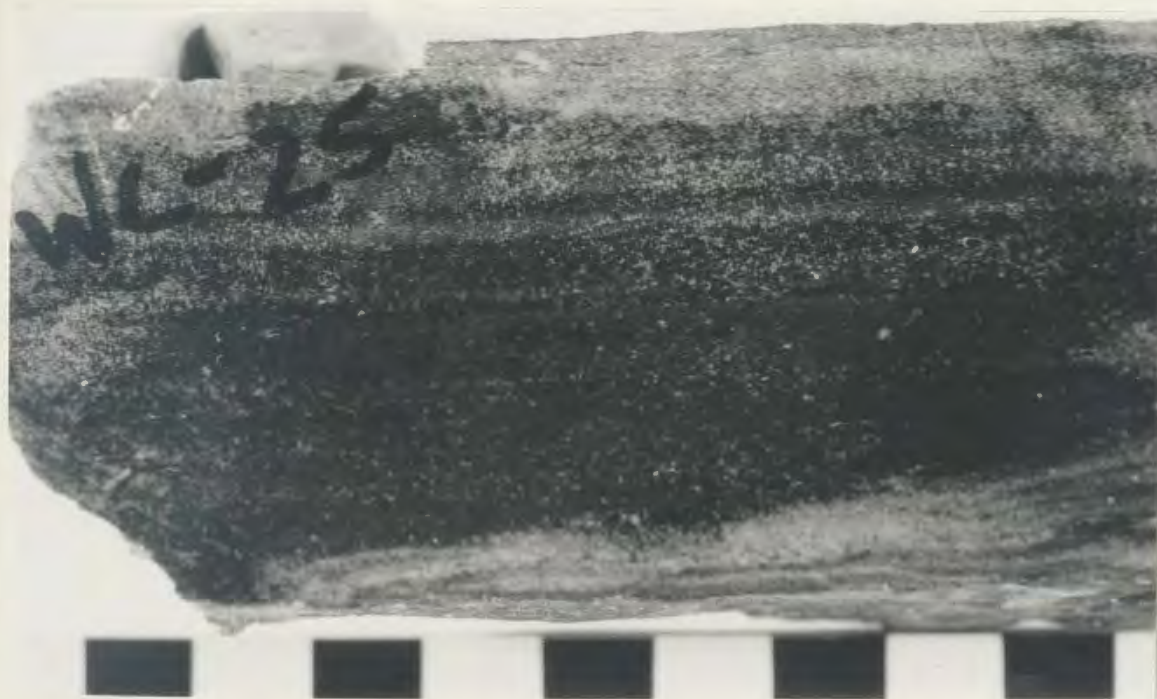


Fig. 2.11 Lower Member silty dolostone bed, scale in cm.



Fig. 2.12 Lower Member interbedded siltstone (light grey) and dolostone (dark grey, foreground).



Fig. 2.13 Upper Member typical gossan, near Zee Lake.

finely laminated siltstone to arkosic arenite. The regional distribution of the Lower Member suggests that this is due in part to structural thickening on east-west trending fold axes, but also to the primary basin configuration of a sequence which onlapped to the east (i.e. the basin was deeper to the west and could hold more material, notably some of the finer silts seen to the west, while the basin was much shallower to the east and only allowed the deposition of the coarser arkosic sediment which is seen directly south of the Archean basement along Warren Creek). A 5 to 10 m thick basal dolostone unit (Unit 2b) occurs in close proximity to the Archean basement throughout the area, but is underlain by approximately 5 to 25 m of siltstone and arkose which lie directly on the unconformity. In the Moran Lake area, approximately 2 km northeast of the last exposure of the dolostone bed in the study area, the dolostone is observed to directly overly the Archean basement at the CANICO Anomaly No. 8 showing (Perry, 1980; Ryan, 1984; D.Wilton, 1986 pers. comm.). This was recognized by earlier workers to represent an onlapping direction of the Moran Lake Group to the east (Ryan, 1984; Smyth et al., 1978) and the present observations on the thickness of the basal sandstone formation support this conclusion.

2.2.2.3 Map unit 3: Upper Member

Decreased relief and outcrop frequency help to define the contact between the basal siliciclastics of the Lower Member, and the recessively weathered, heterogeneous black shale sequence of the Upper Member. These rocks occupy the southern and central part of the map area. This sequence varies from 543 to 3350 m in thickness, and consists primarily of fine-grained and finely bedded black shale, slate, and argillite which are intercalated with numerous grey silt and chert beds (Unit 3a). Massive beige to grey arkose (Unit 3b), banded ironstone (Unit 3e), and vesicular basalt flows (Unit 3f) are locally interdigitated with clastic sedimentary rocks at the top of the sequence. The shales and slates are composed of varying amounts of aphanitic clay minerals, amorphous silica, and fine detrital quartz and may be very graphitic over relatively narrow widths (~1 cm). Pyrite is a ubiquitous constituent of the shales, and as a result nearly all shale outcrops are covered with a distinctive rusty gossan (Fig. 2.13, pg. 28). Stratiform massive pyrite beds (+/- pyrrhotite, chalcopyrite, and sphalerite) were observed in a few localities reaching thicknesses of over 1 m (Fig. 2.14), (Hansuld (1958) described a 6 m thick pyrite bed).

As mentioned in section 2.2.2, the stratigraphy of the Upper Member has always been somewhat problematic due

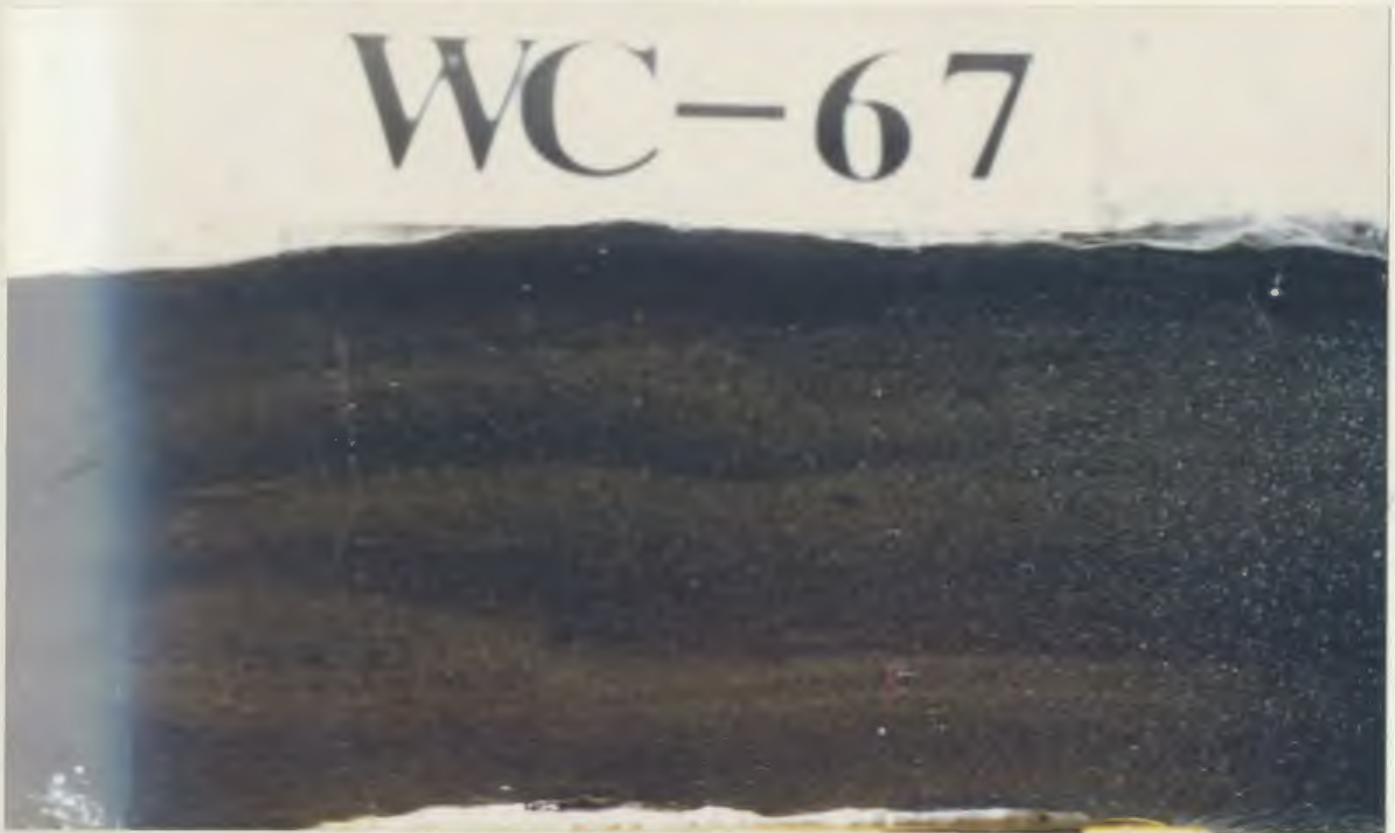


Fig. 2.14 Upper Member typical massive graphitic pyrite bed, slab is 5 cm wide.



Fig. 2.15 Upper Member middle dolostone bed, Date Grid exposure.

to limitations imposed by the thickness of glacial cover and lack of detailed structural analysis of the Moran Lake Group. In particular, three important units have never been accurately fitted into a regional stratigraphic column, viz.: banded ironstone (Unit 3e) which crops out in the Zee Lake area and directly north of Mushroom Pond, a thick dolostone unit (Unit 3c) which crops out north of Croteau Lake and Long Pond, and the arkose bed (Unit 3b) which crops out east of Heart Pond and within the core of a large anticline north of Mushroom Pond. The location of these units within the regional stratigraphic column for the Moran Lake Group is shown in Figure 2.1, pg. 17.

2.2.2.3.1 Middle dolostone

The dolostone unit is well exposed north of Long Pond where it reaches a maximum thickness of 235 m. This unit is also exposed, albeit rather poorly, north of Dragon Pond. The unit is dominated by massive brown ochrous polygonal weathering dolostone (Fig. 2.15, pg. 31), with minor intercalated silt, shale, and chert. North of Dragon Pond the unit crops out approximately 400 m north of the highly sheared contact with the Joe Pond Formation. North of Long Pond the unit is exposed almost in contact with the Joe Pond Formation with 40 m or less of intervening shale, therefore it is suggested that the dolostone occurs within 400 m of the top of the Upper Member.

2.2.2.3.2 Vesicular basalt

Narrow flows of dark green, fine-grained, vesicular, chloritized basalt (Figs. 2.16, 2.17) are interdigitated with clastic sedimentary rocks near the top of the Upper Member, and crop out in two areas; 90 m east of Heart Pond at the Teuva showing, and 500 m southwest of Dragon Pond near the Fault Creek Showing. These rocks consist of 20-30% fine-grained phyrlic plagioclase, 15-20% aphanitic groundmass plagioclase, 10-15% aphanitic microlites of groundmass clinopyroxene, 30-35% chlorite after plagioclase and clinopyroxene, 3-5% very fine-grained equant opaque minerals, and 2-3% fine-grained quartz +/- calcite. The matrix plagioclase is highly altered to carbonate and ultrafine sericite as well as chlorite, giving the rock a cloudy appearance in thin section under crossed polars.

2.2.2.3.3 Arkose bed

The arkose bed (Unit 3b) crops out in the core of a mesoscopic anticline north of Mushroom Pond. Previous workers (Halet, 1946; Smyth et al., 1975, 1978; and Ryan, 1984) have interpreted this to be exposed Lower Member sedimentary rocks which were upwarped into the core of the fold. The present mapping indicates distinct differences between these rocks and the rocks of the Lower Member,



Fig. 2.16 Upper Member basalt flow (light grey, under hammer) hosted in siltstone 600 m south of Dragon Pond.



Fig. 2.17 Upper Member vesicular basalt, note plag. phenocrysts, scale in cm.

namely that the arkose in the core of the anticline is slightly coarser-grained and massively bedded with occasional round quartz pebbles (Fig. 2.18). Primary sedimentary structures are rare, and no chert or calcareous material were observed in the core of the anticline. This contrasts with the thinly bedded and frequently cross-stratified siltstones and sandstones of the Lower Member which contain numerous chert and shale interbeds and calcareous units. Detailed mapping in the fold area revealed the arkose unit on the southern limb of the fold on the north side of a steep hill composed of Joe Pond Formation volcanics directly north of Croteau Lake (Fig. 2.19). The line of section is shown on the geology map in the back pocket. Here the arkose is in contact with poorly exposed steeply dipping cherty siltstone to the south, and forms a mappable unit over 50 m thick. To the north the arkose is bounded by typical shales of the Upper Member, via a gradational contact through a 2 m thick shale-lithic paraconglomerate bed (Fig. 2.20) which indicates that the sequence faces south. This is consistent with the facing direction of the southern limb of the anticline. These relations prove that the arkose is part of the Upper Member and at the top of the sequence, since the arkose bed, and local stratigraphy, are in conformable contact with the Joe Pond Formation. Vesicular basalt flows outcrop to the north and stratigraphically below the arkose

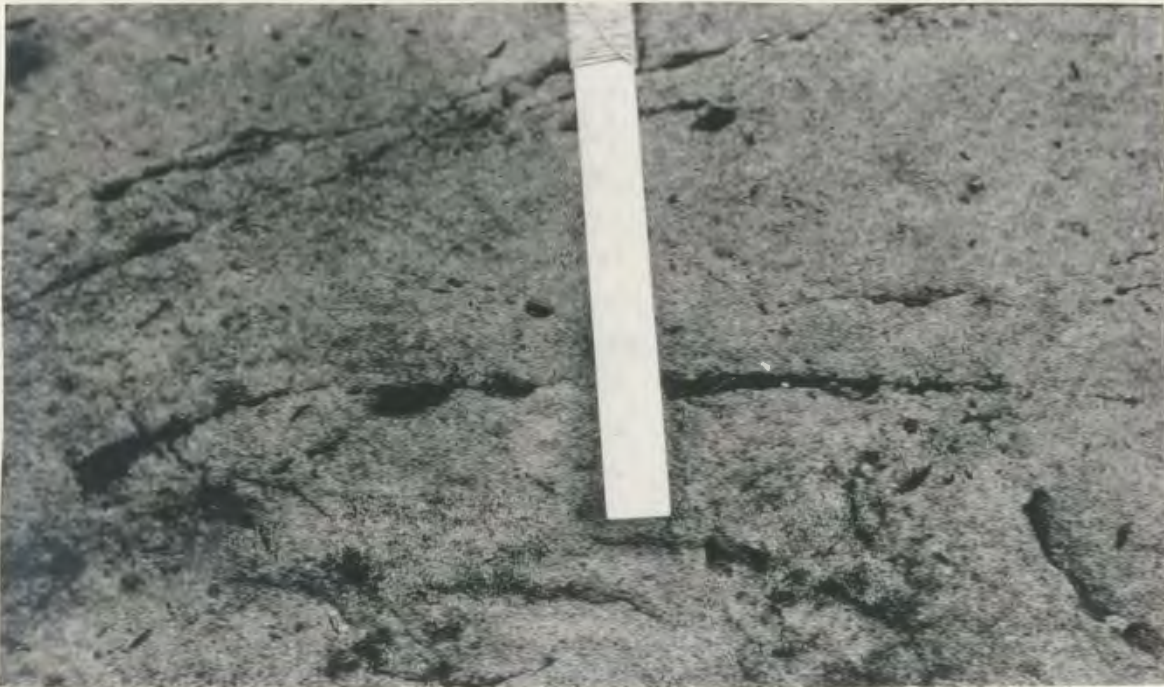


Fig. 2.18 Upper Member arkose bed, note dark grey qtz. pebbles, scale in cm.

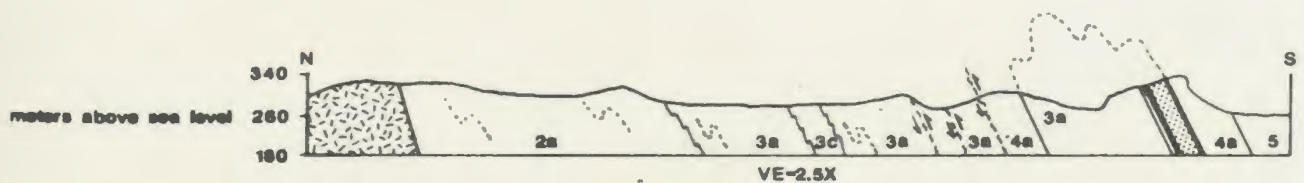


Fig. 2.19 Moran Lake Group structural cross section, note arkose bed (stippled).



Fig. 2.20 Upper Member shale lithic conglomerate, note elongate black shale, and light grey rounded qtz. clasts, scale in cm.



Fig. 2.21 Upper Member ironstone, north of Mushroom Pond.

bed east of Heart Pond, and attest to a more dynamic tectonic regime during the deposition of the upper part of the Upper Member than that of the monotonous typical shale sequence.

Therefore, a re-interpretation of the genesis of the arkose bed in the core of the anticline is proposed. This bed was deposited during a change in depositional and tectonic environments during the last stages of the deposition of the Upper Member shale sequence. Vesicular basalt flows, overlain by shale-lithic conglomerate and 50 m of pebbly arkose were deposited following a gradual change in water depth from deep to shallow, and a change in depositional setting from passive shale and silt accumulation in a deep reducing basin to uplift, and rapid deposition of arkose in a high energy nearshore environment above a minor internal disconformity marked by the shale-lithic conglomerate. Banded hematite-magnetite-chert ironstone indicate that conditions were oxidizing rather than reducing at this stage. The vesicular basalt flows at the top of the Upper Member may be shallow water incipient equivalents of the non-vesicular Joe Pond Formation. Subsequent deformation (D_1) of the Moran Lake Group folded this sequence into a broad westerly plunging, east-west trending anticline. Deep erosion on the hinge of the anticline exposed the arkose in the core of the fold. Deeper erosion of the west end of the anticline along

the east shore of Heart Pond exposed a window of Upper Formation shales which occur stratigraphically below the arkose.

2.2.2.3.4 Banded ironstone

Ironstone (Unit 3e), consisting of rhythmically bedded jasper, specularite, hematite, magnetite, and varied epiclastic impurities (Fig. 2.21, pg. 37), is exposed in two outcrops in the southern part of the map area. The ironstone always crops out in close proximity to the unconformity with the younger^o Bruce River Group, and the Brown Lake Formation conglomerate of the basal Bruce River Group in this area (see section 2.2.4) contains numerous clasts and boulders of the Moran Lake Group ironstone suggesting, at least empirically, that this unit occurs near the top of the Moran Lake Group and not at the base as has been suggested by previous workers (Halet, 1946; Smyth et al., 1975, 1978; and Ryan, 1984). At the CANICO Anomaly 15 showing, 3.4 km northeast of Moran Lake, sandstones of the Heggart Lake Formation (Bruce River Group) unconformably overlie a basal iron formation conglomerate of the Moran Lake Group (Wilton, 1986, pers. comm.).

North of Mushroom Pond, 5 to 10 m of the ironstone is poorly exposed on a hillside marking the contact with the overlying Bruce River Group. The unit is flanked to the north by the arkose bed described in the previous

section. The facing directions in the anticline infer that the ironstone overlies the arkose bed, however, direct correlation with the stratigraphy in the anticline is precluded by the presence of a northwest trending dextral strike-slip fault with an apparent displacement of 500 m which truncates the ironstone. The stratigraphic location of the iron formation in the anticline is inferred because it is largely covered by overburden, however, a cherty siltstone bed was noted in the general area.

The ironstone is also exposed at Zee Lake northeast of the east arm of Pocket Knife Lake. Argillaceous sediments, chert, siltstone, and fine-grained siliceous arkose are intercalated with the ironstone here, but since the exposure is poor, no definite contact was observed between the ironstone and the host rocks. The Zee Lake exposure does not yield much insight into the stratigraphic position of the ironstone other than that it appears to be at the top of the Upper Member sequence and is associated with chert and siliceous epiclastics similar to those of the exposure at Mushroom Pond. Though limited by the amount of available data, the ironstone appears to occur above the arkose bed in association with chert and siliceous siltstone as it does at Mushroom Pond. This would be the last unit to be deposited in the Upper Member and as such represents a period of relative quiescence and low rate of sedimentation prior to the deposition of the Joe Pond

Formation in a sediment-starved basin.

2.2.3 Map unit 4: Joe Pond Formation

Light to dark green, fine-grained, massive and pillowed basalt, with minor interflow chert, and pyritic chert, were deposited conformably over the Warren Creek Formation (Fig. 2.22). The basalt sequence is 100 to 300 m thick and is repeated on the limbs of the Mushroom Pond anticline. Facing directions indicate that the north limb of the fold, which plunges 40° to the west, is overturned to the south by 22° .

The rocks are granular, aphanitic, and moderate to weakly foliated in thin section. Regional greenschist facies metamorphism has pervasively altered the basalt to chlorite and carbonate after plagioclase and clinopyroxene. Remnant plagioclase phenocrysts were observed in the field, however they are usually obscured by regional metamorphism, and difficult to recognize in thin section due to the extent of alteration. Some thin sections of these rocks appear to consist entirely of fine to medium-grained calcite, occurring as irregular masses, and/or idioblastic interlocking rhombs, with minor interstitial anomalous blue chlorite, and exsolved opaque minerals. Secondary quartz-calcite stringers fill microfractures and small cavities.



Fig. 2.22 Joe Pond pillow basalt, north shore of Croteau Lake.



Fig. 2.23 Carbonatized basalt, west end of Long Pond, scale in cm.

The basalts are highly fractured and carbonatized in proximity to the Aphebian-Helikian unconformity, particularly between the northeast bay of Croteau Lake and Long Pond, where highly fractured basalt is exposed directly below the basal conglomerate of the Brown Lake Formation (Fig. 2.23, pg. 42). The basalt here is composed of up to 30-50% calcite as fine-grained pervasive replacement of mafic minerals, and mineralization in fractures with secondary quartz. This unusually intense carbonate alteration is not accompanied by a distinctive or unique strain fabric, suggesting that a regolith was developed in the basalt below the Brown Lake Formation.

2.2.4 Map unit 5: Bruce River Group

Red to buff boulder conglomerate of the Brown Lake Formation, the middle subdivision of the Bruce River Group (Ryan, 1984), is in contact with the highly altered Joe Pond basalt on the northeast shore of Croteau Lake, defining the Aphebian-Helikian unconformity. The conglomerate also unconformably overlies the black shales of the Upper Member of the Warren Creek Formation in the map area. This polymictic conglomerate is a maximum of 100 m thick, varies from clast to matrix supported, and contains unsorted angular to sub-rounded boulders and pebbles of ironstone, quartz arenite, arkose, and siltstone derived from the underlying Moran Lake Group

(Fig. 2.24). Basalt fragments were not observed in the conglomerate.

Felsic volcanic rocks, identified as dust tuff or porcellanite by Ryan (1984), are intercalated with the conglomerate in intervals up to 30 m thick. The tuff contains 1 to 5 cm beige and purple bands, which may represent primary beds, with disseminated 0.1 to 2 mm feldspathic sericitized lapilli or spherulites in a brittle siliceous matrix (Figs. 2.25, 2.26).

Fine to medium-grained, red, mauve, and buff tuffaceous sandstone overlies the basal conglomerate and felsic volcanic rocks of the Brown Lake Formation. These rocks dip gently south and form the rocky southern shoreline of Croteau Lake. These rocks are finely bedded on a scale of 1 mm to 1 cm, and are frequently cross-stratified and internally graded (Fig. 2.27). Selectively sericitized, light green to buff horizons a few mm to a few cm thick, are present in the sandstones. This alteration gives these rocks the appearance of the Brown Lake Formation felsic volcanic rocks described above.

2.2.5 Map unit 6: Gabbro

Dark green, massive, medium-grained gabbro plugs and dikes (Fig. 2.28) intrude all units in the map area. The dikes are 20 to 80 m wide on average, but rounded plugs may reach 1400 m in diameter.



Fig. 2.24 Bruce River Gp. boulder conglomerate, north shore Croteau Lake.



Fig. 2.25 Bruce River Group felsic volcanic west of Heart Pond.



Fig. 2.26 Bruce River Group felsic volcanic, scale in cm.



Fig. 2.27 Bruce River Group volcaniclastic sandstone, note light sericitized laminae, scale in cm.



Fig. 2.28 Gabbro dike 500 m south of Dragon Pond.

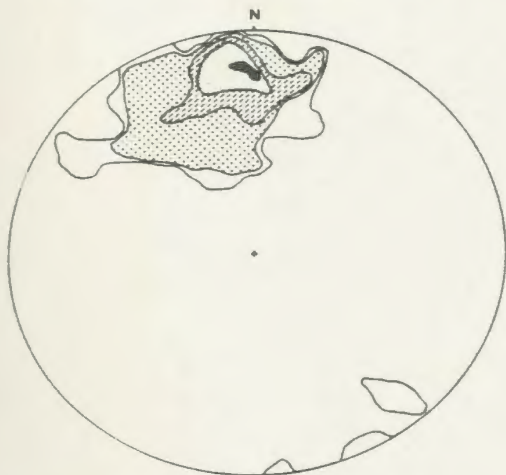
The rocks are medium to coarse-grained, idiomorphic, granular, and are mainly composed of 25-30% plagioclase, 30-40% hornblende, and 10% equant clinopyroxene. Biotite may occur as disseminated fine to medium-grained phenocrysts, but occurs most commonly as (up to 10%) replacement of pyroxene and amphibole. Plagioclase grain boundaries are slightly corroded by alteration to chlorite and sericite with minor calcite.

The gabbros are relatively fresh looking, however secondary quartz-carbonate-sulphide mineralization occurs along fractures and wall rock contacts. This alteration significantly decreases the grain size of the rock, and has resulted in the alteration of plagioclase to sericite and calcite, and amphibole and pyroxene to chlorite and biotite, with the addition of up to 20, to 30% secondary quartz. Disseminated pyrite and chalcopyrite (2-3%) occur in these alteration zones but do not appear to be of any economic interest.

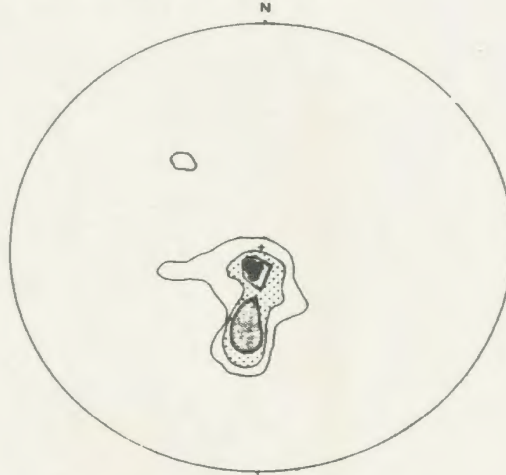
2.3 Structural Geology

The various strain fabrics in the Moran Lake Group are illustrated in Figure 2.29. Two prominent deformational events are preserved in these rocks. The D_1 structures are pervasive, while D_2 structures are less obvious, and are more prevalent in areas of contrasting lithological competencies. D_3 -related structures are preserved

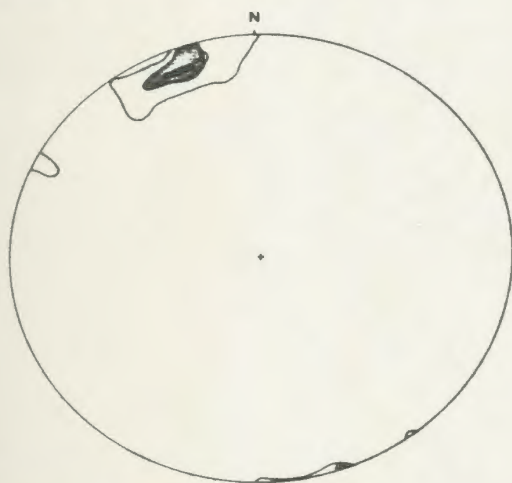
(a) $N=109$, C.I.=2,3,5,7,10%



(b) $N=33$, C.I.=5,7,10,15%



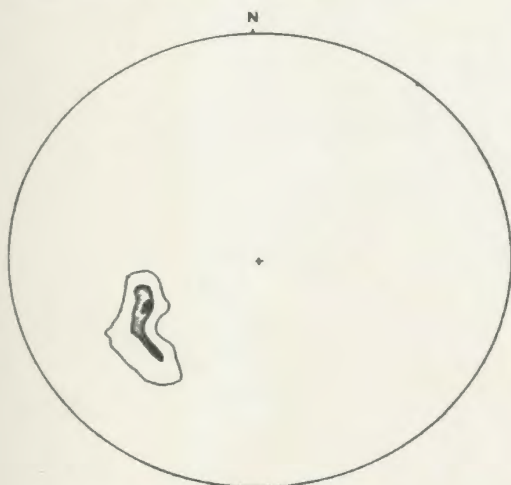
(c) $N=25$, C.I.=8,12,16,20%



(d) $N=52$, C.I.=2,4,6,8%



(e) $N=15$, C.I.=7,14,20%



(f) $N=14$, C.I.=10,15,25,30%

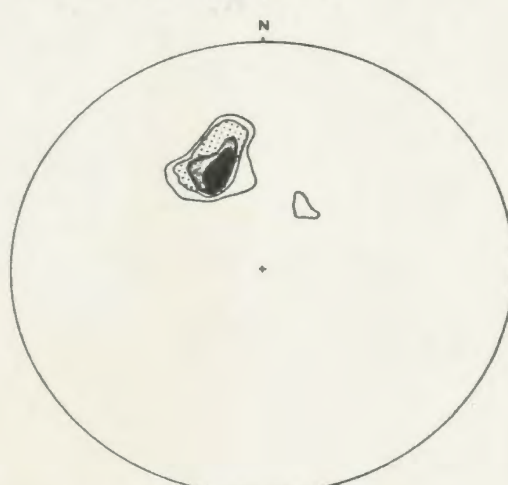


Fig. 2.29 Contoured equal area stereographic projections of poles to S_0 (a), F_2 (b), poles to S_1 (c), poles to joints (d), stretching lineations (e) for Moran Lake Group; and poles to S_0 (f), Bruce River Group.

locally, and characterized by broad, open warping of the stratigraphy and earlier fabrics. D_1 and D_2 structures predate the deposition of the Bruce River Group and are best developed in the ductile shales of the Upper Member of the Warren Creek Formation.

2.3.1 D_1

Bedding (S_0) strikes 076° and is tilted 74° to the south in response to D_1 which isoclinally folded the Moran Lake Group into numerous paired syncline-anticline couples (Fig. 2.30). The south limbs of the synclines and the north limbs of the anticlines are overturned to the north by approximately 16° . F_1 closures are rarely observed due to a significant degree of D_1 axial planar shearing approximately parallel to S_0 (bedding), which is rotated into parallelism with S_1 . The best example of an F_1 fold, occurs north of Mushroom Pond. Here, the limbs of a west plunging anticline are defined by basalts of the Joe Pond Formation which bound a central core of arkose which occurs near the top of the Upper Member. A slatey, axial planar D_1 cleavage (S_1) which trends 071° and dips 79° south, is pervasive in the Upper Member shales, but poorly developed in the Lower Member siliciclastics, and in the Joe Pond Formation basalts. D_1 stretching lineations (L_1), as defined by mineral streaking on micaceous cleavage planes in the Upper Member trend 251° and plunge 49° in the plane



Fig. 2.30 D_1 closure in shale, trench C, Date Grid.

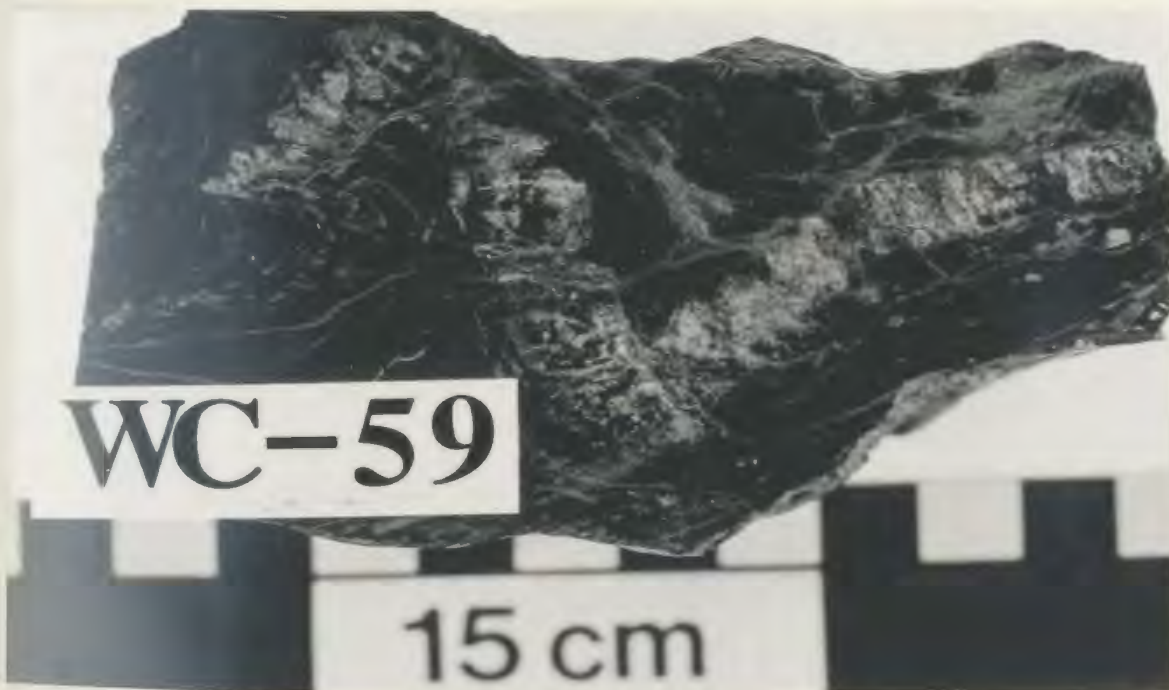


Figure 2.31 D_1 buckle fold in competent chert layer, scale in cm.

of S_1 .

Discordant, steeply dipping sinistral and dextral cross-faults at high angles to S_1 and S_0 , truncate D_1 structures with displacements of up to 2.5 km. These cross-faults are prominent at 160° and 205° . The faults trend close to an observed conjugate joint set at 134° and 211° , suggesting that they are related to the same deformational event. It is suggested that the conjugate joint set and the crosscutting faults formed in response to D_1 , since the bisectrix of the acute angle of these fracture systems is perpendicular to S_1 , and parallel to the maximum direction of crustal shortening which is fixed by the S_1/L_1 relationship (where the S_1/L_1 relationship defines the X-Y plane of the regional strain ellipsoid (Ramsay, 1967, 1976; Hobbs *et al.*, 1976)).

The shales of the Upper Member of the Warren Creek Formation form a broad, central, ductile shear zone in the map area which is bounded by competent and rheologically distinct siliciclastic rocks of the Lower Member to the north, and basalt of the Joe Pond Formation to the south. Shearing is most intense along the contacts with these competent units, and it is possible that some of these shear zones, in particular the east-west trending shear which defines the basalt-shale contact north of Heart Pond, and the complexly sheared basalt-shale contact south of Dragon Pond, represent ancient growth faults along the

contacts of the younger Joe Pond Formation. Primary structures in the ductile shales are often totally masked by shearing which accompanied D_1 layer shortening, while primary structures within silt, chert, and dolostone interbeds are often preserved, since these materials deformed mainly by buckle shortening (Fig. 2.31, pg. 51).

2.3.2 D_2

D_2 folds (F_2) deform S_1 and isoclinal F_1 axes. D_2 folds vary from open asymmetric folds to tight crenulations (Fig. 2.32) with amplitudes generally less than 1 m. These folds trend $194^\circ/82^\circ$ to $187^\circ/60^\circ$, and are developed best in the shales of the Upper Member.

2.3.3 D_3

Open warping, possibly indicative of a D_3 stress, was observed locally. This deformation is not associated with a penetrative "S" fabric and may represent passive folding which developed during the deposition or unloading of the Bruce River Group.

2.3.4 Summary

D_1 and D_2 strain fabrics in the the Morán Lake Group developed during the Makkovikian-Ketelidian orogeny ca. 1810-1790 Ma (Wardle et al., 1986) prior to the deposition of the Bruce River Group, since these fabrics



Fig. 2.32 D_2 crenulations in shale defined by folded D_1 slatey cleavage, Date Grid.

are not developed in the Bruce River Group. The structural fabric of the Bruce River Group was developed by deformation related to the Grenvillian Orogeny ca. 1000 Ma (Ryan, 1984; Wardle et al., 1986). There are no well developed Grenvillian structural fabrics in the Moran Lake Group, however a poor to moderately well developed fracture cleavage was observed in some outcrops of Archean basement, and in some of the more competent sandstones in the Warren Creek Formation.

2.4 Archean-Aphebian unconformity

Laminated sandstone and siltstone of the Lower Member of the Warren Creek Formation unconformably overly Archean basement granitoids. The unconformity is exposed at four locations in the eastern map area (Fig. 2.33):

1. Along Warren Creek, dark green-grey silty shale is in contact with buff, massive, limonitic granite (Fig. 2.34). The siltstone grades into calcareous siltstone and dolostone which attain a maximum thickness of 40 m. The calcareous sedimentary rocks are overlain by 20 m of thickly bedded grey quartz arenite, which is overlain by fissile black shale.
2. The unconformity is well exposed along the southern shore of Moon Pond. Leucocratic, carbonatized, and fractured Archean granitoid material is in contact with 2 m of massive grey quartz arenite, overlain by 5 to 10 m

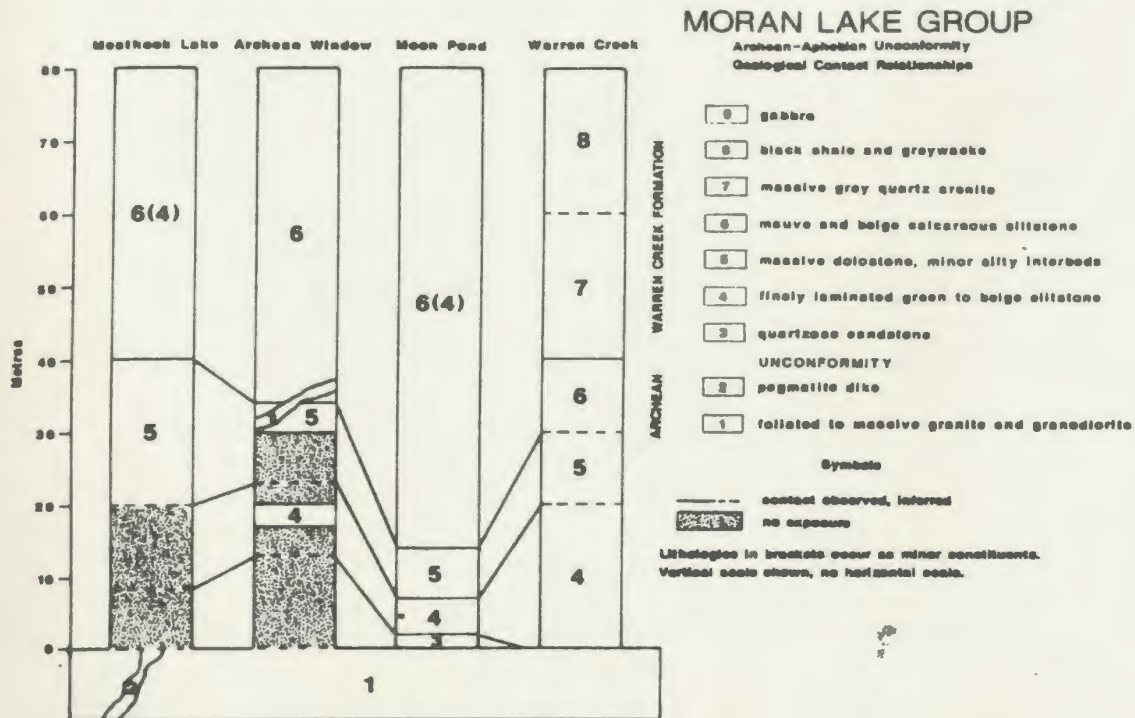


Figure 2.33 Stratigraphy of the Archean-Aphebian unconformity.



Fig. 2.34 Green siltstone (dark) overlying massive granitoid (light), Warren Creek.

of dark green to grey siltstone and chert, and 3 to 7 m of laminated brown silty dolostone and calcareous siltstone. A regolith is developed in the underlying Archean intrusive which is characterized by carbonatized, limonitic feldspars, and rare secondary carbonate-sulphide mineralization in fractures. The regolith penetrates the basement rock for 1 m.

3. Four hundred metres south of Meathook Lake, 20 m of exposure gap intervene between red calcareous slate, siltstone, and brown dolostone, and Archean basement granitoids. The contact is interpreted to be a depositional unconformity. In this area, the Archean granitoids are crosscut by abundant pegmatite dikes and veins which were never observed in the overlying Moran Lake Group.

4. A window of Archean basement is exposed in the Warren Creek valley in the eastern map area. Hansuld's (1958) geology map shows the Archean-Aphebian unconformity at this location, however, in 1986 it was discovered that this exposure of granitoid rocks was simply exhumed basement exposed by erosion along Warren Creek. Seventeen m of exposure gap intervene between the window of granitoid rock, and an outcrop of finely laminated green to beige siltstone. The siltstone is overlain by massive, brown, cross-bedded silty dolostone which crops out approximately 30 m south of the Archean window.

2.5 Aphebian-Helikian unconformity

The basal Brown Lake Formation conglomerate, of the Bruce River Group, is in unconformable contact with the Upper Member of the Warren Creek Formation, and Joe Pond Formation. The angular nature of the unconformity was observed at a number of locations in the eastern map area. The unconformable relationship is established by:

1. The presence of highly deformed clasts of Moran Lake Group sedimentary rocks within the Brown Lake Formation conglomerate.
2. The angular bedding relationship between the ENE-WSW trending ironstone and quartz arenite in the Upper Member east of Zee Lake, which is in fault contact with the overlying northeast-southwest trending conglomerate of the Brown Lake Formation. In addition, the Bruce River Group was deposited over a large D_1 anticline in the Moran Lake Group north of Mushroom Pond, and does not, in any way, reflect the geometry of this early structure within its own stratigraphy.
3. The difference in average bedding attitude of the Moran Lake and Bruce River Groups. One can see at a glance from Figure 2.29 (pg. 49) the difference between the Moran Lake Group, which strikes 58° to 88° and dips steeply south below the gently tilted Bruce River Group which strikes 66° and dips 38° southeast.

2.6 Summary

The rocks of the Moran Lake Group record a marine "first transgression" over Archean granitoid crust under a dominantly tensional tectonic regime.

The fine siltstones, sandstones and calcareous siliciclastics of the Lower Member of the Warren Creek Formation were deposited in a nearshore, oxic environment, as evidenced by the abundance of red weathering sandstone beds, dolostone, and calcareous sandstone beds in this sequence. This sequence of rocks was deposited unconformably upon an Archean granitoid highland which is the source area for the authigenic detritus in the Moran Lake Group (see Chapter 3).

The black shales of the Upper Member of the Warren Creek Formation record a marine transgression over the Lower Member and the Archean basement. Detritus was still being derived from the Archean highland, but reducing conditions prevailed, and black carbonaceous shale and finely interbedded siltstone +/- calcareous siltstone, chert, and dolostone were deposited. Ubiquitous iron sulphide (pyrite) occurs in this shale sequence in contrast to dominantly iron oxide (hematite) in the Lower Member.

Uplift, and the deposition of a shallow water sequence of vesicular basalt flows, shale-lithic conglomerate, and the Arkose Bed, is preserved at the top of the Upper Member of the Warren Creek Formation prior to the deposition of

the non-vesicular pillowed Joe Pond Formation basalts in deep water.

Deformation (D_1 and D_2) and uplift during the Makkovikian-Ketilidian Orogeny (1810-1790 Ma) post-date the deposition of the sulphide-bearing horizons in the Moran Lake Group. These events were not associated with the mineralization (i.e. sulphide mineralization is not transgressive to the hosting sediments, and no significant concentrations of sulphides were structurally emplaced).

The basal Brown Lake Formation of the Bruce River Group was deposited on the uplifted Moran Lake Group in an alluvial fan-flood plain setting. This continental succession may have been deposited within fault-bounded intracontinental basins (Ryan, 1984). These rocks were deformed ca. 1000 Ma during the Grenvillian Orogeny.

CHAPTER 3
GEOCHEMISTRY

3.1 Archean Basement

Eight samples of Archean basement granitoid were submitted for whole rock chemical analysis (see Appendix 2). Sample A-15 was collected from the regolith south of Moon Pond therefore the data from this sample is not used in the chemical classification of the basement rocks (see discussion below). The normative mineral compositions of the rocks are listed in Table 3.1.

Texturally the rock varies from grey-buff granodiorite gneiss with alternating lamina of fine-grained biotite, quartz, and feldspar, and fine to medium-grained interlocking quartz and feldspar, to pink equigranular massive to weakly foliated granite and granodiorite. The rocks are frequently augen textured with well developed gneissic banding and disseminated elongate xenoblasts of ribbon quartz up to 5 mm X 20 mm. Coarse-grained pink pegmatite dikes were observed in these rocks south of Meathook Lake.

The compositions of the basement rocks are shown on Figure 3.1, based on O'Connor's (1965) normative feldspar plot. Most of the samples plot in the trondjemite field, except sample A-1 which plots in the granite field near the trondjemite boundary. Each of the samples were highly

Table 3.1 CIPW norm compositions of Archean basement

	A-1	A-2	A-4	A-5	A-6	A-14	A-18
Qtz	51.70	31.32	31.67	26.43	28.33	27.84	14.53
Corund	0.78	2.37	3.45	2.05	0.00	0.00	1.22
Or	14.36	9.22	14.01	13.59	8.63	8.63	8.22
Ab	28.68	44.00	34.27	37.06	38.75	42.47	36.80
An	1.72	3.51	5.24	8.08	6.79	11.09	12.33
Diop	0.00	0.00	0.00	0.00	9.20	0.39	0.00
Hypers	0.44	5.63	8.00	7.18	2.98	5.79	18.37
Mag	0.02	0.37	0.47	0.42	0.36	0.41	1.11
Ilm	0.00	0.76	0.84	0.76	0.23	0.61	1.44
Hydrap	0.02	0.17	0.33	0.24	0.07	0.17	0.78

total	97.73	97.34	98.28	95.80	95.33	97.39	95.35

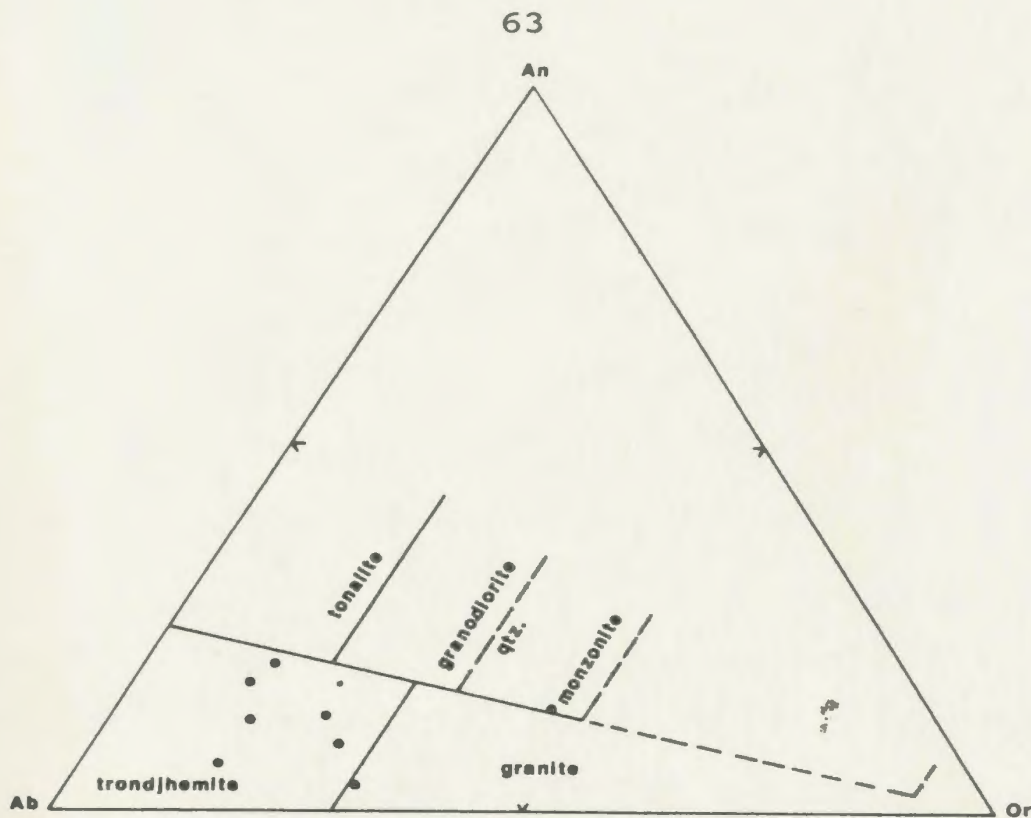


Fig. 3.1 Normative feldspar plot of Archean basement, Or = orthoclase, Ab = albite, An = anorthite, fields after O'Connor (1965).

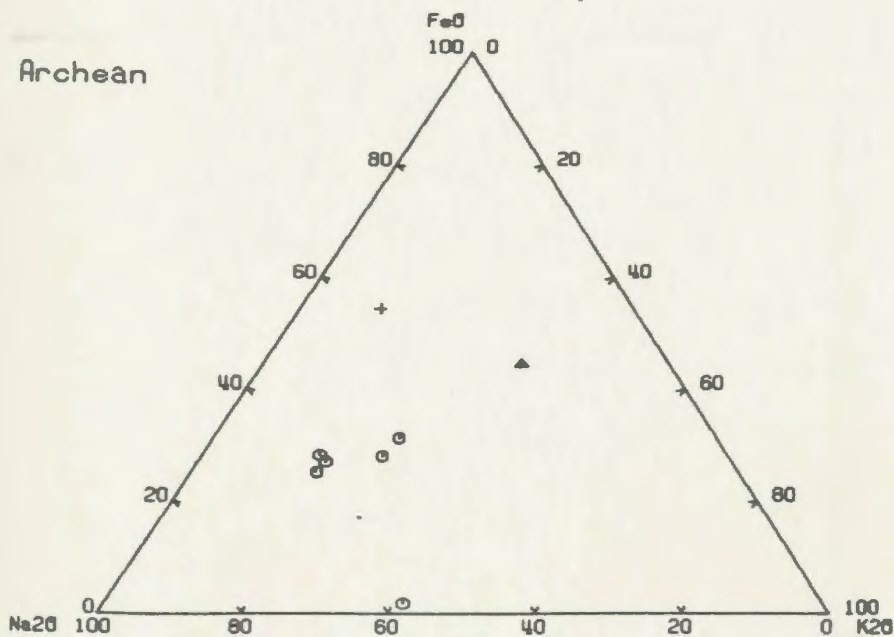


Fig. 3.2 Archean basement, sample A-18 (cross), A-15 (triangle, from regolith).

albite normative, and consistently contain 15 to 25 % normative Ab, with Na_2O contents commonly more than twice that of K_2O . Normative anorthite content of these rocks is generally less than 5 %.

The basement rock compositions are illustrated on the ternary plot of $\text{FeO}-\text{Na}_2\text{O}-\text{K}_2\text{O}$ (Fig. 3.2, pg. 63). Sample A-18, which was collected near the Archean-Aphebian unconformity north of Lupus Lake, is particularly iron-rich relative to the other samples, due to the fact that it contains 20-25% biotite. Sample A-1, which contains almost no biotite, plots along the $\text{Na}_2\text{O}-\text{K}_2\text{O}$ axis.

Sample A-15 was collected from highly fissile, carbonatized saprolite directly below the basal unit of the Moran Lake Group. The rock is slightly depleted in Al_2O_3 relative to the unaltered granitoids, and is highly orthoclase normative with 7.26 mole % Or. Normative albite is relatively decreased with respect to unaltered basement with 6.35 mole % Ab. Quartz content of the granitoid was not significantly affected, but regolith development caused a significant enrichment in FeO and depletion in Na_2O . A 1 cm pyrite/galena-bearing carbonate vein was observed in a fracture in the regolith at this location. Quantitatively, this does not represent a significant Pb discovery, however the style of mineralization is similar to the epigenetic quartz-barite-sulphide veins at the Ellingwood showing near Moran

1 Lake. These showings also occur near the Aphebian-Archean unconformity, and are thought to have been formed by the remobilization of base metals from the Archean basement during the Grenville Orogeny (Wilton, 1986).

3.2 Warren Creek Formation

3.2.1 Upper Member

The geochemical compositions of the Upper and Lower Members of the Warren Creek Formation are similar. Since many more samples of Upper Member rocks were analyzed, these rocks are described first, and the Lower Member will be compared with them in Section 3.2.2.

The Upper Member consists of a monotonous sequence of poorly sorted black shale and grey siltstone which are locally intercalated with narrow beds of dolostone and massive sulphide horizons. As previously described, pyrite is a ubiquitous constituent of the shales and in some cases is associated with significant enrichments in Cu, and Zn. The shale sequence can be broken down into three data sets viz.: typical (shale +/- graphite, pyrite, and siltstone), showings (>300 ppm Zn; or >70 ppm Cu; or >5% iron sulphides), and the Teuva showing. The typical shale and showings data sets are not mutually exclusive, and have similar geochemical characteristics, however the Teuva Showing samples are geochemically exotic in many ways with

respect to the first two data sets.

3.2.1.1 Typical shale, showings, Teuva showing

The typical (i.e. background) shale and showings geochemical data (Appendix 2) were derived from rocks deposited in a marine shelf environment above a thick unit (the Lower Member) of feldspathic siltstone, arkose, dolostone +/- shale. These titaniferous sedimentary rocks were undoubtedly derived in part from the underlying siliciclastic Lower Member, and ultimately from the Archean basement, with the addition of a significant allogenic organic (carbon) component.

The geochemistry and detrital mineralogy of the shales reflect the composition of the Archean basement in a number of ways. Firstly, monazite $((\text{Ce}, \text{La}, \text{Th})\text{PO}_4$, or $(\text{Ce}, \text{La}, \text{Nd}, \text{Pr})\text{PO}_4$) which occurs as a common accessory mineral in the basement trondjemite, was commonly observed as a detrital component of the shales (Figs. 3.3, 3.4).

Aluminium (as clays), zirconium (in zircon), and titanium (in ilmenite, rutile, anatase, pseudobrookite) would comprise significant detrital components in sediments derived from a granitoid source area (Vine and Tortelot, 1970), and anatase and rutile were observed as authigenic detritus in the shale sequence (Figs. 3.5, 3.6). Anatase was also observed in the basement rock (see Section 2.2.1). The morphology of some titanium-bearing minerals in the

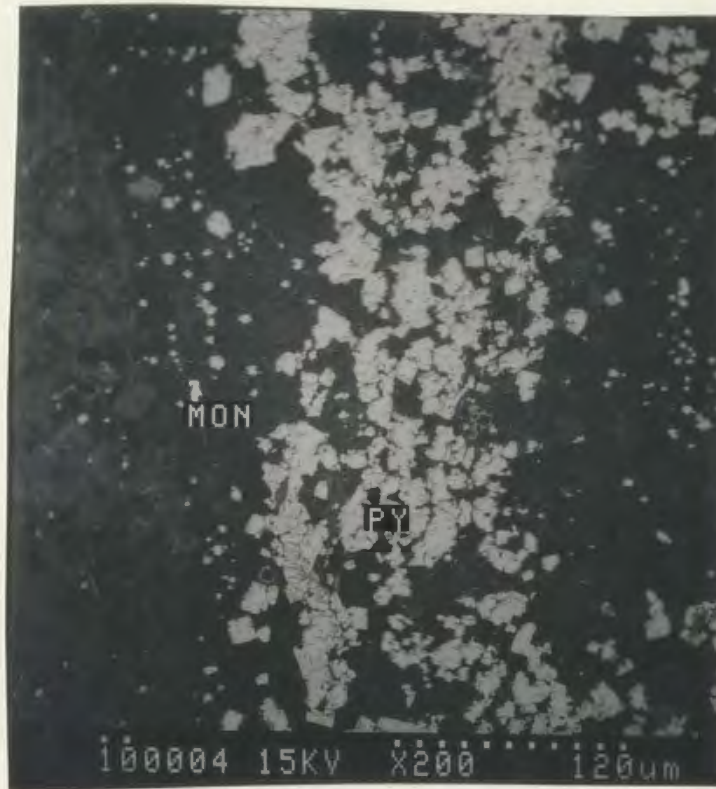


Fig. 3.3 Detrital monazite (mon) in pyritic shale, Date Grid, note finely bedded nature of pyrite (py).



Fig. 3.4 Monazite (white) enclosed in pyrite grain, Date Grid, possibly diagenetic pyrite formation.

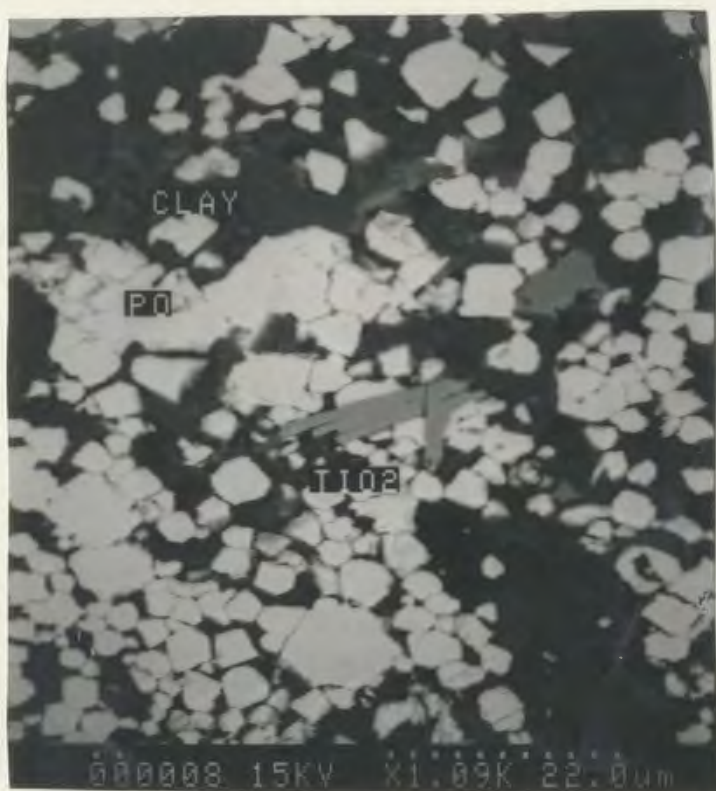


Fig. 3.5 Detrital rutile needle (TiO_2) in pyrrhotite-rich (po) shale bed, Three Ponds showing.

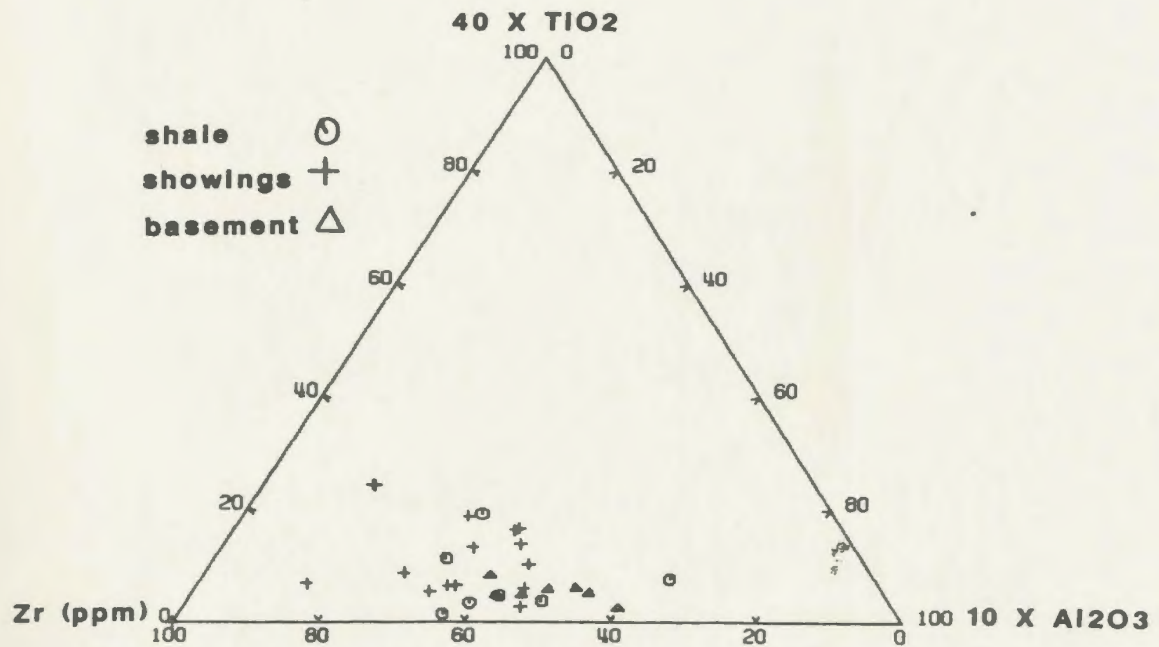


Fig. 3.6 TiO_2 (anatase) rim (light grey) on black detrital qtz. grain in centre of photograph.

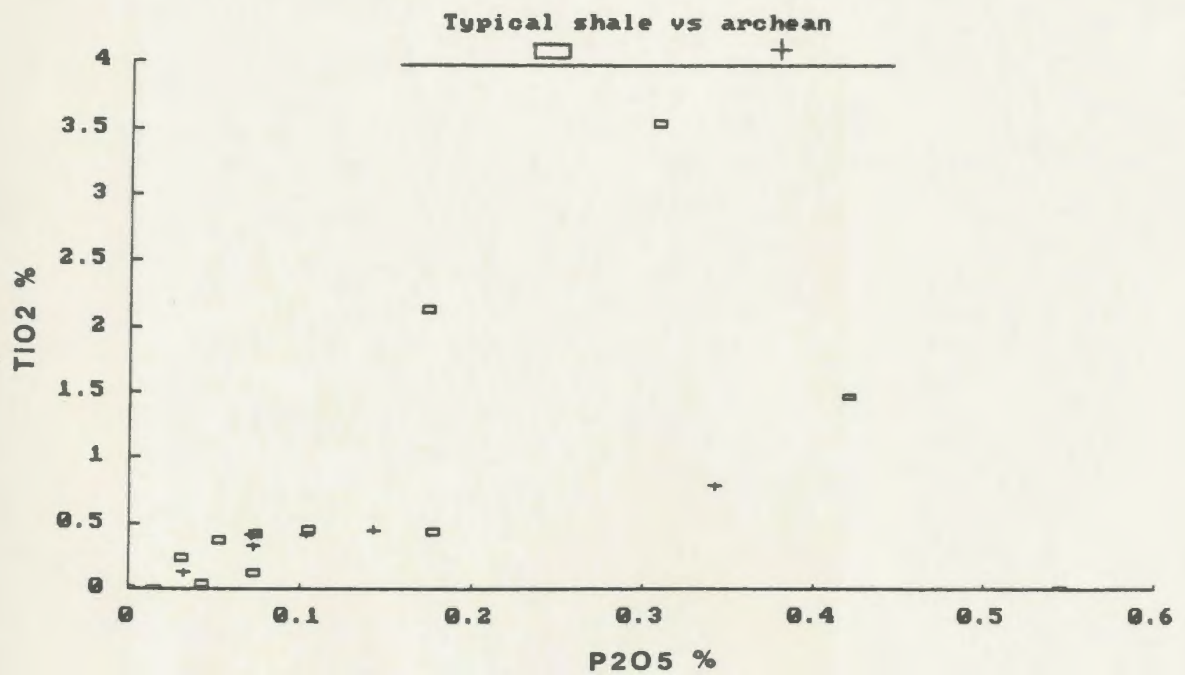
shale samples; ameboid overgrowths on detrital quartz, and amorphous flames intergrown with paticulate detrital mineralogy, suggest that diagenetic recrystallization of some minerals has occurred.

The ternary $\text{TiO}_2\text{-Al}_2\text{O}_3\text{-Zr}$ plot indicates similarities in the ratios of these components for detritus and basement rocks (Fig. 3.7a). There is an enrichment in zirconium and depletion of aluminium in the showings and typical shales data with respect to the basement. This is probably due to the winnowing out of aluminous clays from the sediments prior to lithification, but overall the data for each of the sets are most closely grouped midway along the $\text{Al}_2\text{O}_3\text{-Zr}$ boundary.

TiO_2 vs P_2O_5 for typical shale and Archean basement are plotted on Figure 3.7b. Since TiO_2 is established as a detrital component of the shales which is derived from the basement, it was plotted against P_2O_5 or monazite, (since no other phosphorous-bearing phase has been recognized in the sedimentary rocks) to establish whether the Archean basement is the source of this mineral in the shale. The data group together rather closely, again indicating that detrital monazite from the basement trondjhemite is the source of P_2O_5 in the shale, and further implicating Archean basement rocks as the donor for the bulk chemistry of the shale sequence. There is a slight increase in TiO_2 in some of the samples, again suggesting that some



(a)



(b)

Fig. 3.7 Comparison of resistate mineral chemistry, TiO_2 and Zr (a), and P_2O_5 (b), for basement and detritus.

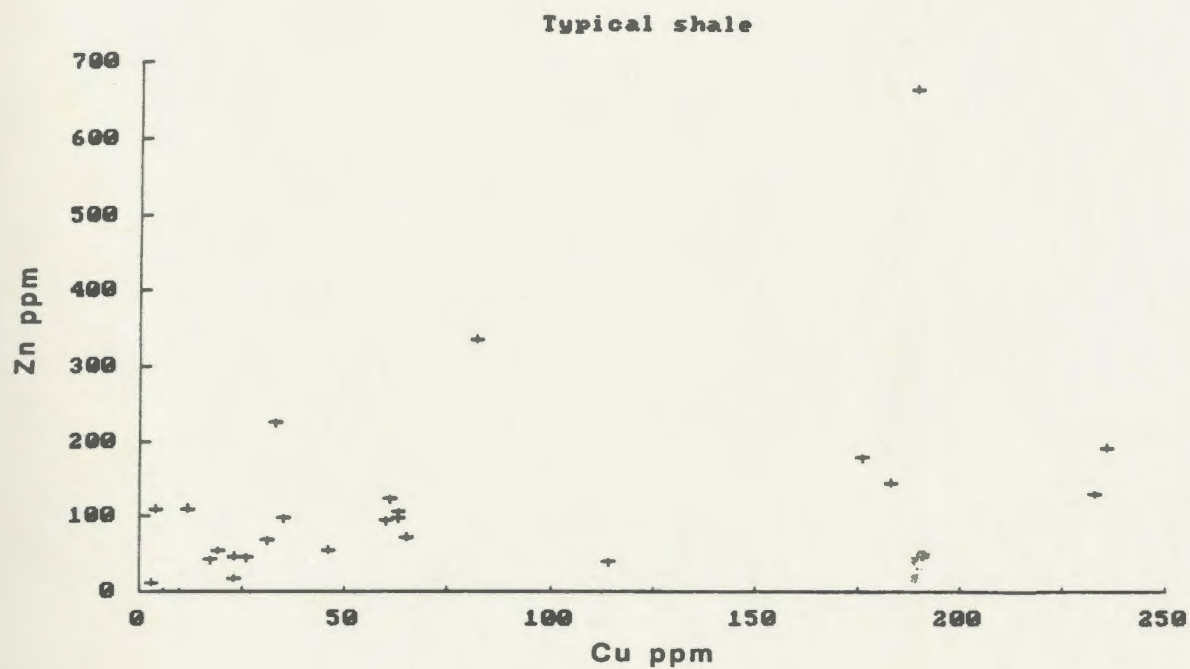
of the heavier Ti-bearing minerals were concentrated by winnowing.

Since base metal concentrations may be economically significant in the Moran Lake Group shales, several variation diagrams were constructed comparing base metal abundances with each other, and with abundances of selected elements typically associated with gangue minerals in sedex deposits.

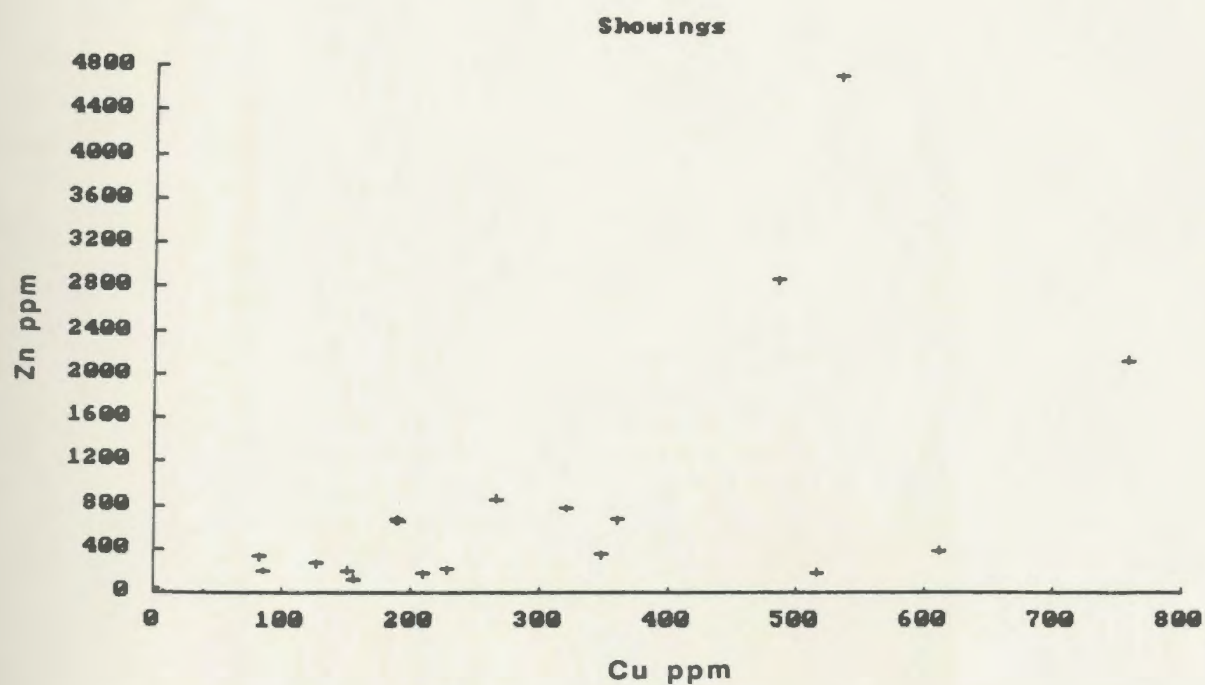
The shales contain a wide range of Cu (0-250 ppm) and Zn (0-300 ppm). When plotted against each other, there is a weak positive correlation between Zn and Cu, but Zn contents are generally lower than Cu (Fig. 3.8a). Zn vs Cu for the showings data (Fig. 3.8b) indicates a similar trend to that of typical shale, however Zn is much more abundant (0-4700 ppm) than Cu (0-700 ppm).

Pb concentrations are low in typical shale and showings, (2-26 ppm and 0-70 ppm respectively) and do not correlate with Cu or Zn (Fig. 3.9, 3.10). This is probably due in part to the paucity of lead in the sedimentary rocks and underlying basement granitoid (see discussion below).

A small lead occurrence was discovered in the field, however the mineralization is unrelated to the stratiform sulphide beds. The occurrence consists of a 1 to 5 cm wide discordant galena-bearing carbonate vein which filled an irregular fracture in massive white quartzite. The geochemistry of this showing was not investigated, however



(a)



(b)

Fig. 3.8 Zn vs Cu variation diagram for typical shales (a), and showings (b).

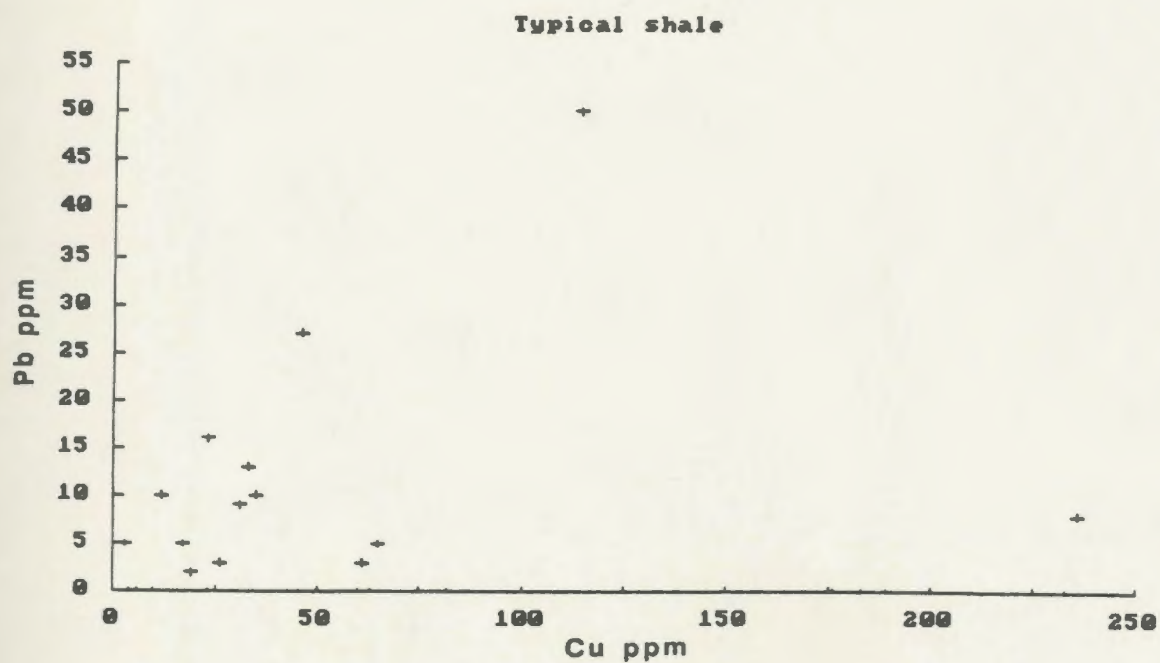
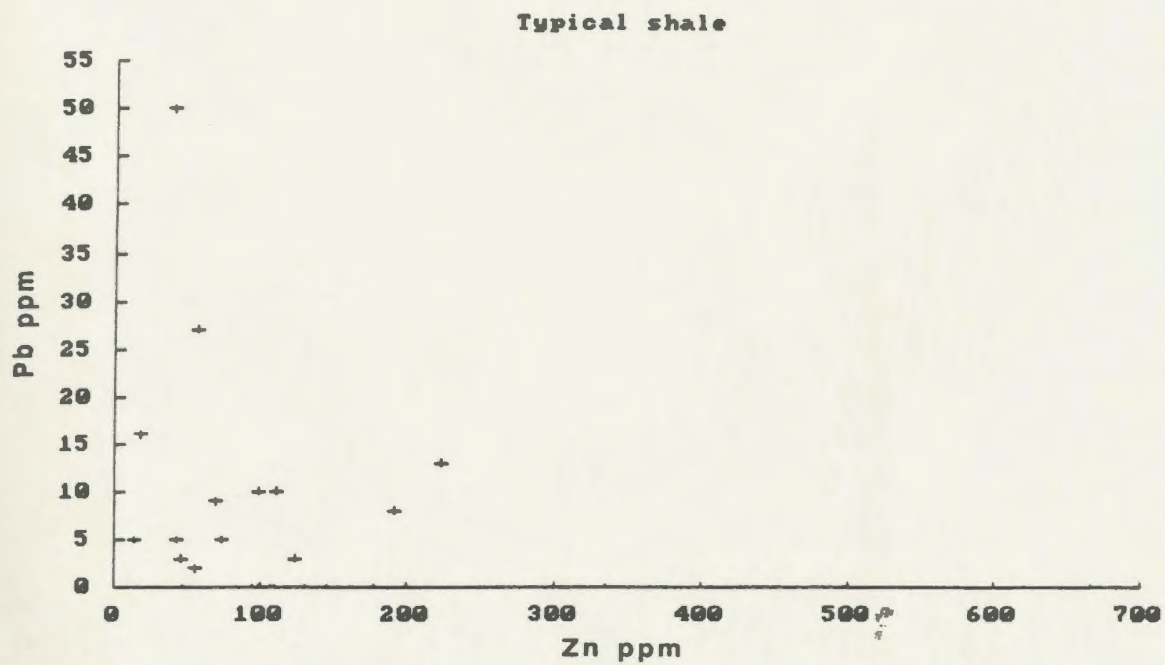


Fig. 3.9 Pb vs Zn, and Pb vs Cu variation diagrams for typical shale.

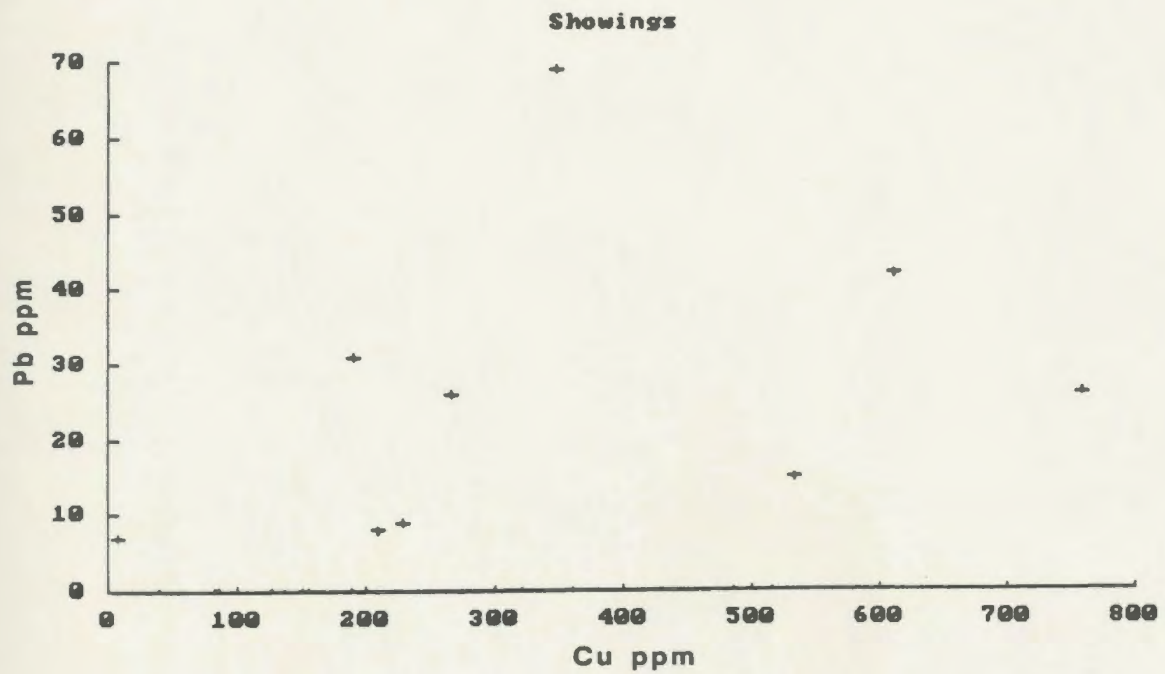
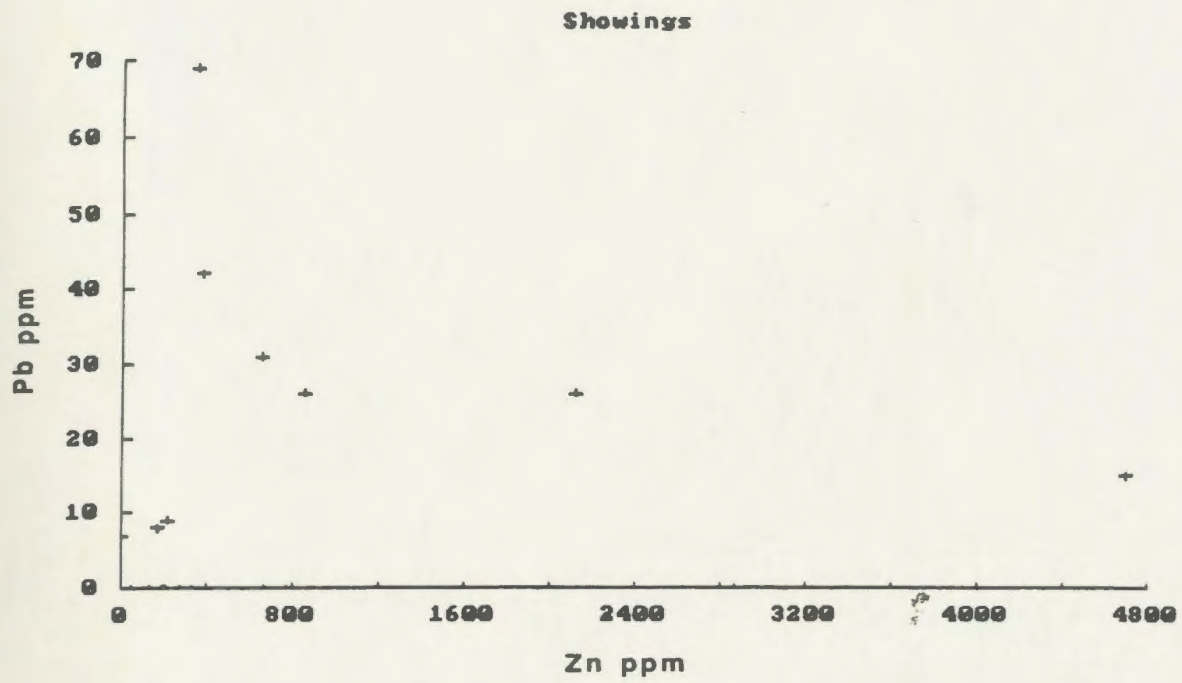


Fig. 3.10 Pb vs Zn, and Pb vs Cu variation diagrams for showings.

the style of mineralization is reminiscent of the base metal-bearing veins in the Warren Creek Formation at the Ellingwood showing which are thought to have formed from the remobilization of metals from Archean basement during the Grenvillian Orogeny (Wilton, 1986).

Ba is frequently enriched in sedimentary exhalative mineral deposits, and may occur as a hydrothermal gangue mineral which increases in abundance laterally away from the core or vent area of the typical sedex deposit (Lydon, 1983; Large, 1983), or may increase vertically within an ore zone such as in the Rammelsberg deposit (Large, 1983).

Ba was plotted against Cu, Pb, and Zn for typical shale (Fig. 3.11) and showings (Fig. 3.12). In each of these plots Ba varies over a wide range of values (approximately 0 to 1500 ppm), without a significant correlation with base metal values in either data set. Hence, barium is not related to base metal concentration.

Ternary plots of base metal (Pb-Zn-Cu) ratios for typical shale, showings, and Archean basement are similar (Fig. 3.13). The absolute base metal content of these rocks is discussed in Chapter 4. In each of the three data sets, the samples plot on, or very close to, the Cu-Zn axis, and favour the Zn apex. This is not surprising since the base metals in the shales, especially the "ambient" concentration of base metals in the typical unmineralized

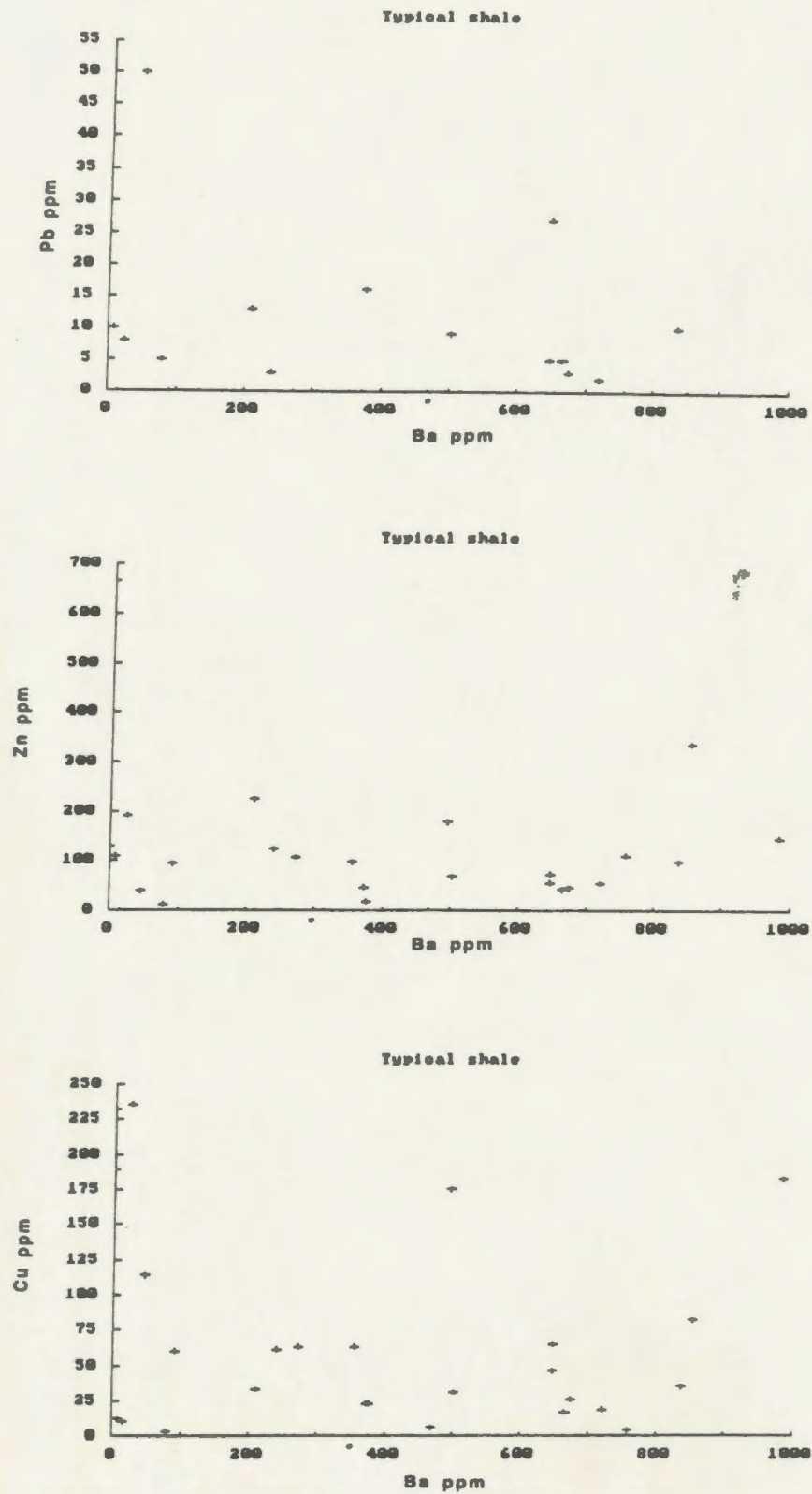


Fig. 3.11 Ba vs Pb, Zn, and Cu variation diagrams for typical shale.

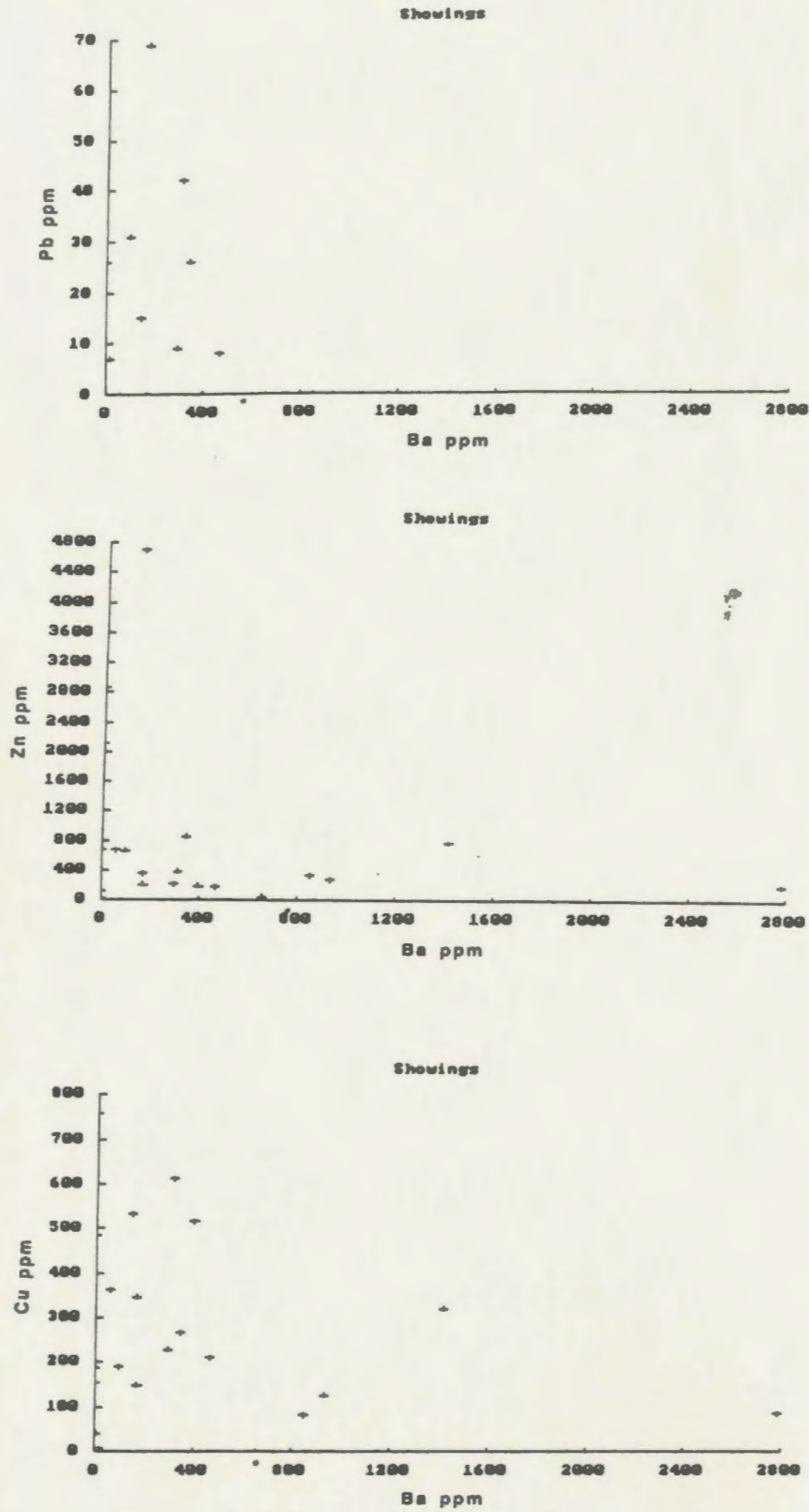


Fig. 3.12 Ba vs Pb, Zn, and Cu variation diagrams for showings.

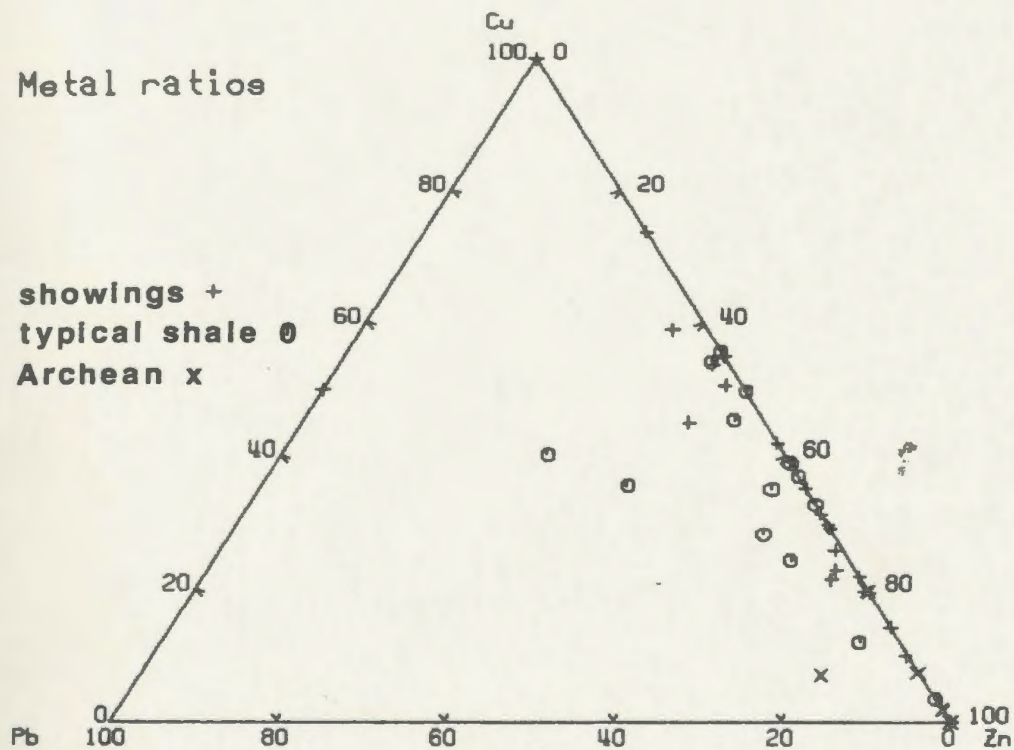


Fig. 3.13 Comparison of base metal ratios in basement, typical shale, and showings.

shales, would be derived from the parent Archean trondjhemite without intermediate concentration stages by convective brine circulation to produce anomalously enriched or depleted metal ratios. Oddly enough though, base metal ratios for the showings are almost identical to that of typical shales. Since these metals have different mobilities (Haak et al., 1984; Barrett and Anderson, 1982), and were probably deposited as sulphides from sea water (Lydon, 1983) subsequent to a stage of concentration from ambient basement abundances (and abundances of the underlying Lower Member and hosting Upper Member), this relationship was not expected. A partial explanation for the similarity in showings base metal ratios to that of typical shale and Archean basement is the lack of complexity due to Pb participation in the base metal content of these sediments. This is due to the paucity of lead and uranium (hence low radiogenic lead donation from the basement) in the Archean source area (Appendix 2).

In addition to detrital source area, the geochemistry of these rocks would be affected by hydrologic and diagenetic conditions within the basin of deposition. These conditions were the subject of studies by Bonatti (1975), Robertson and Boyle, (1983), and to some extent Vine and Tortelot (1970).

Bonatti's (1975) ternary plot of $(\text{Ni}+\text{Co}+\text{Cu})\times 10$ vs Fe/Mn distinguishes hydrogenous (slow precipitation of metals

from sea water wherein the metals are derived primarily from terrigenous material) pelagic sediments from spreading centre "hydrothermal" ferromanganese sediments which contain anomalous enrichments of transition metals and are very highly enriched in Mn and Fe. Figure 3.14 illustrates the fields for Upper Member typical shales, showings, the Teuva showing, and the established fields for hydrologic and hydrothermal pelagic sediments. Each of the data sets from the Warren Creek Formation plot close to the Fe apex, indicating that they are affiliated with a hydrothermal enrichment trend, and contain almost no manganese, thus these sediments do not have any affinities with mid-ocean spreading centres. The typical shale data are the least enriched in Fe, because these samples contained much less sulphide than the showings and Teuva samples. However, all of these samples still plot on the Fe-rich side of Red Sea sediments which are metalliferous hydrothermal sediments associated with an active spreading centre, and which were deposited in restricted, stagnant, brine pools (hence no Fe/Mn fractionation by quick precipitation of Fe into oxygenated water (ibid.)), and also no Cu/Zn fractionation since all of the sulphides in solution would be precipitated under restricted conditions). Thus, since the sediments of the Warren Creek Formation are intrinsically Mn-poor and show an extreme Fe enrichment, they have a strong affinity with massive sulphide deposits.

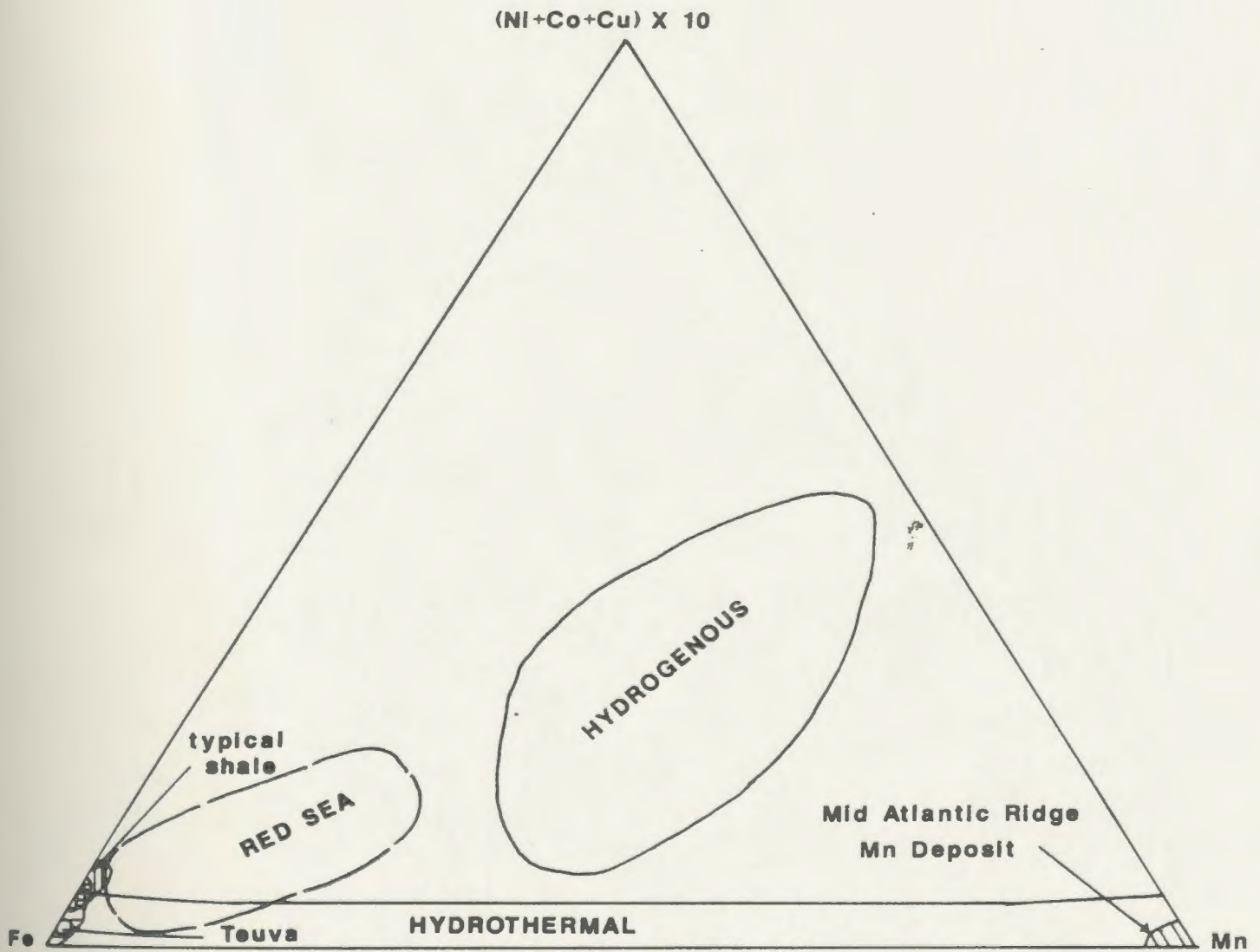


Fig. 3.14 Established fields for hydrothermal and hydrogenous pelagic sediments from Bonatti (1975). The field for showings (vertical bars) is a small field within the larger typical shale field.

Bonatti (1975) also used a very simple and practical plot of SiO_2 vs Al_2O_3 to distinguish hydrogenous from hydrothermal pelagic sediments. Figure 3.15 shows the fields for hydrogenous and hydrothermal pelagic sediments, and the fields for Upper Member typical shale, showings, and the Teuva showing. Silica is abundant in hydrothermal solutions and will be enriched in hydrothermal sediments relative to Al_2O_3 which is deposited as fine detritus. The silica content of data sets from the Upper Member are slightly enriched in SiO_2 relative to Al_2O_3 , and plot within, and slightly more SiO_2 -rich than, the field for hydrogenous sediments.

Robertson and Boyle (1983) classify metalliferous marine sediments on the basis of Al versus Mn/Fe. Again hydrothermal pelagic sediments are extremely enriched in Fe and Mn and depleted in Al and thus, are easily distinguished from typical aluminous pelagic sediments (Fig. 3.16). The Upper Member typical shales, showings, and Teuva showing plot along the Al-Fe axis of this ternary diagram in the vicinity of modern Pacific (hydrogenous) pelagic sediments. The pyritiferous showings obviously plot closer to the Fe apex.

The fields for typical shale and showings are shown on ternary base metal plots, and compared with the data from Lydon (1983; Fig. 3.17). Lydon compiled data from

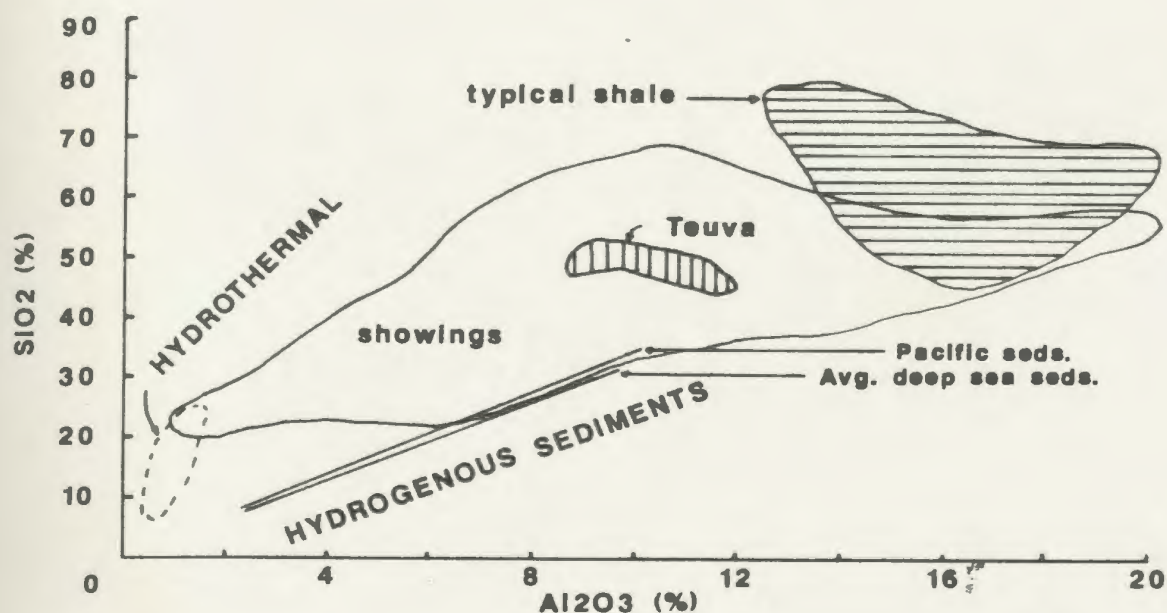


Fig. 3.15 Established fields for hydrogenous and Hydrothermal sediments from Bonatti (1975). Pacific seds. from Landergren (1964), avg. deep sea seds. from Turekian and Wedopohl (1961).

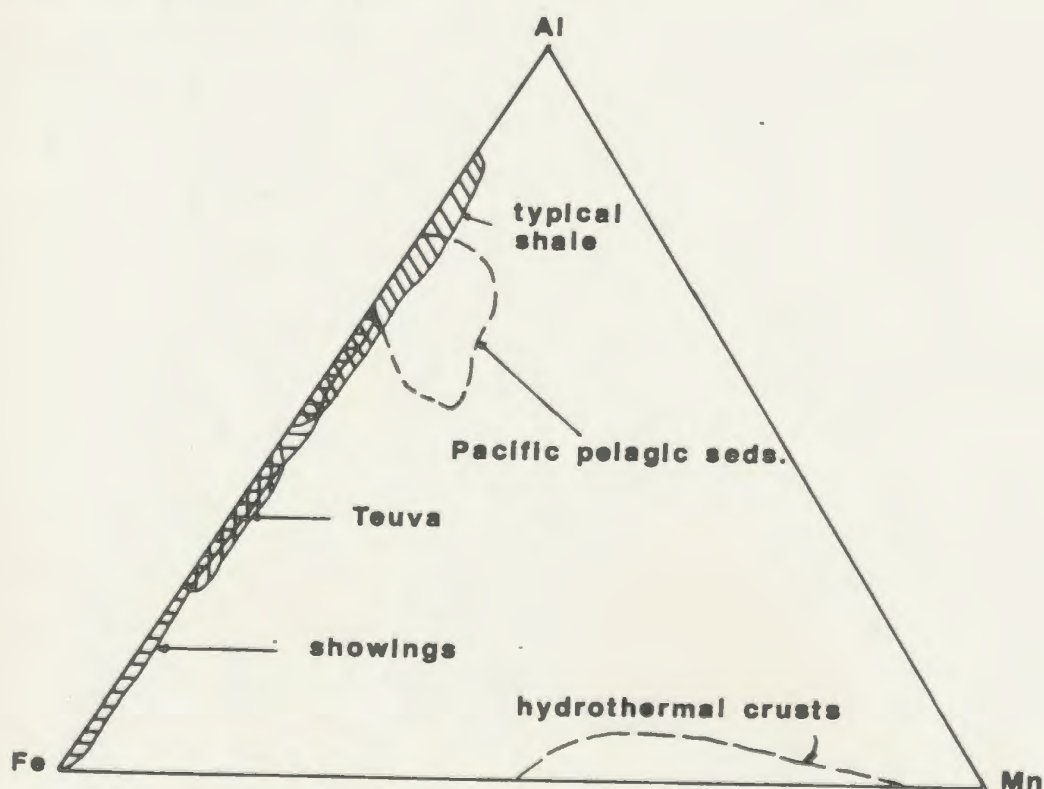


Fig. 3.16 Established fields for pelagic sediments from Robertson and Boyle (1983).

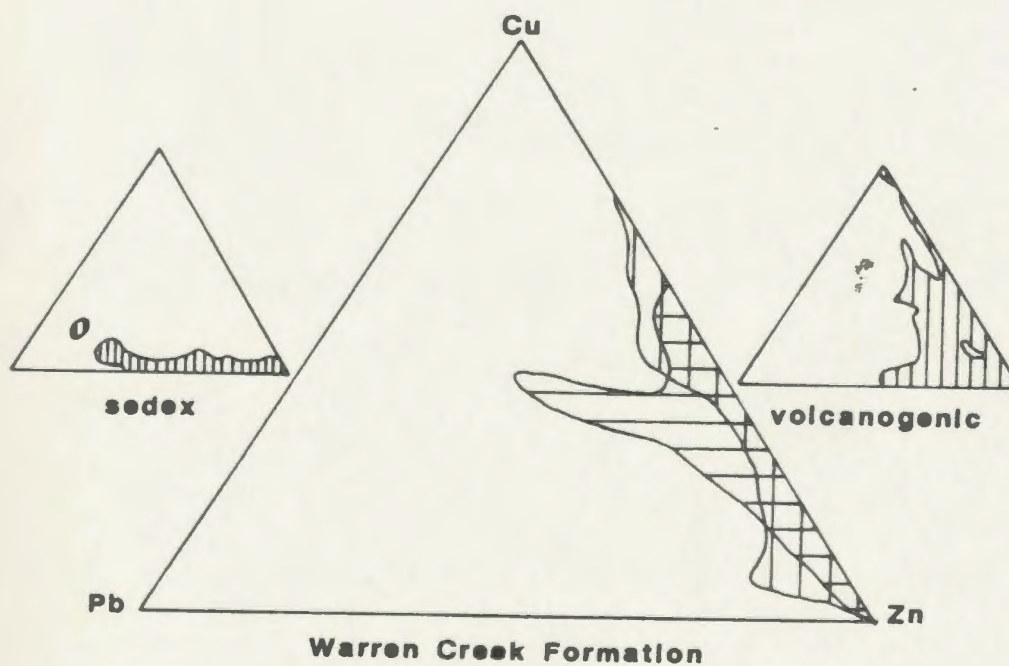


Fig. 3.17 Comparison of base metal ratios in Upper Member shales (horizontal bars) and showings (vertical bars), with established fields for sedex and volcanogenic base metal massive deposits worldwide, from Lydon (1983).

38 Proterozoic and Phanerozoic sedex Pb-Zn deposits, and compared their metal ratios with Archean and Phanerozoic volcanogenic massive sulphide orebodies. The ternary plots for sedex Pb-Zn deposits have lower Cu/Pb+Zn ratios than the volcanogenic massive sulphides, and an even distribution of Zn/Pb ratios distributed near the Zn apex along the Zn-Pb axis. When the three data sets from the Warren Creek Formation are compared with this data, the Warren Creek Formation shows affinities with volcanogenic massive sulphide deposits, having much higher Cu/Zn+Pb ratios than average sedex Pb-Zn deposits. The field for the Teuva showing was not plotted, these rocks plot on the Zn apex of the diagram.

To summarize, these plots indicate that these rocks are affiliated with a massive sulphide deposit iron-enrichment trend (Bonatti, 1975) which is similar to that of volcanogenic massive sulphide deposits (Lydon, 1983) and that these sediments were not deposited near a mid-ocean spreading centre, since these types of deposits are typically manganiferous (Scott et al., 1974; Fehn, 1986, Bonatti, 1975; Robertson and Boyle, 1983;).

Trace element abundances of typical Warren Creek Formation shales, showings, and Archean basement trondjhemite are compared with "average shale" of Vine and Tortelot (1970) in Table 3.2. The mean composition of typical Warren Creek (W.C.) shale is very similar to

Table 3.2 Trace element abundances

Parts per million

V&T 1970 WC Shale Showings Archean

Cu	70	70	270	1.4
Pb	20	6	11	.7
Zn	<300	118	753	41
Cr	100	241	278	3.8
Ni	50	80	229	1.3
V	150	264	463	41
Sc	10	5	.86	N/A
Ba	300	397	433	650
Ga	20	17	10	14.6
Sr	200	83	47	174
Y	30	25	31	11
Zr	70	209	157	112

"average shale" of Vine and Tortelot with no significant element enrichments or depletions indicated (considering the wide variety of geologic environments from which this average was calculated). The transition metals Cu, Zn, Ni, Cr, and V are significantly enriched in the showings relative to typical Upper Member shale, Archean basement, and average shale of Vine and Tortelot (1970). These metals are considered to be enriched in the organic fraction of metalliferous shale (*ibid.*), and graphite is abundant in the Upper Member shales, suggesting an organic association for metal concentration.

3.2.1.2 Extended REE plots (spider diagrams)

Spider diagrams of Archean basement, typical shale, showings, and Teuva showing are illustrated in Figure 3.18. The data are normalized to primitive mantle (or bulk Earth, from values published in Taylor and McLennan, 1981, and Jenner *et al.*, 1987). The Archean basement spidergrams slope steeply downward to the right, and display a strong fractionation of light rare earth elements (LREE) from heavy rare earths (HREE), a feature characteristic of granitoid rocks (Arth, 1976). Two samples of typical Upper Member shale are plotted with the spidergram for the North American Shale Composite or NASC (Gromet *et al.*, 1984). The shape of the Upper Member spidergrams are similar to the NASC, but have lower overall Th, Nb, Ta, and total REE. The

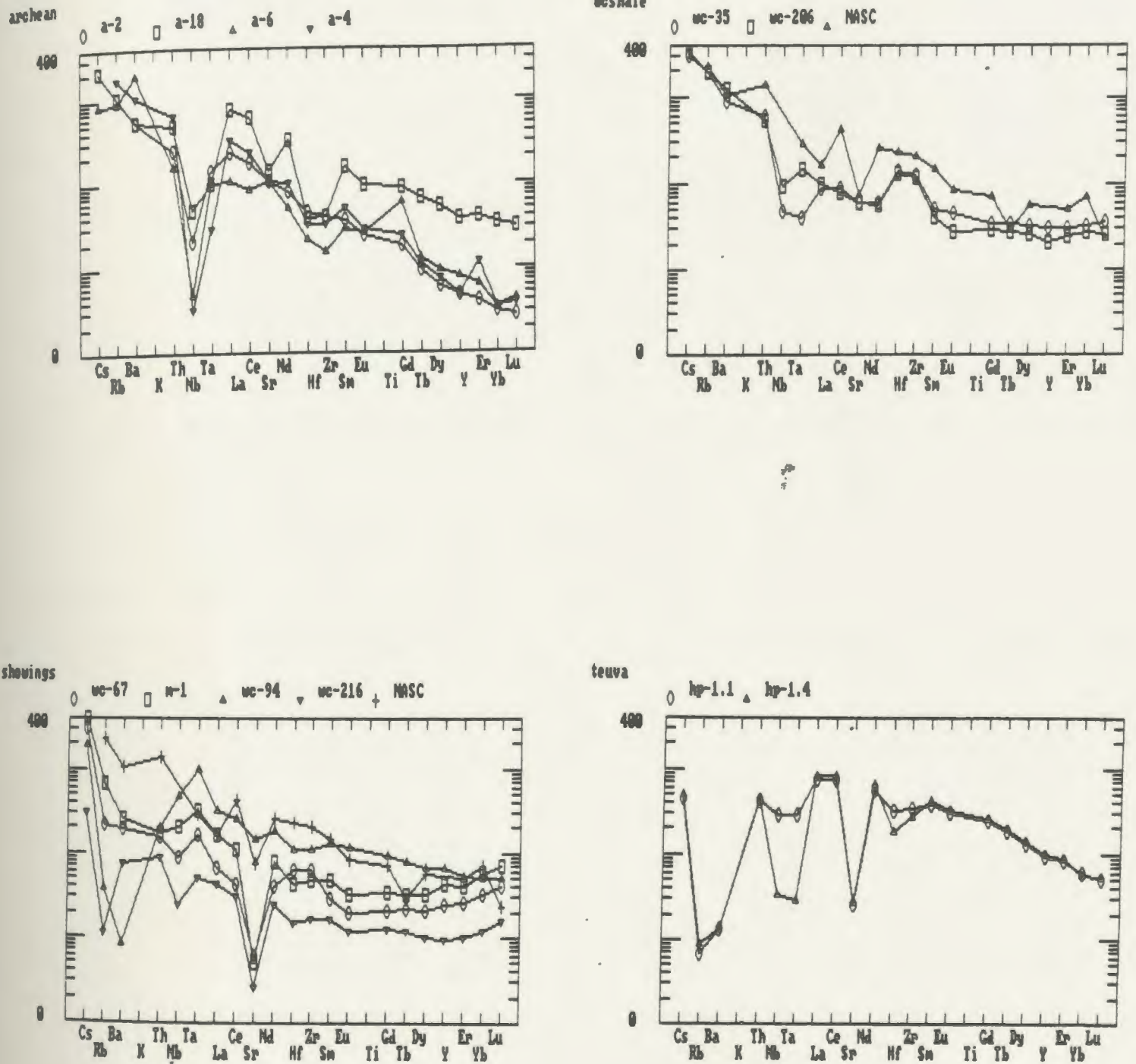


Fig. 3.18 Extended REE plots for Archean, typical shale (wchale), showings, and Teuva.

pattern of fractionated HREE from LREE is not as pronounced, in the Upper Member shales as it is in the detrital source area (Archean) spidergrams. This is probably due to the sedimentary process of averaging total REE from a source area with highly fractionated HREE, by the enrichment of HREE in detrital resistate minerals (Gromet et al., 1984; Wronkiewicz and Condie, 1987). Basement rocks and typical shale have an Nd depletion which the NASC does not exhibit, further elucidating their genetic link. The REE pattern for typical shales is slightly concave upward suggesting that a moderate degree of winnowing occurred prior to lithification which concentrated HREE in heavy detrital minerals. The positive Zr anomaly suggests that the HREE are contained in detrital zircon.


Spidergrams for four Upper Member massive sulphide beds have enriched Th, Nb, Ta, and contain 10 to 150 times as much REE as typical shale, however the shapes of the spidergrams are similar to that of the typical shales. The showings have a pronounced negative Sr anomaly, lower Ba and Rb, and lack the positive Zr anomaly present in typical shale suggesting that detrital zircon, and possibly Sr, Ba, Rb-bearing feldspars, were not concentrated by winnowing prior to lithification.

Bonatti (1975) states that hydrogenous sediments have total REE abundances that are commonly 10 to 100 times greater than hydrothermal sediments. Since REE in the Upper

Member showings are enriched at least this much above typical shale, contain negative Sr anomalies, and lack positive Zr anomalies (i.e. no winnowing) they are interpreted to have been deposited in a low energy environment by hydrogenous precipitation from seawater.

The showings spidergrams are similar to the NASC, but lack a positive Ce anomaly. Robertson (1981) and Bonatti (1975) state that hydrogenous manganiferous sediments usually have pronounced positive Ce anomalies which are caused by the precipitation of Ce into pelagic sediments as seawater Ce^{3+} is oxidized in surface waters to insoluble Ce^{4+} (*ibid.*). The lack of a positive Ce anomaly in the hydrogenous sulphide-rich showings of the Upper Member probably indicates that there was not abundant dissolved (reduced) Ce in these waters, or that excess oxidized sedimentary Ce was reduced by diagenetic reactions in the organic-rich sediments, and later expelled in pore waters, or lost by diffusion across the sediment-seawater interface.

The data from the two Teuva showing samples is very difficult to interpret, since only subtle (fortuitous?) similarities exist between these, and the spider diagrams for Archean basement, and showings. The difficulties arise from the inability to differentiate between geochemical characteristics contributed to the rock by the authigenic detrital mineralogy (see Chapter 4.2.5), and chemistry



contributed, or removed, by the mineralizing fluids (this problem is obviated with typical shales and showings, since the gänge in the showings is basically typical shale). Therefore, the spidergrams for the Teuva showing will be compared with each of the three data sets, and the interpretation will be minimal.

The shape of the Teuva spidergrams are similar to that of Archean basement rocks however, there are significant negative Rb and Ba anomalies in the Teuva samples, and the total REE in the Teuva are approximately 50% greater than in the basement. An interesting common feature of these two diagrams is the small positive Ce and La anomalies. This may be due to the contribution of authigenic detrital monazite to the Teuva sediment which was derived from the basement.

The Teuva and showings spidergrams are very similar (low to strongly negative Ba, Rb, and Sr anomalies), but the Teuva contains greater total REE. This would be expected since the Teuva samples contain much less sulphide, and much more detrital silicate and/or oxide minerals which could contain REE. The coinciding negative Ba, Rb, and Sr anomalies result from the paucity of feldspars in the showings samples (see discussion above on winnowing) and lack of feldspars in the Teuva samples (Chapter 4.2.5).

The Teuva spidergrams do not share any common

characteristics with the typical shale spidergrams. Total REE are much higher in the Teuva showing, the typical shale does not have the negative Ba and Rb anomalies characteristic of the Teuva showing, and the typical shales do not have the pronounced inflection from a negative Sr to a positive La-Ce anomaly that the Teuva showing exhibits.

To summarize, the Teuva showing has common characteristics with the Archean basement and showings. The similarities in the shape of Teuva showing and Archean basement spidergrams arise from the sedimentary concentration of REE in resistant authigenic detritus which was derived from the basement. Total REE however, are greater in the Teuva showing. The negative Ba, Rb, and Sr anomalies in the Teuva showing are probably due to the diminution of Ba-Rb-Sr-bearing feldspars prior to deposition.

3.2.1.3 Summary

The geochemistry of Upper Member typical shale and showings reflects the composition of the Archean basement trondjhemite, implicating this as the source of detritus in the basin. Although transition metals are more abundant in the sulphide-rich showings, the Cu-Pb-Zn ratios are similar to those of typical Upper Member shale and Archean basement, indicating that no fractionation of base metals has occurred by any of the intermediate stages of metal

leaching, concentration, and deposition.

The iron-rich Warren Creek Formation sedimentary rocks do not have affinities with hydrothermal manganiferous pelagic sediments. This is not surprising, since these sediments were deposited by a marine transgression over granitoid basement in a marine shelf environment, and not upon ophiolite, near an oceanic spreading centre.

The sulphide-rich showings contain 10 to 150 times as much REE as typical shale, and lack any features suggesting that winnowing occurred prior to lithification, further suggesting that the depositional mechanism was hydrogenous precipitation from seawater.

The transition metals found to be enriched in Upper Member showings relative to typical Upper Member shale are those typically found in the organic fraction of "average shales" (Vine and Tortelot, 1970), suggesting that the depositional mechanism for base metals in the Moran Lake Group is due to biogenic activity under reducing conditions.

The paucity of Mn, and abundance of Fe in the typical shales, and the lack of Cu, Pb, Zn fractionation in the showings together support a massive sulphide affinity for the sulphide-bearing horizons in the Moran Lake Group. The lack of fractionation of base metals in the mineralized rock suggests that sulphide deposition occurred in restricted brine pools, where the metals Cu, and Zn, which

each have strong affinities for sulphur, were deposited rapidly from solution.

3.2.2 Lower Member

Three samples of the Lower Member siltstones were analyzed and the data (Appendix 2) indicate similarities with typical shales of the Upper Member, and thus, to the Archean basement trondjhemite. The relationships have similar features to those of the typical shale-basement relationship described previously, i.e. the detrital component of these rocks was derived from the Archean basement.

The samples each consist of finely interbedded, grey feldspathic, siltstone interdigitated with fine lamina of dark brown to black shale. Cu-Zn-Pb ratios (Fig. 3.19) plot well within the field of the typical shales (Fig. 3.17, pg. 84). The Lower Member plot of TiO_2 vs P_2O_5 (Fig. 3.20) illustrates the similarity of these ratios with the field for typical Upper Member shale. The $TiO_2-Al_2O_3-Zr$ plot (Fig. 3.21) shows that the data points occur within the field of data for typical shales (Fig. 3.7a, pg. 70).

In short, to summarize this small set of data, it is reasonable to suggest that the detritus that formed the Lower Member was derived from the basement rocks and was the first detritus in a continuum succeeded by the overlying Upper Member typical shales. (i.e. there

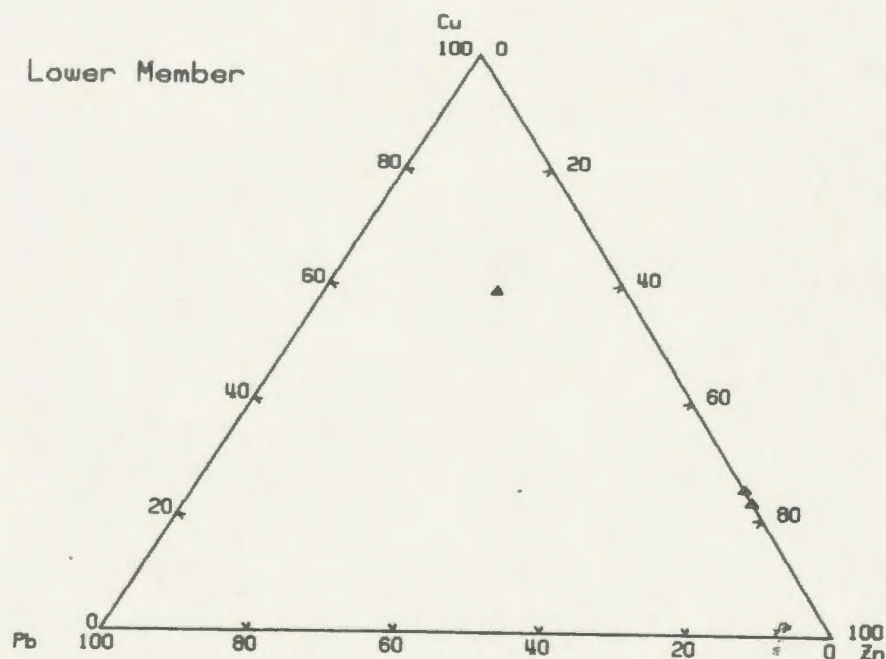


Fig. 3.19 Cu-Pb-Zn ratios in Lower Member siliciclastics.

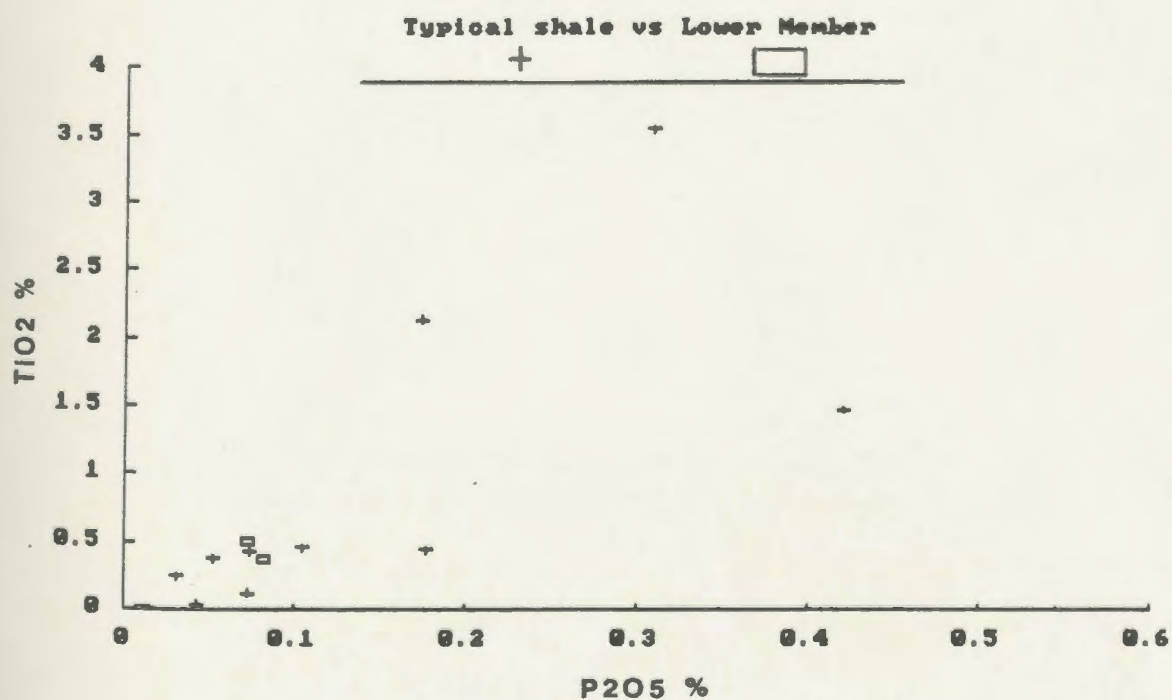


Fig. 3.20 Comparison of Lower and Upper Member TiO₂ vs P₂O₅.

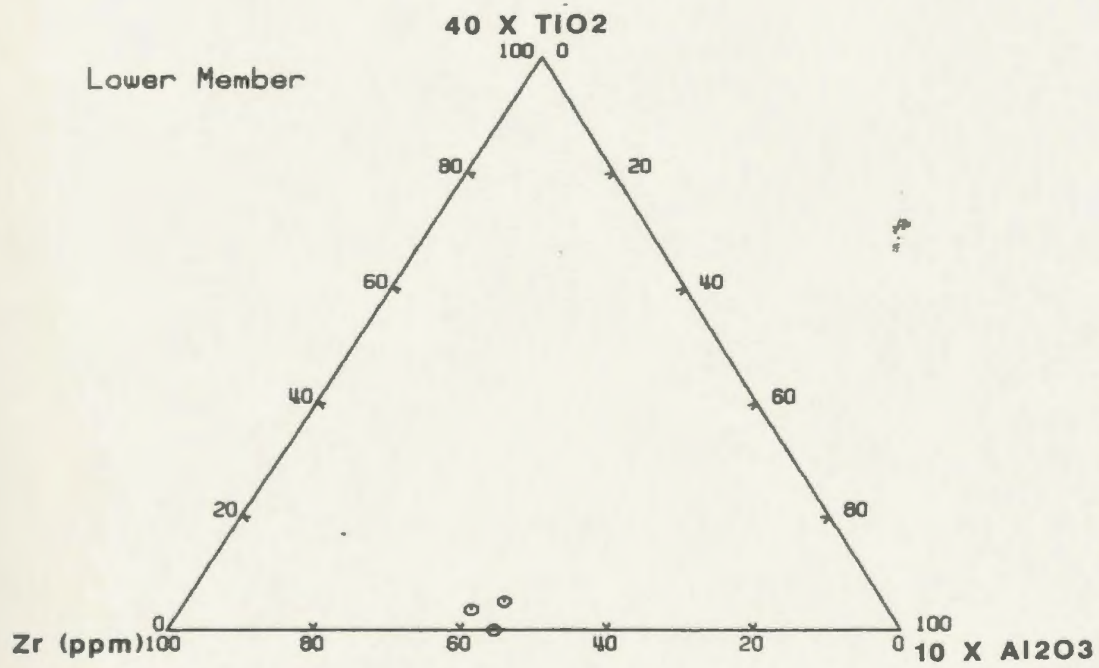


Fig. 3.21 Lower Member ratios of resistate mineral components (TiO_2 , Al_2O_3 , Zr).

is no geochemical evidence to suggest that this marine sequence is allochthonous with respect to the basement).

3.3 Basalt Geochemistry

3.3.1 Joe Pond Formation

Ryan (1984) classified the Joe Pond Formation basalts as having komatiitic affinities but being more closely analogous in chemical composition to olivine tholeiites (more CaO and MgO and less Al_2O_3 than average tholeiites but less TiO_2 than true olivine tholeiites).

The Joe Pond Formation basalts fall within the major subdivisions for subalkalic and tholeiitic rocks (Figs. 3.22, 3.23; after Irvine and Baragar, 1971) and are relatively MgO-rich. Sample WC-16 falls in the alkali-rich fields of both diagrams, which may reflect an increase in Na_2O by spilitization. These basalts are also TiO_2 -poor, and plot in the LKT-OFB field (Fig. 3.24; after Pearce and Cann, 1973). The Ti and Cr contents of these rocks are primitive relative to typical low K tholeiites, hence these data plot within the OFB field as well as the LKT field of Pearce's (1975) log Ti vs log Cr diagram (Fig. 3.25). On the $\text{Al}_2\text{O}_3/\text{TiO}_2$ vs TiO_2 plot (Fig. 3.26; after Sun and Nesbitt, 1978) most of the samples plot in the field for MORB, although four samples plotted in the very high Ti range (a possible explanation for the seemingly bimodal

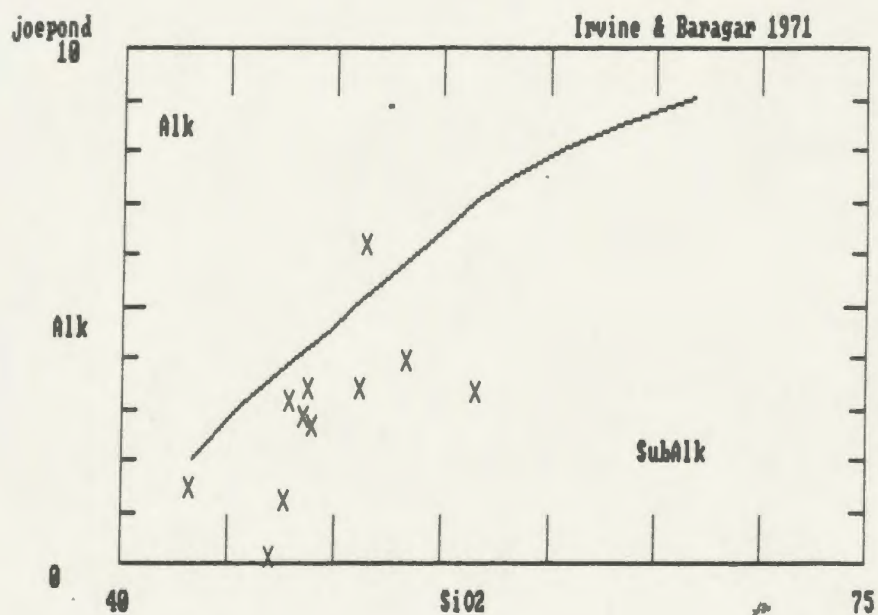


Fig. 3.22 Joe Pond Alk vs Subalk discrimination diagram.

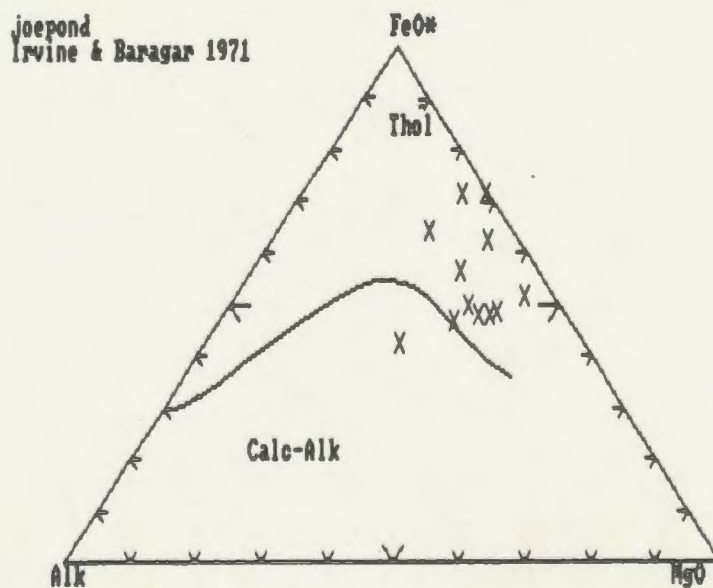


Fig. 3.23 Joe Pond tholeiitic vs calc-alkalic discrimination diagram.

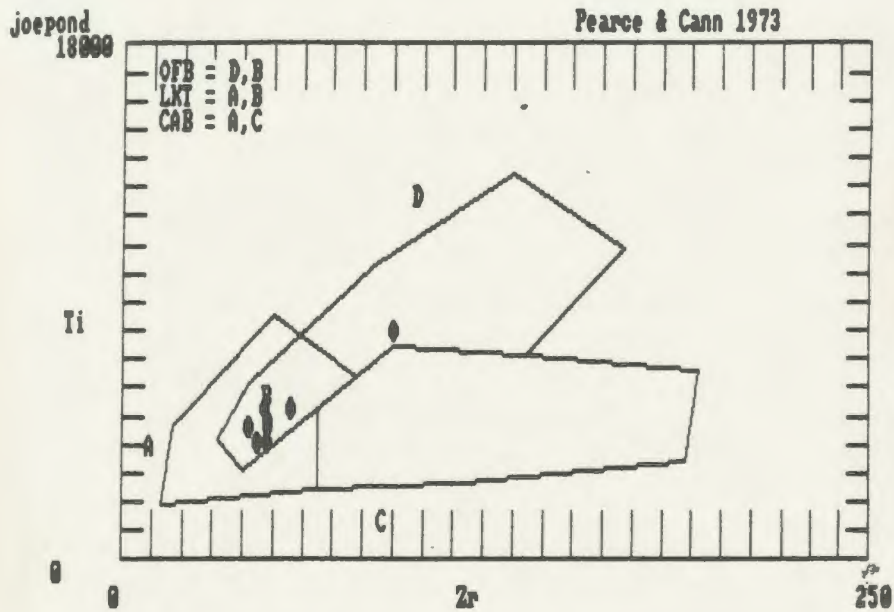


Fig. 3.24 Joe Pond OFB-LKT-CAB discrimination diagram.

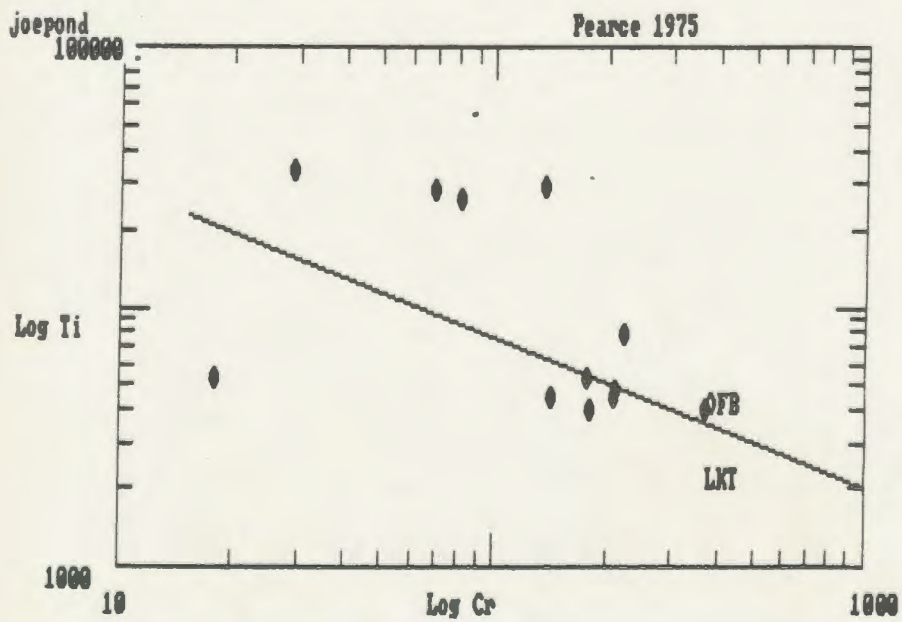


Fig. 3.25 Joe Pond OFB-LKT discrimination diagram.

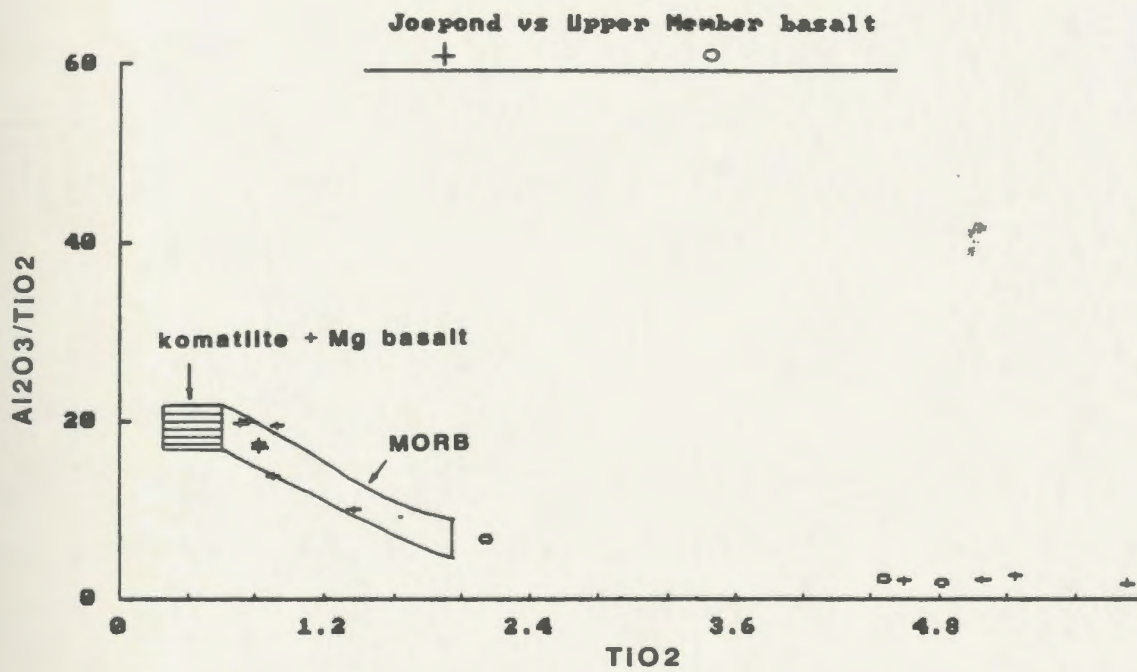


Fig. 3.26 Joe Pond, Upper Member basalt MORB-komatiite discrimination diagram.

nature of the Joe Pond basalts on this diagram is discussed in Section 3.3.3). Thus, although the basalts have a tholeiitic affinity, the Cr and Mg contents are high relative to average tholeiites and overall, are low in TiO_2 . These rocks probably formed from a relatively primitive (high Mg, Cr, and low K) source by rifting in a tensional setting near the continental margin, without contamination from exotic pre-existing crust, or extensive fractionation which would reduce the MgO contents to that of typical mid-ocean ridge tholeiite.

3.3.2 Upper Member basalt

Narrow (< 5 m), vesicular and massive, dark green basalt flows are interdigitated with clastic sedimentary rocks at the top of the Upper Member. The top of this sequence is well exposed at the Teuva Showing 90 m east of Heart Pond, and in a complexly faulted and sheared area near the Fault Creek Zn showing 500 m southwest of Dragon Pond. Field exposures of these rocks typically consist of narrow flows, which are usually vesicular, occurring as interbeds in shale, or siltstone. The flows have unknown lateral extent, but consistently outcrop within 200 m of the contact with the Joe Pond Formation. The obvious conclusion is that these rocks mark a period of extensional tectonism during the last stages of deposition of the Upper Member, and are shallow water analogues of the Joe Pond

Formation basalts, marking the incipient stage of these younger volcanics.

Three samples were collected from flows hosted within clastic sediments of the Upper Member (Appendix 2). These rocks fall within Middlemost's (1980) chemical composition range for basaltic rocks (Table 3.34), and are listed with the composition of the Joe Pond Formation basalts (the data represent mean compositions for each group). These rocks are clearly more primitive than Joe Pond Formation, containing less SiO_2 , Al_2O_3 , and alkali oxides but more FeO .

These rocks plot in the tholeiitic field of Irvine and Baragar (1971), but are clearly alkali-poor compared to the Joe Pond basalts (Fig. 3.27). These rocks plot within the ocean floor basalt (OFB) field (Fig. 3.28; after Pearce, 1975), and two of the samples plot within the OFB field of Pearce and Cann (1973). Sample WC-82 (Fig. 3.29) falls within the island arc basalt (IAB) field of Pearce and Cann (1973), the reason for the high Sr content of this sample is not known. These basalts are much too rich in TiO_2 to fall within Sun and Nesbitt's (1978) MORB field (Fig. 3.26, pg. 100). On the plot of $\log \text{Cr}$ vs $\log \text{Ti}$ the Upper Member basalts plot in the high Ti and high Cr part of the ocean floor basalt field, while Joe Pond rocks straddle the OFB-LKT boundary for rocks with a lower range of Ti and Cr contents. In summary, the Warren Creek basalts

Table 3.3 Basalt screen, percent oxides
From Middlemost (1980)

	Middlemost 1980	Warren Creek	Joe Pond
SiO ₂	44 to 53.5	45.66	48.45
Al ₂ O ₃	10.5 to 21.5	10.04	13.54
FeO	2.5 to 15	20.16	15.12
CaO	5 to 15	7.24	7.48
Na ₂ O	1 to 3.9	0.48	1.9
K ₂ O	0 to 2.5	0.57	0.85

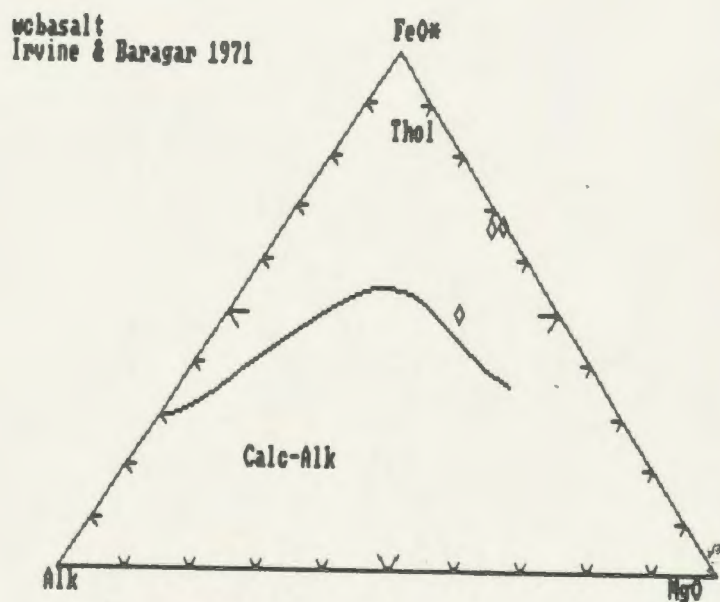


Fig. 3.27 Upper Member basalt tholeiitic vs calc-alkalic discrimination diagram.

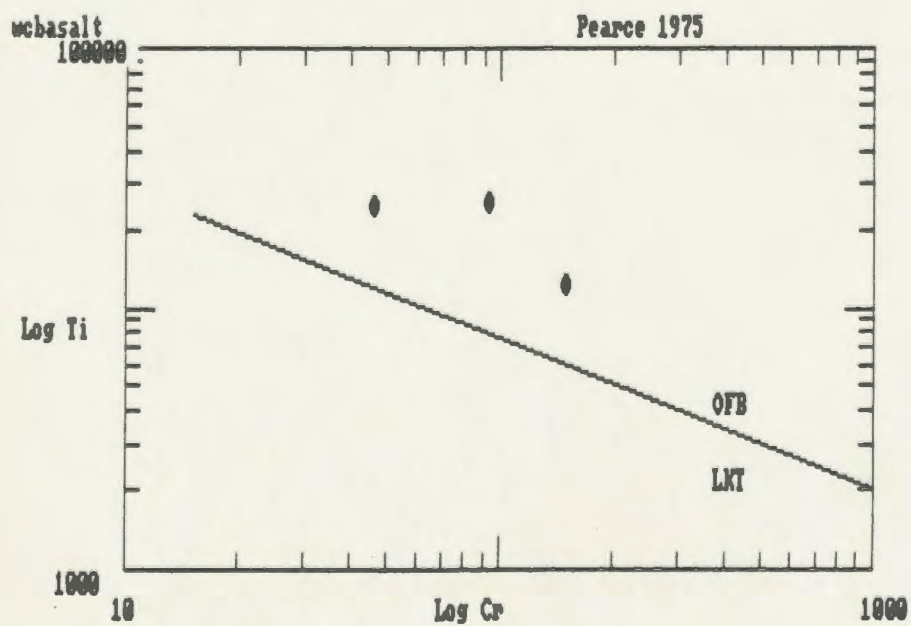


Fig. 3.28 Upper Member basalt LKT-OFB discrimination diagram.

webasalt
Pearce & Cann 1973

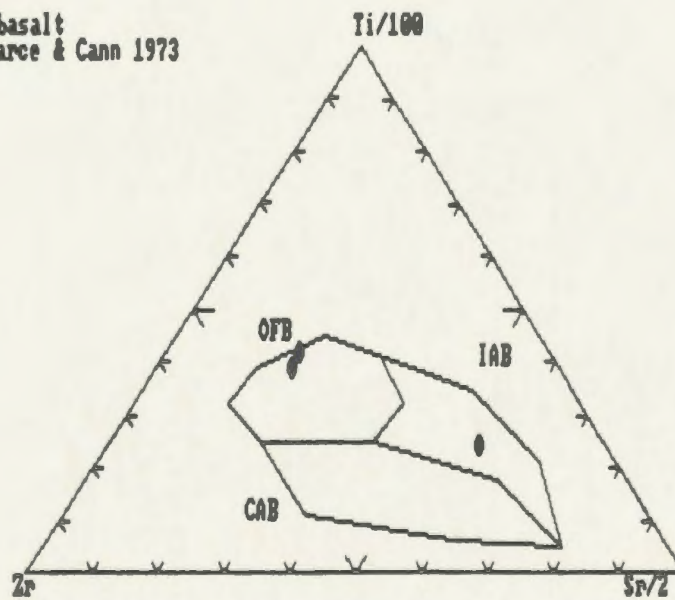


Fig. 3.29 Upper Member basalt OFB-CAB-IAB discrimination diagram.

have a primitive (high Ti, Cr, Mg, and low $\text{Na}_2\text{O} + \text{K}_2\text{O}$) OFB affinity, while the Joe Pond sequence is a LKT rock with OFB affinities (low Ti but high Cr and Mg).

3.3.3 Extended REE plots (spider diagrams)

Trace and rare earth element (REE) data for selected samples of Upper Member and Joe Pond basalt are plotted on spider diagrams (Figs. 3.30, 3.31). The data are normalized to primitive mantle (or bulk Earth, from values published in Taylor and McLennan, 1981, and Jenner et al., 1987). The spidergrams for Upper Member basalt display the typical concave downward shape of ocean island basalts (OIB; after Sun, 1980; Thompson et al., 1984). Samples WC-41 and WC-82 have enriched (approximately 10X primitive mantle) REE profiles sloping steeply downward to the right, a feature attributed to generation from a fertile OIB source mantle (Thompson et al., 1984). The positive Ta/Nb anomaly in WC-41 is characteristic of basalts formed from OIB source mantle (ibid.).

Spider diagrams for Joe Pond Formation basalts have a bimodal distribution between; an enriched (10 to 100X primitive mantle) group (JP-15, JP-17) with an incompatible element pattern similar to the pattern for typical OIB (and Upper Member basalt), and a group (JP-1, JP-10, JP-14) with slightly enriched (less than 10X primitive mantle) REE and trace element abundances, and relatively flat REE profiles.

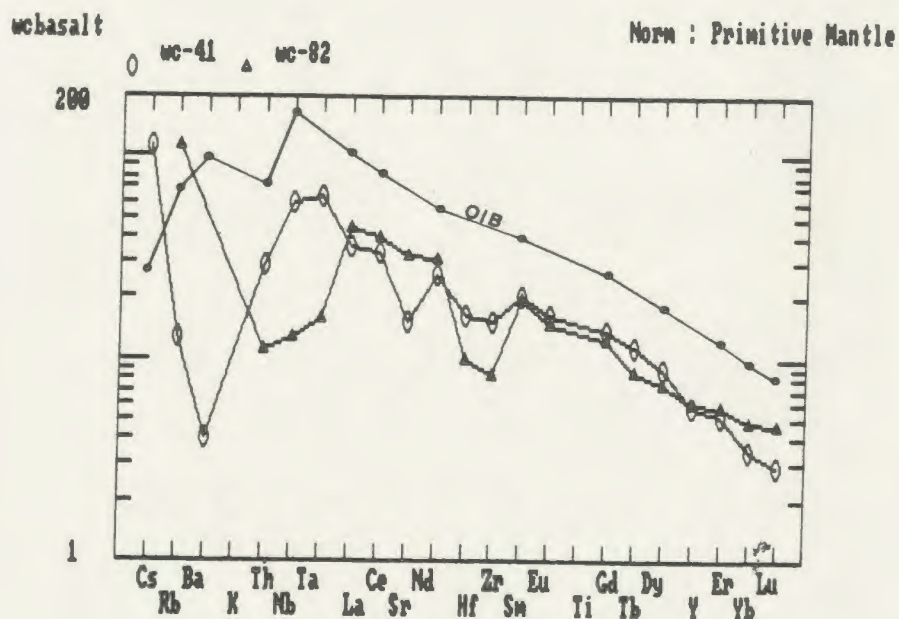


Fig. 3.30 Upper Member basalt extended REE plot, Cs and Ba are off scale in sample WC-82 (>1000X, and >500X respectively).

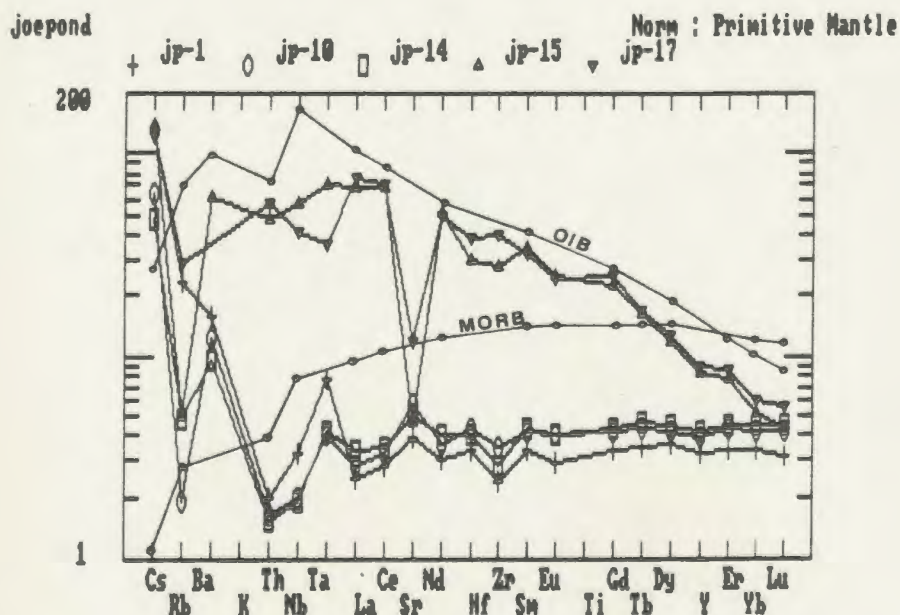


Fig. 3.31 Joe Pond Formation extended REE plot.

The spidergrams for JP-1, JP-10 and JP-14 are similar to that of the more evolved mid-ocean ridge basalt (MORB) i.e. flat REE profiles, and an overall gentle slope upwards from left to right (*ibid.*). There is a small positive Ta anomaly, and significant positive Ba and Cs anomalies, the former probably reflects a relatively primitive MORB source mantle, and the latter alteration.

The samples of Joe Pond Formation with OIB affinities probably represent lavas geochemically related to the underlying Upper Member flows, if it is assumed that the Upper Member and Joe Pond basalts are end members in a comagmatic series. The samples with MORB affinities probably represent typical Joe Pond basalt, since this is in agreement with the discrimination diagrams discussed previously. The bimodality of the Joe Pond Formation may be explained by the small number of samples analyzed (5), and risk of not having analyzed a sample geochemically midway between these two groups.

The Upper Member REE profiles strongly resemble those of the Teuva showing (Fig. 3.18, pg. 88). This similarity may reflect contamination of the Teuva sedimentary rock with REE contained in circulating juvenile fluids, or an exsolved gaseous phase related to this volcanism. Contamination of this type would certainly not be surprising when the effect of this volcanism on the metallogeny of the basin as a whole is considered. This

also supports the hypothesis that the Teuva mineralization is a consequence of the incipient stages of Joe Pond Formation mafic volcanism (see Chapter 5.2).

3.3.4 Summary

The appearance of narrow vesicular basalt flows hosted in clastic sedimentary rocks of the Upper Member, within 200 m of the contact with the overlying Joe Pond Formation basalts, suggests that these rocks are comagmatic (Chapter 2.6). The basalt geochemistry also suggests, but does not prove, that these rocks are comagmatic.

A single phase of magmatism is used to explain the genesis of these rocks. The primitive composition of the Upper Member basalt represents an early eruption (or leakage) of magma, prior to the eruption of Joe Pond Formation basalt, which evolved geochemically in a stable magma chamber during the last phases of deposition of the Upper Member. The spidergrams for each of these basalt types indicate that the Upper Member basalt was derived from OIB source mantle. Eruptions such as these must penetrate the more geochemically evolved MORB source mantle in order to reach the earth's surface (Thompson et al., 1984), therefore they are thought to originate over convecting mantle plumes or so called "hot spots." Thus, to invoke a single phase of magmatism requires that the Joe Pond Formation basalt is the product of differentiation of

primitive (OIB) magma by crystal fractionation in a stable magma chamber to produce geochemically evolved (MORB) magma.

Another plausible explanation involves eruption of Joe Pond Formation basalt from MORB source mantle due to partial melting induced by pressure release in a rifting episode caused by earlier OIB (Upper Member basalt) eruption. This second explanation requires that dissimilar magmas erupt via common structural conduits without a detectable degree of mixing. A discussion of the geochemical and thermodynamic complexities inherent in this explanation are beyond the scope of this work.

The former explanation is the most practical since it gives a simple account of the genesis of both types of basaltic rocks, and explains two outstanding tectonic and stratigraphic features of the Moran Lake Group namely; that the hot spot which gave rise to the Upper Member basalt, and ultimately the Joe Pond basalt, formed a basin by crustal expansion and rifting in the Archean basement over an inferred stable magma chamber, into which the marine transgressive sequence of the Warren Creek Formation was ultimately deposited.

3.4 Gabbro

Dark green, medium to fine-grained gabbro sills and dikes crosscut all lithologies of the Moran Lake Group.

These rocks are most commonly allotriomorphic granular and melanocratic, however amphibole and biotite-phyrlic melanocratic varieties were observed. These intrusives are probably related (Ryan, 1984) to the pre-Grenvillian Micheal Gabbro (Fahrig and Larochelle, 1972), which crops out as east-northeast trending linear intrusions throughout eastern Labrador. In this study area gabbro crosscuts both the Moran Lake and Bruce River Groups, and may be weakly foliated to massive. Effusive equivalents of these rocks have not been recognized in the area, however their geochemistry will be treated as though volcanic analogues did exist.

The gabbro data fall within the subalkalic field of Irvine and Baragar (1971), and straddle their discrimination line for tholeiitic and calc-alkalic rocks (Figs. 3.32, 3.33). Ryan (1984) noted that ultramafic compositions were observed in "gabbros" north of Pocketknife Lake. Three samples of gabbro from this study fall within the komatiitic field of Sun and Nesbitt's (1978) CaO/TiO_2 vs TiO_2 plot (Fig. 3.34), and five samples plot in a region of high $\text{Al}_2\text{O}_3/\text{TiO}_2$ on the plot of $\text{Al}_2\text{O}_3/\text{TiO}_2$ vs TiO_2 (Fig. 3.35; *ibid.*) for rocks of ultramafic composition. Thus these rocks are probably contaminated MgO-rich magmas which have fractionated TiO_2 , and assimilated some alkalis. The alkalic contamination may have been inherited from the Archean granitoid basement or

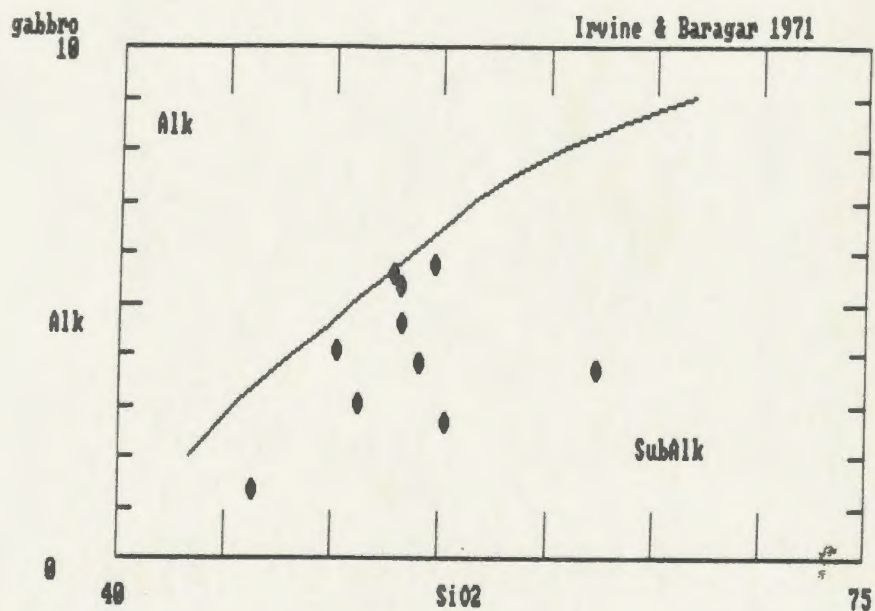


Fig. 3.32 Gabbro Alk vs Subalk discrimination diagram.

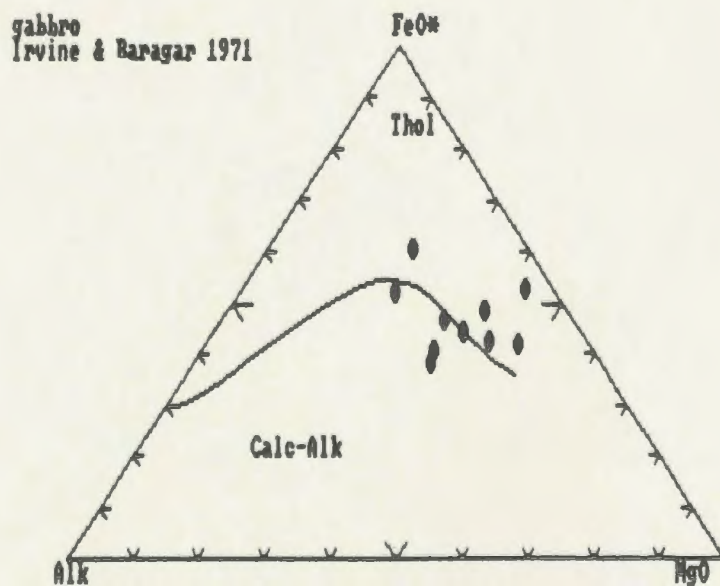


Fig. 3.33 Gabbro tholeiitic vs calc-alkalic discrimination diagram.

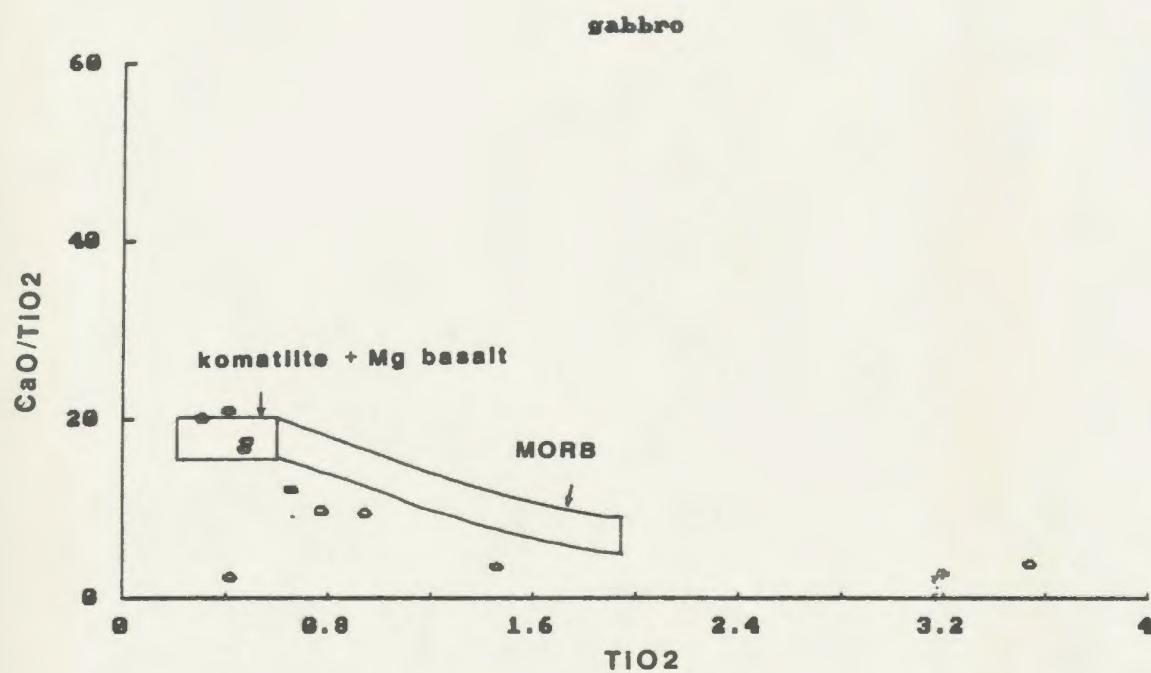


Fig. 3.34 MORB vs komatiite discrimination diagram for gabbro using TiO₂ and CaO.

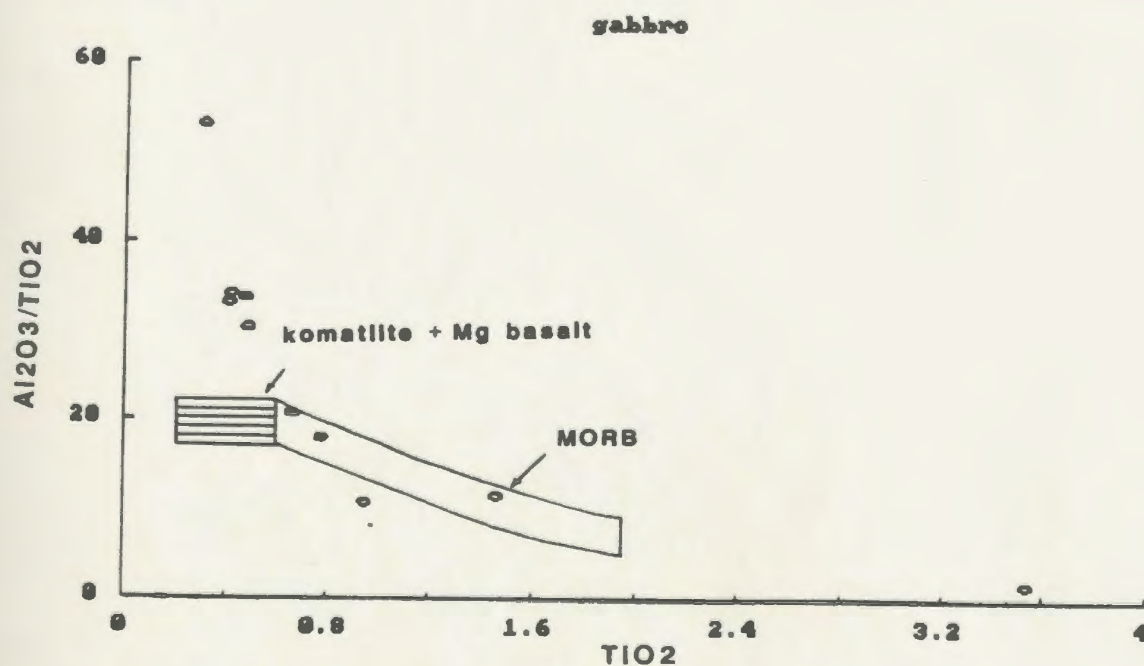


Fig. 3.35 MORB vs komatiite discrimination diagram for gabbro, using TiO₂ and Al₂O₃.

underlying sediments.

CHAPTER 4

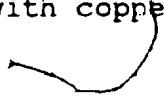
ECONOMIC MINERALIZATION

4.1 General introduction

The geology and mineral occurrences of the Moran Lake Group are shown in Figure 4.1. Economic mineralization in the Moran Lake Group consists of gossanous, massive and disseminated, stratiform, iron and base metal sulphides hosted in the Upper Member of the Warren Creek Formation black shale-siltstone sequence.

The sulphide gossans are an important rock-forming constituent of the member, and exhibit remarkable consistency of character in the field. Graphite content, however, varies considerably and, where present in abundance, is associated with massive pyrite beds up to 2 m thick. Typical sulphide gossans consist of black graphitic shale and interbedded grey siltstone, with 5 to 15 % finely laminated, stratiform pyrite beds, and laminae rich in disseminated pyrite and traces of pyrrhotite, chalcopyrite, and sphalerite.

Since previously documented geochemical and geological data for these rocks are very limited (e.g. Hansuld, 1958; Ryan, 1984), and there are no known showings of sediment-hosted base metal mineralization in this study area, the term "mineral occurrences" refers to those showings with copper or zinc abundances above an



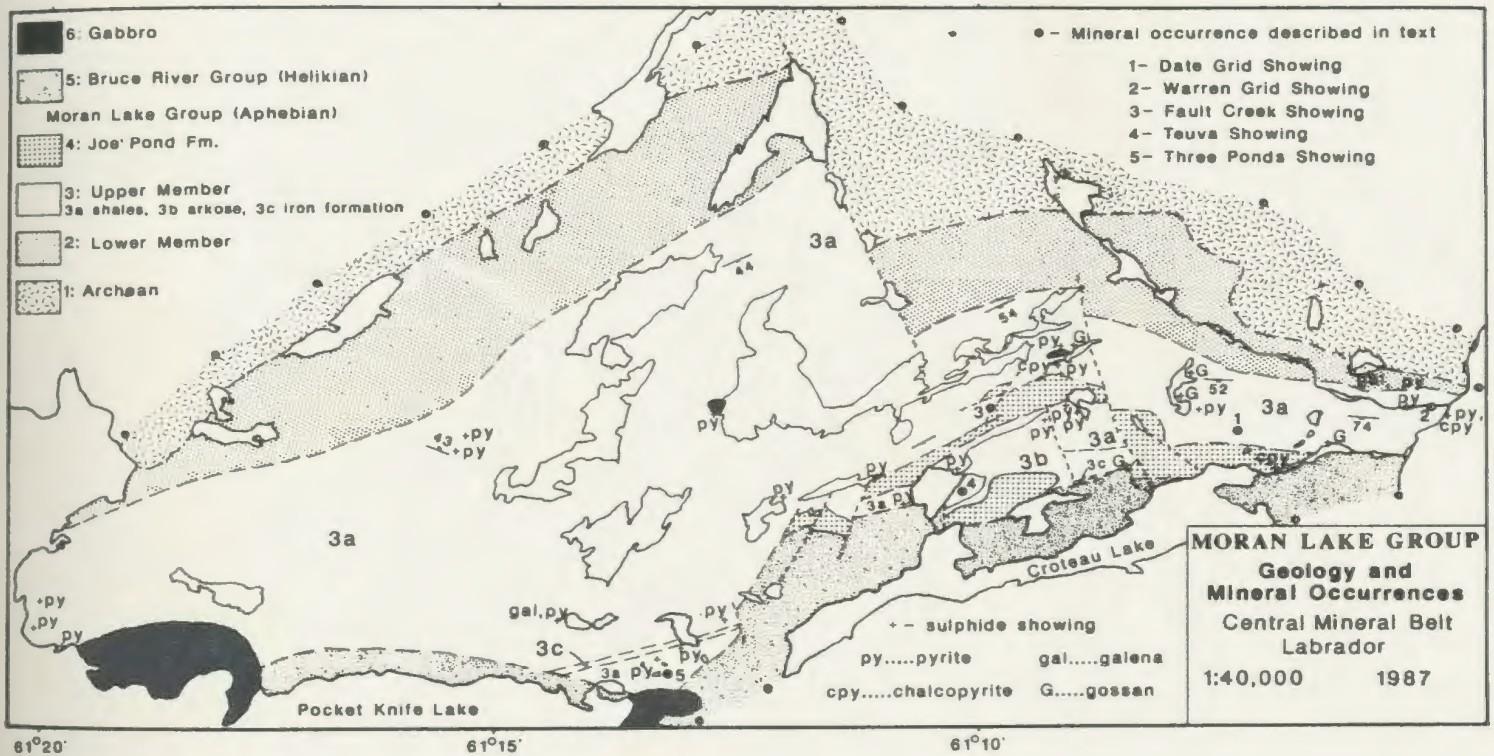


Fig. 4.1 Moran Lake Group geology and mineral occurrences.

arbitrarily set minimum concentration.

Table 4.1 lists the average base metal concentrations for shales from three studies (Green, 1959; Turekian and Wedopohl, 1961; and Vine and Tortelot, 1970). From this data comparison, mineral occurrences were defined as sediment-hosted sulphide mineralization containing >750 ppm Zn, and/or >300 ppm Cu, and thus, are also included in the data set for showings (> 300 ppm Zn, or > 70 ppm Cu, or >5% sulphide mineralization) which were discussed in Chapter 3.

The absolute metal contents of mineral occurrences in the Warren Creek Formation are very low (750-5000 ppm Zn, with no significant Pb, Cu, or Ag; Table 4.2) when compared with the reported average grades of several giant Proterozoic Pb-Zn deposits (McArthur River, Mt. Isa, Sullivan, Broken Hill) which contain 5.7-11.1% Zn, 4.1-14.0% Pb, and 44 to 200 ppm Ag (Lambert, 1983). Thus, the definition of mineral occurrences does not imply that the showings contain economically significant Zn or Cu abundances, rather, it serves to define geochemically anomalous horizons in the Upper Member which may have some economic significance when put into the regional stratigraphic framework.

Grab samples from four previously documented (Hansuld, 1958) pyrite-rich showings (i.e. the Date Grid, Warren Grid, Fault Creek, and Three Ponds Showings) contained

Table 4.1
Shale base metal contents (ppm)

	Vine & Tortelot 1970	Green 1959	Turekian & Wedopohl 1961
Cu	70	38	45
Zn	<300	80	95
Pb	20	20	20

Table 4.2. Metal contents of Upper Member
mineral occurrences in ppm.

<u>Showing</u>	<u>Sample</u>	<u>Zn</u>	<u>Cu</u>	<u>Pb</u>	<u>Au ppb</u>
Date Grid	TRC-3	772	320	nil	N/A
Date Grid	TRE-1	658	191	31	28
Warren Grid	WC-67	4702	533	15	N/A
Warren Grid	M-1	353	347	69	78
Warren Grid	M-2	383	612	42	70
Fault Creek	WC-94	2865	486	nil	19
Three Ponds	WC-216	2126	759	26	N/A
Teuva	HP-1.1*	20759	99	nil	<5
Teuva	HP-1.2*	17929	162	"	"
Teuva	HP-1.3*	18484	123	"	"
Teuva	HP-1.4	37295	121	"	N/A

*Samples with high Zn were checked by atomic absorption,
results are as follows:

<u>Sample</u>	<u>Zn%</u>
HP-1.1	2.69
HP-1.2	2.09
HP-1.3	2.22

Note: N/A means not analyzed, all samples contained less
than 5 ppm Ag.

over 750 ppm Zn.

Several new sulphide-bearing horizons were discovered in 1986, and one in particular (Teuva showing) contains up to 2.69% Zn within a zone of stratabound disseminated sphalerite mineralization. The Teuva showing is a pyrite-poor mineral occurrence, and is treated as a separate data set.

4.2 Geology of mineral occurrences

4.2.1 Date Grid showing

A typical gossan, located 420 m north of the northeast bay of Croteau Lake, is exposed in a complexly interdigitated sequence of pyritic shales, chert, siltstone, massive pyritic graphite, and dolostone (see inset on Geology Map, back pocket). The mineralization is exposed in 5 trenches for 35 m along strike. All assays reported from a diamond drilling program in this zone by Brinex (Hansuld, 1958) contained trace amounts of copper, zinc, and nickel.

Up to 35 % disseminated to massive, fine-grained pyrite occurs as irregular, 1 to 3 mm laminae along sheared siltstone and shale bedding planes, and as fine disseminated grains throughout all rock types. Traces of pyrrhotite, chalcopyrite, and rare sphalerite (Fig. 4.2) occur throughout the trenches. Remobilized pyrite and



Fig. 4.2 Sphalerite in shale, trench C, Date Grid.

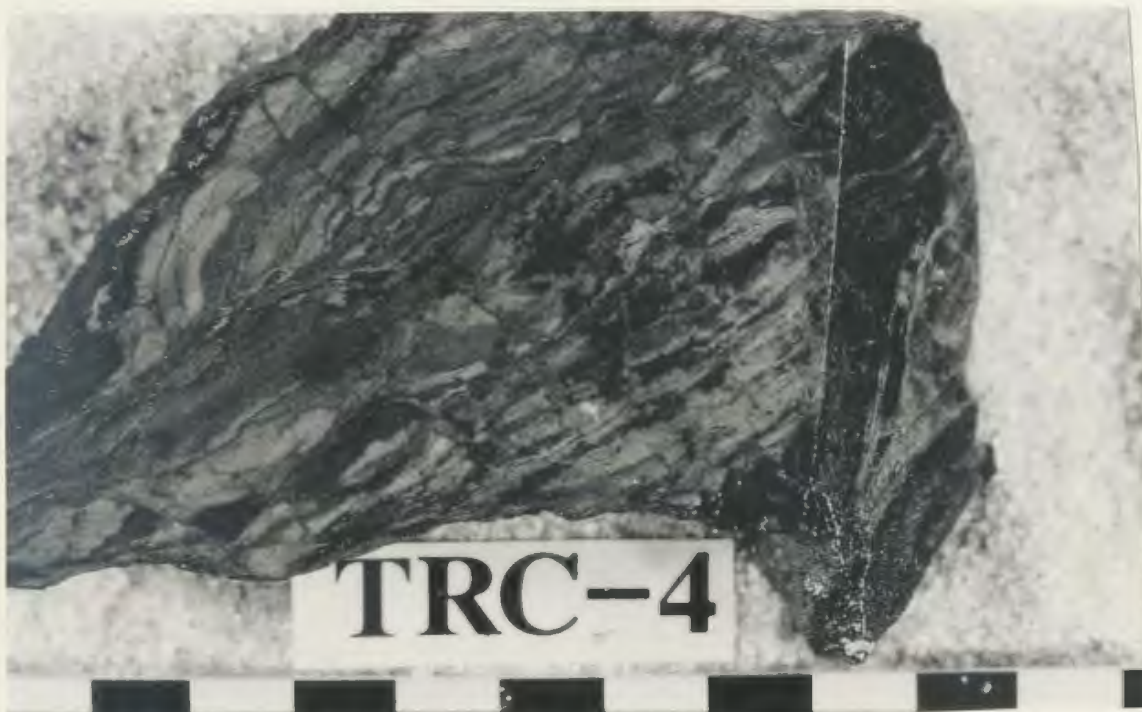


Fig. 4.3 Brecciated siltstone, Date Grid.

pyrrhotite form 1 to 3 mm discordant stringers in F_1 and F_2 hinge line fractures and tension gashes in cherty and calcareous interbeds.

Sample TRC-3 contained 772 ppm Zn. The rock consists of brecciated siltstone (Fig. 4.3, pg. 121) containing 3 to 5 % discordant fine-grained, 1 to 2 mm pyrite stringers filling interstices in a melange of light and dark grey, elongate 5 mm to 3 cm silt fragments. Sample TRE-1, located 15 m west of TRC-3, contained 658 ppm Zn, and 28 ppb Au. This sample was collected from a black, shale-hosted massive pyrrhotite-pyrite horizon 0.5 to 1 m thick, on the south flank of a massive limonite stained chert bed. Much of the pyrrhotite in this brittle unit is remobilized into a network of fine discordant stringers.

4.2.2 Warren Grid Showing

A massive 2 m thick graphitic pyrite bed, containing over 50 % pyrite (Figs. 4.4, 4.5) and traces of fine-grained pyrrhotite, chalcopyrite (Fig. 4.6), and sphalerite (Fig. 4.7), is exposed 1 km northeast of Long Pond and could be traced in outcrop intermittently for 400 m along Warren Creek. The sulphide bed consists of massive, 5 mm to 1 cm beds of yellow, fine-grained pyrite, with minor interstitial graphite and amorphous quartz, which are finely interbedded with massive black earthy graphite, amorphous clays, and quartz (chert?) (Fig. 4.8).

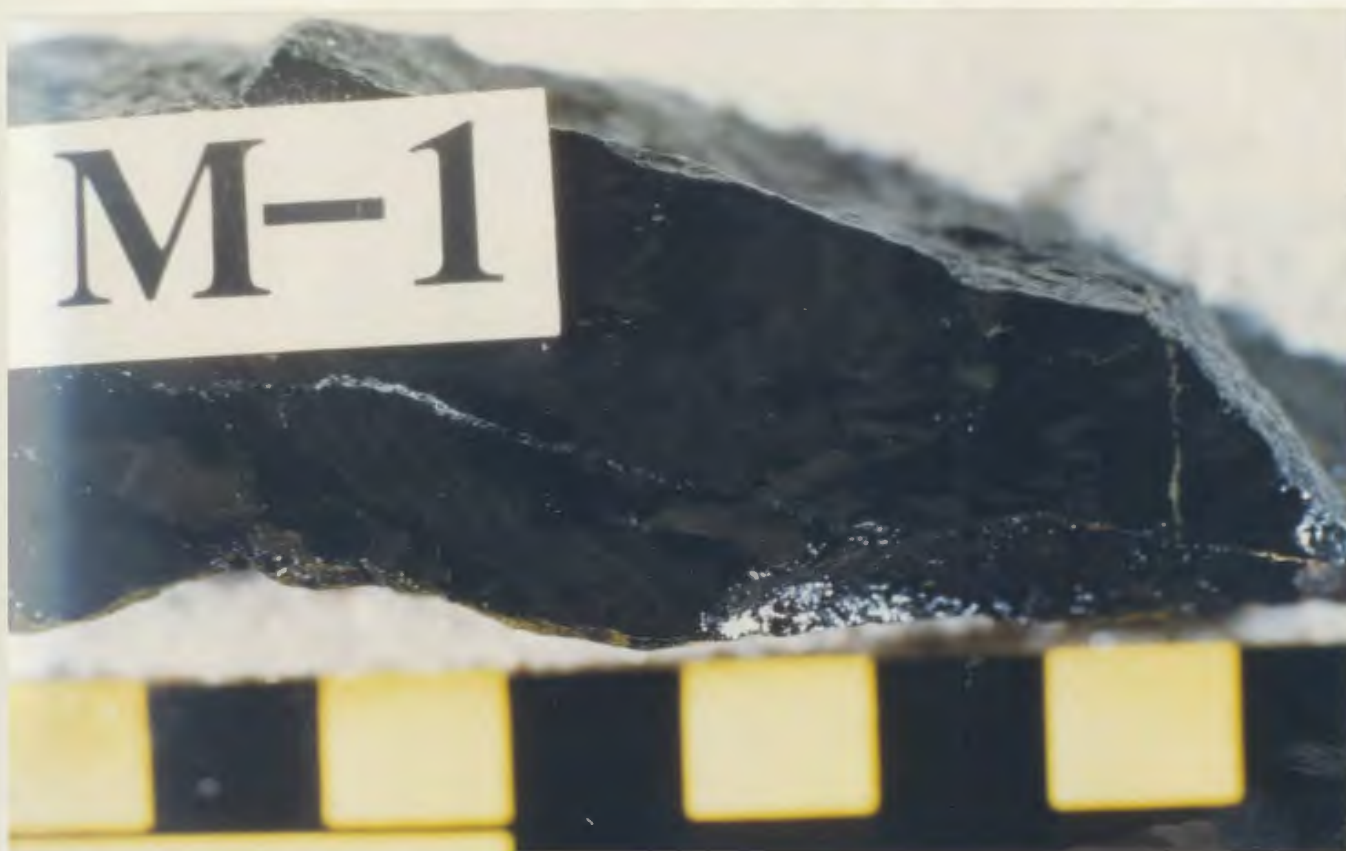


Fig. 4.4 Warren Grid graphitic massive sulphide bed, scale in cm.



Fig. 4.5 Warren Grid graphitic massive sulphide bed, scale in cm.



Fig. 4.6 Chalcopyrite (light grey) intergrown with pyrite in Warren Grid graphitic massive sulphide bed.



Fig. 4.7 Irregular sphalerite grain (light grey) intergrown with pyrite (grey), Warren Grid massive sulphide bed.



Fig. 4.8 Finely interbedded pyrite (light grey) and amorphous clay/graphite (dark grey), Warren Grid massive sulphide bed.

Samples WC-66, and 67, contained 664 ppm Zn, and 361 ppm Cu, and 4,702 ppm Zn, and 533 ppm Cu respectively.

Samples M-1, and M-2 were collected from the same horizon two hundred metres east of this exposure. Sample M-1 contained 353 ppm Zn and 347 ppm Cu; M-2 contained 383 ppm Zn and 612 ppm Cu.

4.2.3 Fault Creek Showing

Sample WC-94 contained 2,865 ppm Zn and 486 ppm Cu. The sample was collected from highly sheared, black, gossanous shale 820 metres northeast of Heart Pond. The exposure occurs along a fault escarpment near the contact with the Joe Pond Formation basalts. Thin basalt flows occur locally in the Warren Creek Formation here.

Sample WC-94 contains 15 to 25% pyrite as massive, 2 cm thick, fractured beds and fine, disseminated grains. Minor, very fine-grained, disseminated sphalerite (Fig. 4.9) was noted in the field. The rock is highly sheared, and it appears as though much of the sulphide has been remobilized into planar laminae following S_1 , and as trains of fine grains along S_1 .

4.2.4 Three Ponds Showing

Sample WC-216 contains 2,126 ppm Zn and 759 ppm Cu. This sample was collected from angular, gossanous, massive sulphide float (over 1 m in maximum dimensions) 460



Fig. 4.9 Sphalerite (light grey) intergrown with pyrite (dark grey), Fault Creek showing.



Fig. 4.10 Isolated sphalerite grain (light grey) in Three Ponds showing.

m northeast of the east arm of Pocket Knife Lake. Halet (1946) reported significant shale-hosted sulphide mineralization at this location, and blasted two test pits. These pits were not located during this study, and have probably since collapsed or filled in, however the size and shape of the abundant massive sulphide float in this area suggest a nearby bedrock provenance which is likely related to the mineralization described by Halet.

Sample WC-216 consists of contorted, massive, 2 mm to 1 cm beds of aphanitic pyrrhotite and pyrite with abundant interstitial graphite, giving the rock a jet black colour on fresh surface. The massive sulphide beds are intercalated with rare, primary, 1 mm pyrrhotite-chalcopyrite laminae, and contain traces of galena and sphalerite (Figs. 4.10, pg. 127, 4.11). A pervasive network of 0.1 mm to 1 mm quartz stringers containing fine remobilized pyrite, pyrrhotite, and chalcopyrite crosscut the bedding at high angles (Fig. 4.12).

4.2.5 Teuva Showing

Samples HP-1.1 to 1.4 inclusive were collected from massive, gossanous, green greywacke, 140 m east of Heart Pond. Each of the four samples contained between 2.09 and 2.69% Zn with no significant Cu or Pb enrichment. Sample HP-1.4 has been analyzed by X-ray fluorescence methods only which yielded a value of 37,295 ppm Zn. This number

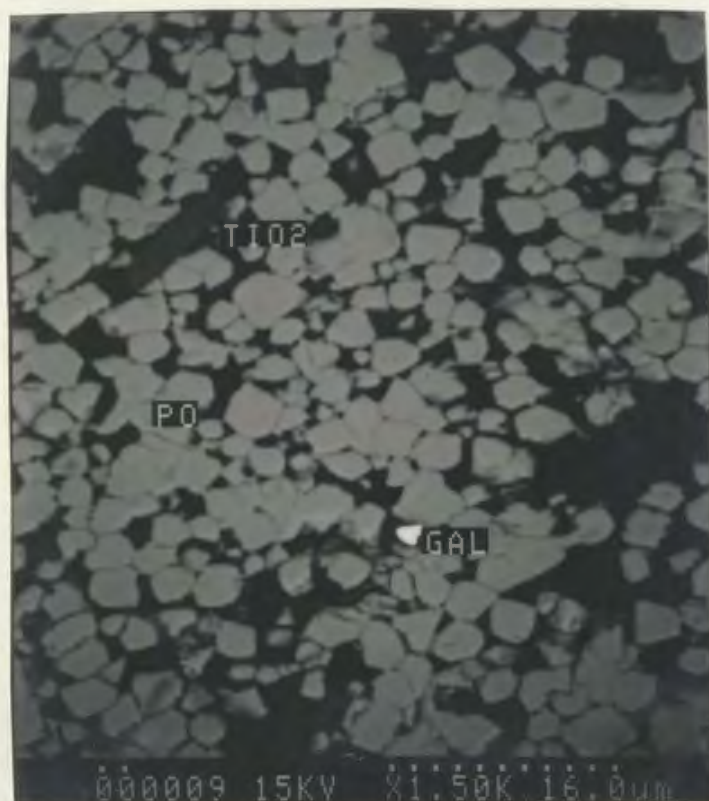


Fig. 4.11 Isolated galena grain (white) in Three Ponds showing, note detrital rutile needle (dark grey).

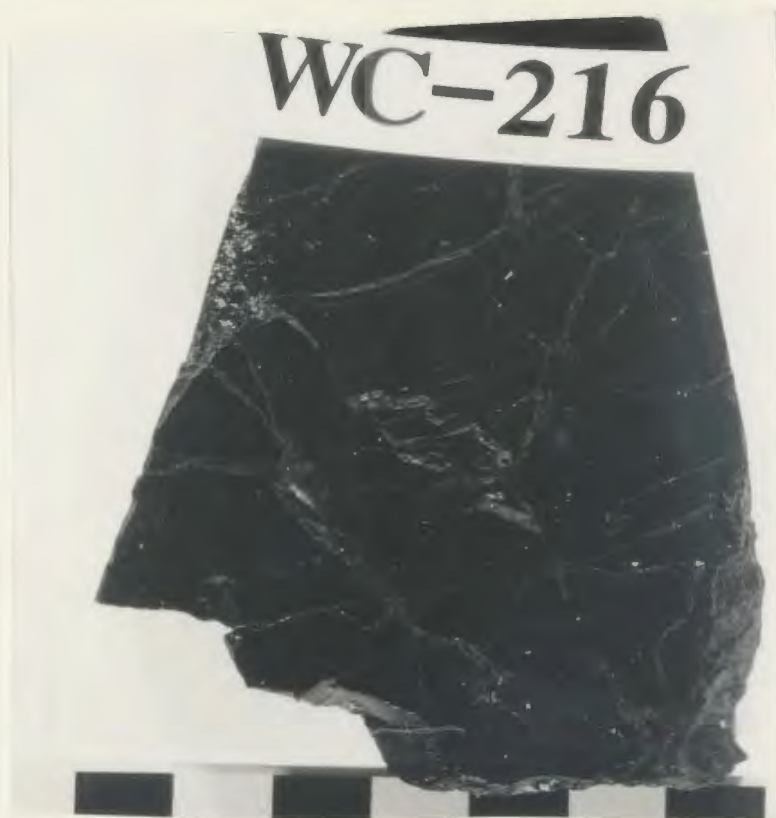


Fig. 4.12 Highly fractured, graphitic, massive sulphide bed, Three Ponds showing.

has not been re-checked by atomic absorption or neutron activation and therefore is not listed as the highest zinc value from the area due to the innacuracy of 'X-ray fluorescence analyses on trace elements in such high concentration (Longerich and Veinott, 1986). HP-7 and HP-8 were also collected from this horizon but did not contain any significant enrichments in base metals.

The host rock for this mineralization is a very "dirty", poorly sorted, fine-grained, chloritic sediment. The chemistry of this rock is very unusual, however the chemical characteristics can be related to its mineral composition. The rock is very MgO-rich (10-15% MgO), and CaO-poor (0.68-1.08% CaO), with the exception of HP-8 which contains 9.6% CaO due to the presence of 50-60% calcite. The MgO is probably contained in ubiquitous fine-grained brown-green chlorite which constitutes 20-25% of the rock. SiO₂ is always less than 50%, this is not surprising since there is very little detrital quartz visible in thin section. Detrital quartz, where observed, occurs as very fine angular broken grains. Na₂O + K₂O are less than .02% in every sample from this horizon, reflecting the paucity of authigenic plagioclase and orthoclase. Where feldspars were observed, they occur as aphanitic groundmass grains, and rare 0.2-0.5 mm subangular broken grains. The sediment is rich in titanium (1.4-4.04% TiO₂), and zirconium (154-402 ppm) indicating that heavy

detrital minerals such as rutile, ilmenite, and zircon were highly concentrated in these sediments by winnowing prior to lithification. Abundant acicular idiomorphic rutile was observed in petrographic thin sections and scanning electron microscope studies of this unit (Fig. 4.13).

The horizon is hosted in a complexly interdigitated sequence of chert, basalt, shale, and greywacke, with sheared shale and siltstone to the north, and vesicular basalt, shale, and arkose (arkose bed) to the south.

The sphalerite-bearing horizon is 2-2.5 m wide, and traceable for 20 m to the west. The zone is covered by overburden to the east. Mineralization consists of 3 to 5% sphalerite, mainly in fine disseminated grains, with subordinate 1 to 2 mm discordant remobilized stringers (Fig. 4.14). Rare pyrite occurs as disseminated fine grains, occasionally intergrown with sphalerite (Fig. 4.15). The sphalerite mineralization in this horizon is not laterally extensive, and appears to be confined to a small pod as illustrated on the rock sample location map of the showing (Fig. 4.16). The base metal contents of the samples are listed in Table 4.2 (pg. 119). HP-7 and HP-8 were collected 15 m west and 2 m east respectively, of the sphalerite-bearing samples HP-1.1 to 1.4. Samples HP-7 and HP-8 contained 206 and 110 ppm Zn respectively indicating that the mineralization has a strike length less than 17 m at this showing.



Fig. 4.13 Rutile needles (light grey) in Teuva showing.

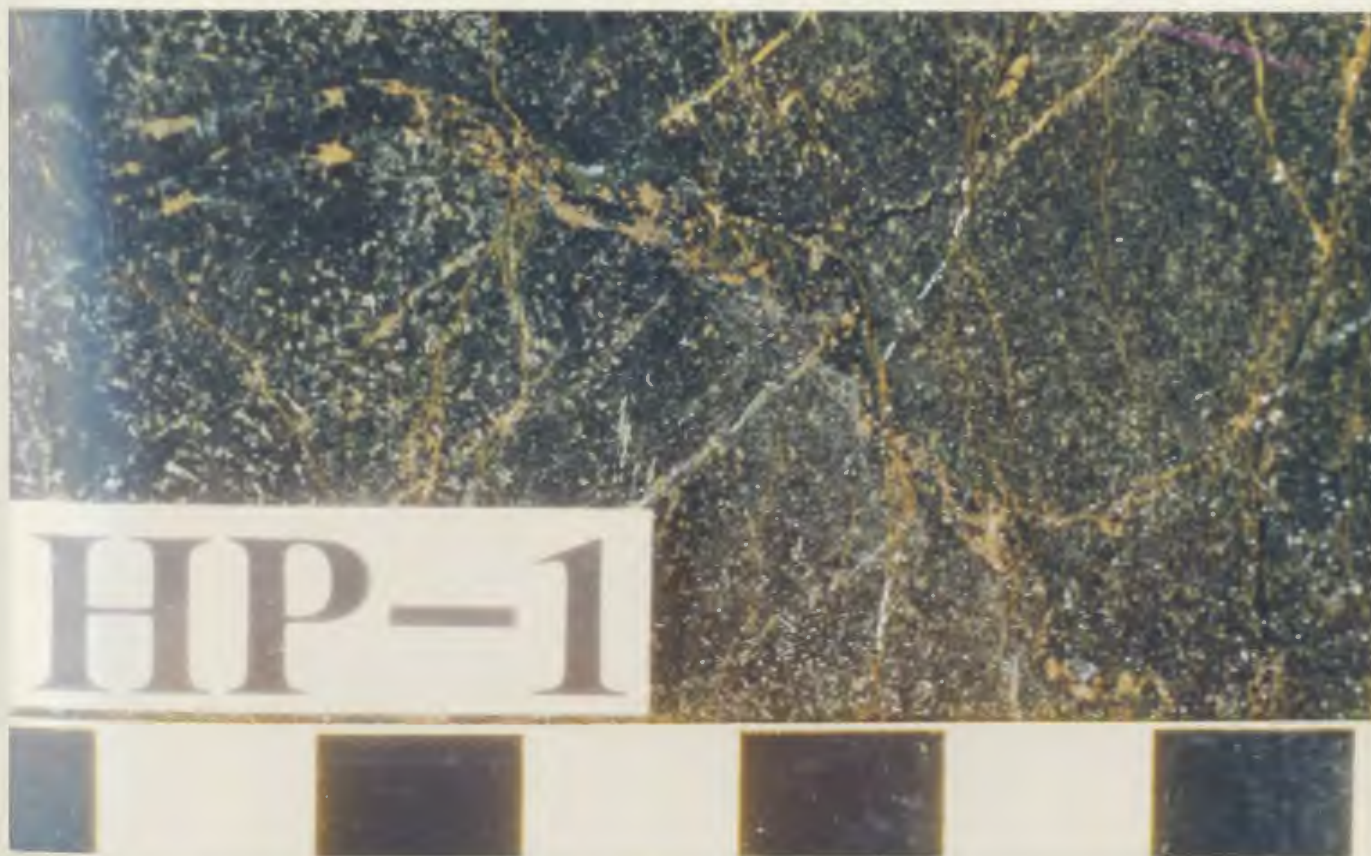


Fig. 4.14 Disseminated and stringer sphalerite (brown), in chloritic host sediment, Teuva showing.



Fig. 4.15 Intergrown pyrite (grey) and sphalerite (light grey), Teuva showing.

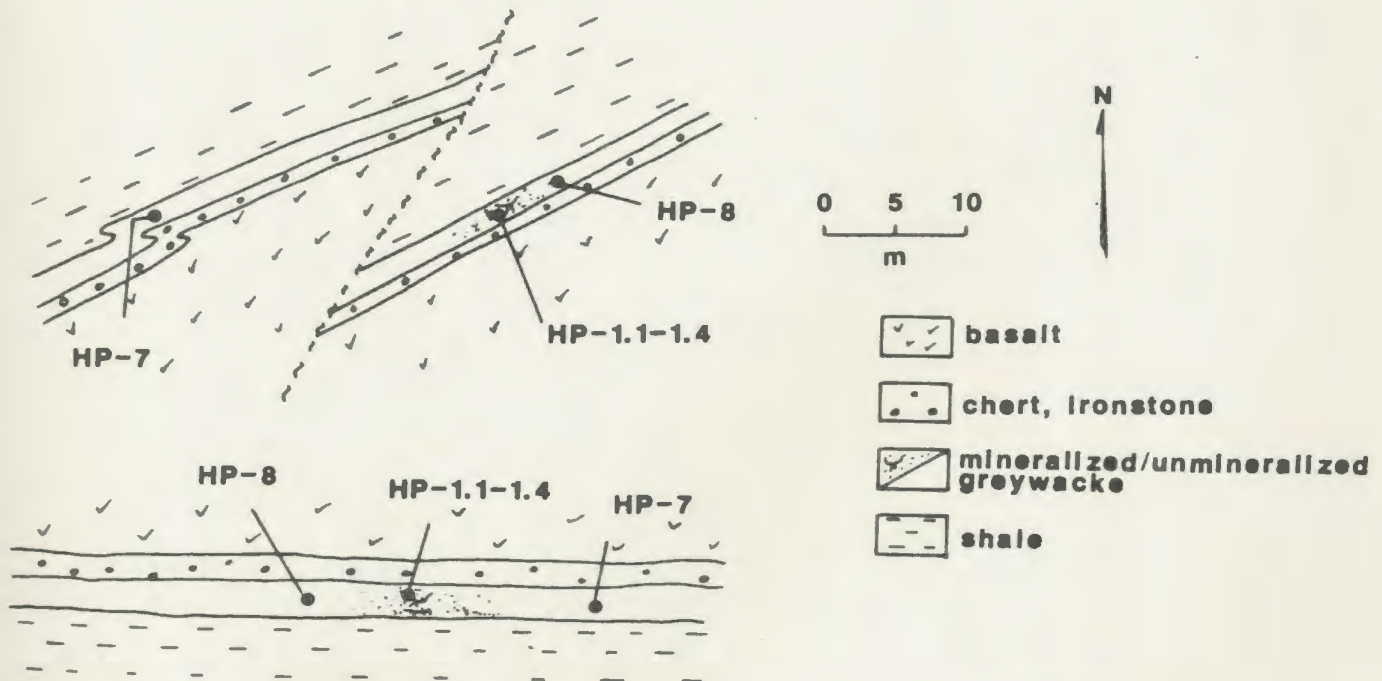


Fig. 4.16 Teuva showing sample location map and geological sketch, and hypothetical reconstruction (lower sketch).

In thin section and hand sample, fine-grained, equant sphalerite grains are evenly distributed throughout the mineralized (HP-1.1-1.4) samples and show some elongation parallel to S_1 . These elongate disseminated grains also form in small clusters and trains parallel to S_1 , possibly representing an original bedding fabric (S_0). The small sphalerite stringers appear to have been remobilized from the groundmass during later deformational events.

Eighty metres south of this horizon, a 2 m thick pyritic shale and siltstone bed was sampled yielding an assay of 859 ppm Zn (sample WC-40b). The shale is bounded to the south by the arkose bed, and to the north by vesicular basalt flows. The sample consists of typical fissile sheared brown shale mineralized with up to 7% fine grains and irregular masses of pyrite. This shale bed follows the trend of the sphalerite-bearing greywacke to the north. The pyritic shale hosting this mineralization is distinct from the pyrite-poor, sphalerite-bearing greywacke to the north, and is included in the data set for showings, not the Teuva showing.

4.2.6 Summary

With the exception of the Teuva showing, mineral occurrences consist of sulphide laminae rhythmically interbedded with their hosting clastic sedimentary rocks. There is no metal zonation, footwall alteration

(chloritization, silicification) or evidence for hydrothermal fluid focusing (breccias, discordant disseminated or stringer sulphide mineralization) with the mineral occurrences. These features suggest that the sulphides were deposited in very saline, restricted, (possibly third order) basins at low temperatures (e.g. Sato, 1977; Hodgson and Lydon, 1977; Carne and Cathro, 1981; Large, 1983; Lydon, 1983). The temperature of the mineralizing solutions are inferred from textural and morphologic features to be on the order of 120⁰-150⁰C (Type 1 fluids of Sato (1972)) based on the delicate layering of sulphides, lack of metal zonation and overall low Cu, and lack of alteration haloes near the sulphide-bearing horizons (Lydon, 1983; Sawkins, 1984; Carne and Cathro, 1981). These solutions would have been very saline (17-20 wt.% NaCl) in order to form stable brine pools in which the delicate layering of the sulphides could be deposited and preserved (Lydon, 1983).

While pyritic gossans (showings) occur throughout the map area, mineral occurrences have a tendency to occur near the top of the stratigraphic section of the Upper Member, 1.5 to 2.2 km above the base of the Warren Creek Formation. Figure 4.17 illustrates the relationship between depth to basement, and abundance of Zn in each of the mineral occurrences. The affinity of economic sedex mineralization for the upper portions of thick

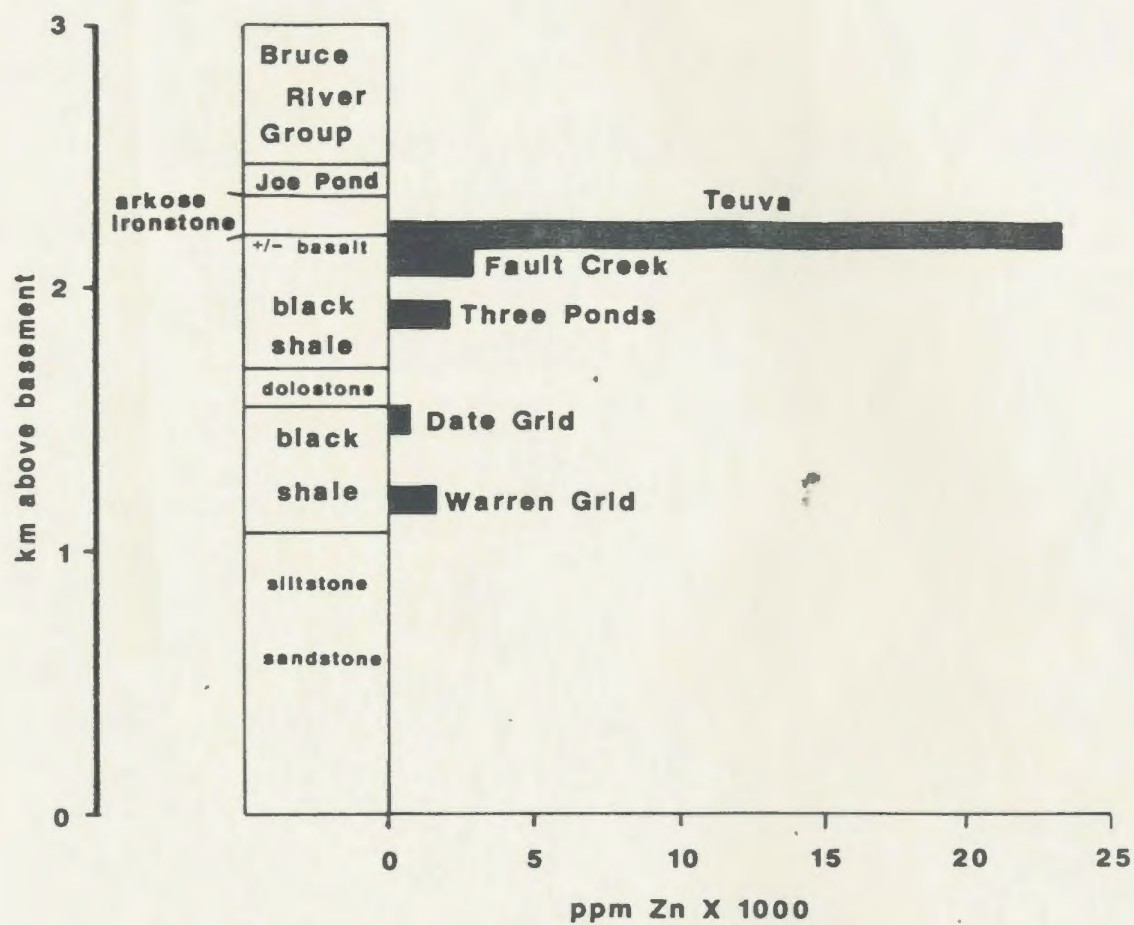


Fig. 4.17 Position of mineral occurrences vs depth to basement.

clastic/evaporitic sequences is well known from the studies of the giant McArthur River (Murray, 1975), Mt. Isa (Mathias and Clark, 1975), Broken Hill (Stanton, 1976), and Sullivan (Hamilton et al., 1983) sediment-hosted Zn-Pb orebodies, which all occur in excess of 3 km from the base of their host clastic/evaporitic sequences.

In addition, all of the mineral occurrences, with the exception of the Warren Grid and Date Grid showings, occur above the middle dolostone bed. The middle dolostone would have been deposited during a local marine regression and period of stagnation, this would be accompanied by increased salinity, and possibly seawater density stratification (Goodfellow, 1987). The increased salinity, and associated chemical precipitate deposition (dolostone) would enhance the production of organic carbon (Eugster, 1984) and facilitate the precipitation of metals from seawater due to bacterial reduction of seawater sulphate (Dexter-Deyer et al., 1984) which would result in the deposition of stratiform syngenetic sulphide horizons.

The highest grade zinc mineralization in the study area was discovered at the Teuva showing which is stratigraphically higher than any of the mineral occurrences in the area. Since there is no discernable metal zonation or fractionation of Zn from Cu in the Upper Member (Section 3.2.1.3), the Zn-rich Teuva showing does not represent the culmination of a chemically stratified

sequence of rocks, rather it appears to be related to a previously unrecognized style of mineralization in the Upper Member.

The Teuva showing was deposited in a more dynamic tectonic environment than the mineral occurrences and sulphide showings stratigraphically lower in the Upper Member. This is evidenced by the stratigraphic proximity of a thick arkose bed (uplift, high energy nearshore depositional environment), a banded ironstone bed (oxidizing rather than reducing waters), and vesicular basalt flows (crustal expansion, rifting, increased heat flow).

An increase in geothermal gradient is frequently implicated as a means of circulating sufficient brines for sedex mineralization (Large, 1983; Russell, 1983; Russell et al., 1981). In the Moran Lake Group this was facilitated by the presence of vesicular basalt flows in a stage of active rifting and uplift at this stage of Upper Member deposition, and also by the incipient Joe Pond mafic volcanism.

4.3 Geochemistry

The pyrite-rich, shale-hosted mineral occurrences (Date Grid, Warren Grid, Three Ponds, and Fault Creek), and the sphalerite-rich Teuva showing are characterized by the Fe-enrichment trends for hydrothermal massive sulphide

deposits (Chapter 3.2.1.1).

On a diagram of SiO_2 vs Al_2O_3 , the laminated pyrite-rich mineral occurrences and showings plot within the field for hydrogenous sediments, and the Teuva showing plots in the centre of this large field (Fig. 3.15, pg. 83) indicating that this disseminated Zn-rich mineralization is associated with a similar hydrologic regime (silica-poor, probably low temperature, and very saline) even though the sulphide mineralogy and host rocks are unique with respect to the showings. Zn is fractionated from Cu in the Teuva showing, while no fractionation has occurred in the Fe-rich mineral occurrences, and sulphide showings lower in the sequence. The base metal fractionation exhibited by the Teuva showing is therefore the signature of a unique style of mineralization in the Warren Creek Formation.

It is therefore proposed that the characteristics of the Teuva Zn mineralization are related to the previously described change in sedimentary and tectonic setting prior to Joe Pond volcanism.

The greywacke hosting the Teuva showing is relatively porous, in contrast to the relatively impermeable shales of the underlying Upper Member, and would be a suitable reservoir for migrating fluids. If metalliferous fluids collected in this unit by diffusion, or advection from adjacent or underlying units, the mineralization would not consist of finely laminated sulphides such as that seen in

the typical pyrite-rich mineral occurrences elsewhere in the Upper Member, rather the mineralization would exhibit disseminated and stringer textures seen in this occurrence. The extent of this type of mineralization in the upper part of the Upper Member is unknown, however the maximum duration of this mineralizing event might be constrained stratigraphically by the deposition of the arkose bed. Since this is also a porous lithology, it would seem likely that podiform Zn-rich mineralization would be found in the core of the Mushroom Pond anticline where this bed is well exposed, and it was not. Further prospecting of this bed is required though, before concluding that there is no economic mineralization in the arkose, since discordant iron sulphide mineralization was noted.

Copper was effectively removed from the Teuva mineralizing fluids. A possible geochemical mechanism for the secular enrichment of Zn from Cu is described by Hallberg (1972), whereby reaction with a lower relatively oxidized sequence (such as the sandstones of the Lower Member) would preferentially precipitate Cu on the oxide coatings of clastic detritus. A similar mechanism envisages selective Cu precipitation within the compacting sediments by reaction of circulating metal-bearing brines with a basinal redox boundary (Sverjensky, 1987) as proposed for the Angolan Copper belt (Van Eden, 1978). This model may provide a plausible explanation for the secular enrichment

of Zn from Cu in the Teuva showing, if uplift accompanying an increased geothermal gradient prior to Joe Pond mafic volcanism formed a redox boundary near the top of the Warren Creek Formation by the percolation of oxidized waters into the upper strata of the reduced Upper Member. The problem with these hypotheses is that there were no Cu-rich, Zn-poor showings found below the Teuva showing. This strongly suggests that the paucity of Cu in the Teuva showing is due to the development of a unique, low temperature ($\leq 150^{\circ}\text{C}$), hydrothermal system which acquired its metal load in a different manner than the metalliferous formation brines which precipitated stratiform sulphide beds in the lower parts of the Upper Member.

4.4 Summary

Two styles of economic base metal mineralization occur in the Upper Member of Warren Creek Formation. The most common style consists of finely bedded pyritic sediments which formed by sulphide precipitation at low temperatures, in saline, restricted basins. These mineral occurrences increase in abundance above the middle dolostone bed, which signifies a local regression, stagnation of seawater, and increase in salinity.

The second style of mineralization is characterized by disseminated sphalerite, with minor pyrite, in porous

greywacke near the top of the Upper Member. The sedimentary horizon was probably mineralized by circulating Zn-rich brines ($\leq 150^{\circ}\text{C}$) which were trapped in this aquifer as a result of the development of a unique hydrothermal regime which formed in a period of increased geothermal gradient and uplift in an active tensional setting.

CHAPTER 5

BASIN EVOLUTION AND METALLOGENY

5.1 Introduction

In Section 5.2, the evolution of the Moran Lake Group will be described based on the stratigraphy of the Group as a whole, and the position of massive sulphide horizons in the Upper Member of the Warren Creek Formation. The model of basin evolution ultimately culminates with a description of the metallogenic setting of the Moran Lake Group in Section 5.3, and a summary of the stratiform sedimentary exhalative Zn-Pb-Cu (Ag) deposit potential of the Moran Lake Group.

5.2 Model for basin evolution: evidence from sulphide deposition

Stage 1: In this stage (Fig. 5.1), the detrital material which formed the basal siliciclastic rocks of the Lower Member of the Warren Creek Formation were being shed off of the Archean basement trondjhemite highland under oxidizing conditions. The detritus was deposited as fine-grained siltstones, sandstones, and shales, with minor carbonate in a nearshore environment. Red beds were also deposited throughout this stage. A dolostone bed which occurs near the Archean-Aphebian unconformity indicates

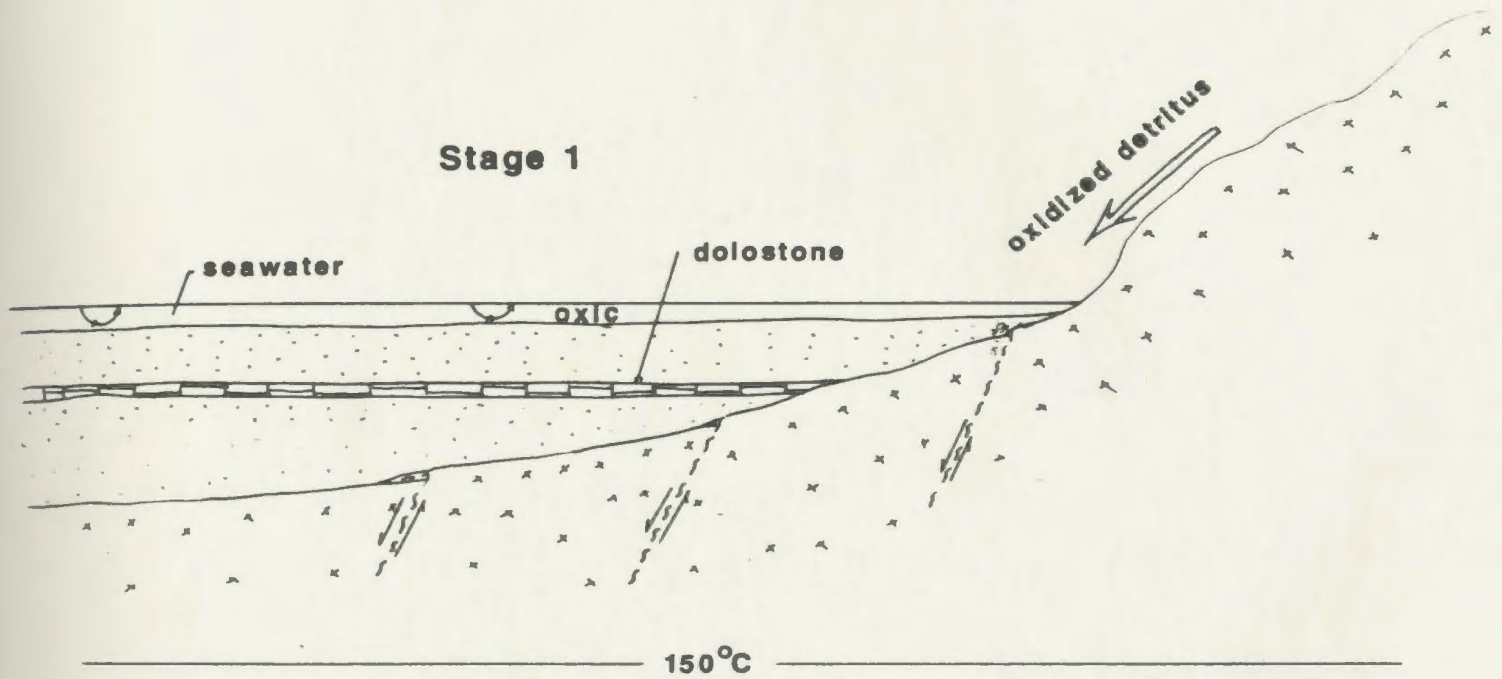


Fig. 5.1 Stage 1 of basin evolution, looking west.

that the sequence overlapped to the east.

Stage 2: Basin subsidence was greatly increased, and normal faults developed in response to tension from increased heat flow and concomitant crustal expansion. Detritus was still being supplied to the basin from the Archean highland, however the supply of detritus was decreased and black shale deposition dominated over siltstone and sandstone. The sediments were deposited into deep water below the photic zone, and red beds were no longer deposited.

At this stage, hydrologic and lithostatic conditions had evolved to the point where conditions were favourable for disseminated and massive sulphide deposition. These conditions resulted from the massive expulsions of pore water from the ever thickening sedimentary pile undergoing compaction (e.g. Krishnan and Oertel (1980) calculated that some phyllosilicate-bearing rocks from the Labrador trough underwent a 68% decrease in volume by compaction and loss of pore water). Sulphide deposition occurred in the Upper Member of the Warren Creek Formation according to the following reactions as illustrated in Figure 5.2:

1: Reactive metal (Fe, Zn, Cu) oxides and/or hydroxides (MeO) contained in authigenic detritus, or as pigmentation, or coatings, (Figs. 5.3, 5.4) on sandstone clasts (i.e. red beds) in the Lower Member siliciclastics, are dissolved by Cl^- -rich formation waters (Lydon, 1983) to

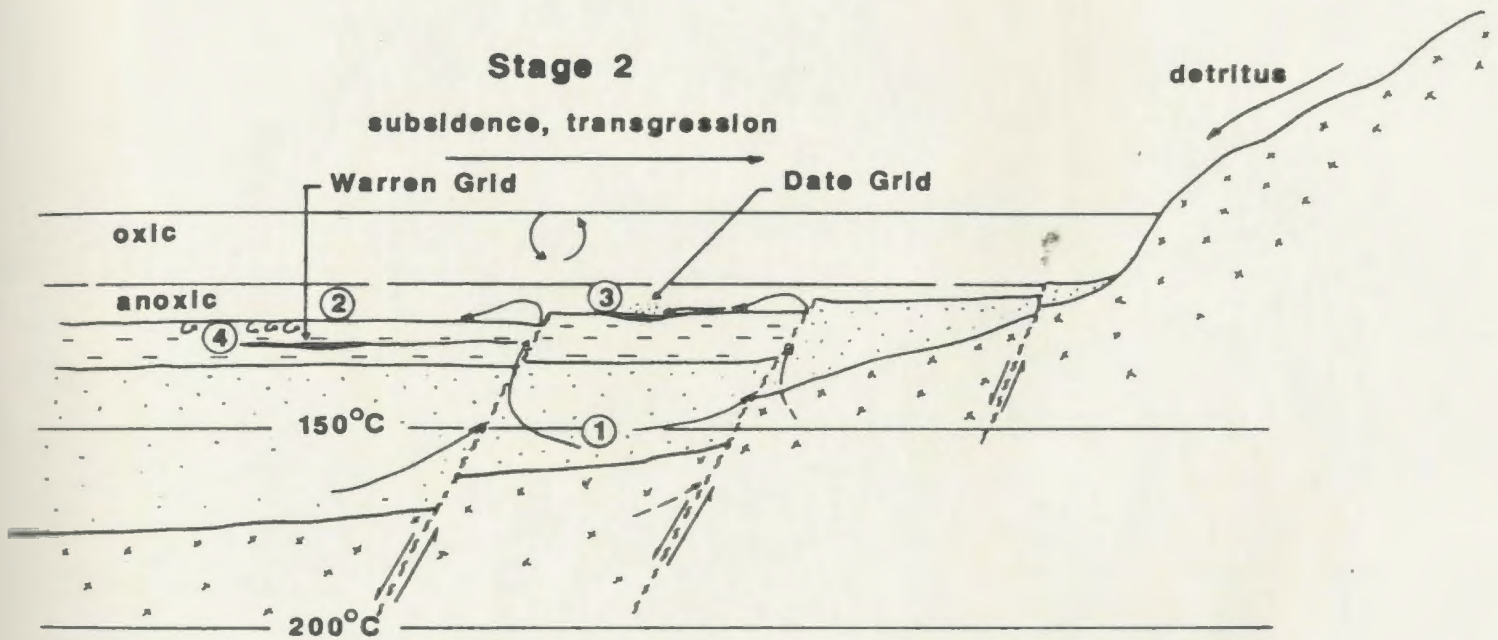


Fig. 5.2 Stage 2 of basin evolution, looking west, note reactions 1 to 4.



Fig. 5.3 Oxidized clastic detritus from Lower Member, note rounded detrital Fe-oxide grains (white) and detrital qtz. clasts (dark grey).

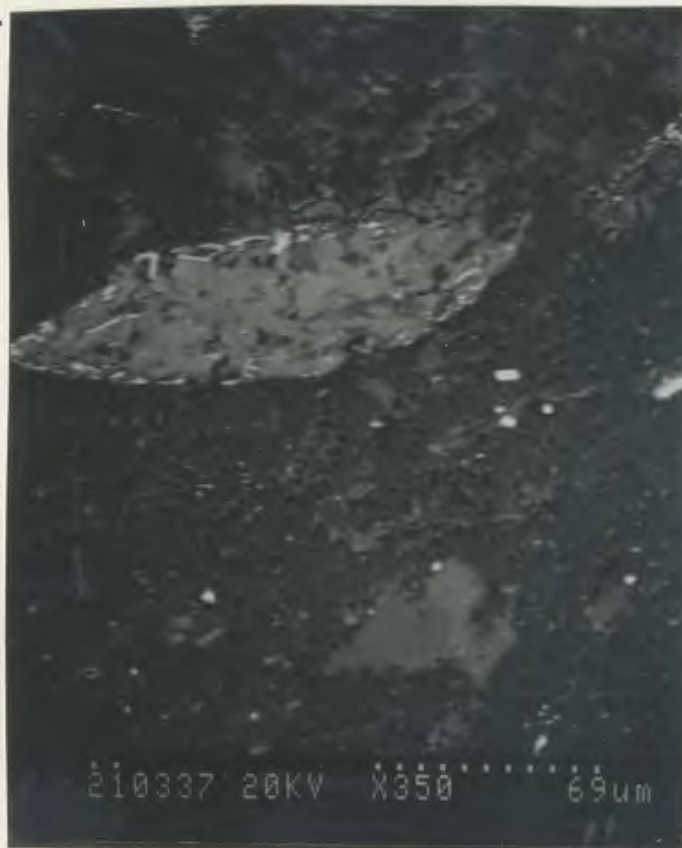


Fig. 5.4 Fe-oxide coating (light grey) on detrital qtz. clast, Lower Member.

form metal chloride (MeCl) rich brines. A simplified reaction for the solution of zinc oxide by a chloride-rich brine is as follows (Bourcier and Barnes, 1987):

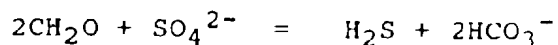


Periodic, and ephemeral, fluid residency in secondary porosity caused by fluid overpressurization and crack nucleation enhances the solute content of the brines (Etheridge et al., 1984) which ascend along lithostatic pressure gradients and normal faults to the sediment-sea water interface. Seismic pumping along normal faults (Sibson et al., 1975) may have also facilitated brine expulsion, and would explain the periodic deposition of the massive sulphide horizons in the Upper Member which are separated by as much as several hundred m of intervening barren shale. The seismic fluid pumping mechanism is facilitated by similar physical conditions as Etheridge et al.'s (1984, p. 4351) "crack seal fluid pump" which causes upward advection of pore fluids due to crack nucleation parallel to the direction of maximum shortening as P_{fluid} (in pore spaces) exceeds the minimum compressive stress + T (the tensile strength of the compacting sediments). The net fluid flow at this stage was vertical, away from the base of the sedimentary pile, causing a net volume decrease (compaction) of the sediments. No downward penetration of fluids (i.e. seawater) occurred in this stage as the formation brines were heated by the ambient geothermal

gradient of the subsiding basin and were expelled upwards from the compacting sediments by slow advective flow along normal lithostatic pressure gradients.

The Cl^- content, and thus base metal capacity (Barrett and Anderson, 1982) of the formation waters may have been increased by Cl^- contribution from the dolostone which occurs near the Archean-Aphebian unconformity. The resulting dense, saline fluids would probably correspond to Type 1 fluids of Sato (1972), at 120°C , and 3 m (17.6 wt.%) NaCl (Fig. 5.5).

2: Sea water sulphate (SO_4^{2-}) undergoes reduction below the seawater redox boundary by anerobic bacteria which decompose organic matter to produce H_2S according to the following simplified reaction (Westrich, 1983):



The energy derived from the reduction of sulphate by anerobic bacteria is used to drive cellular metabolic reactions (Dexter-Dyer et al., 1984) and thus, is a very common reaction in the reduced bottom waters of euxinic environments, and in the uppermost layers of organic-rich pelagic sediments (Berner, 1983; Dexter-Dyer et al., 1984).

3: Metal chloride complexes are expelled on to the sea-floor. The 3 m NaCl brines at 120° to 150°C would have a density greater than seawater (Sato, 1972; Lydon, 1983; Shanks et al., 1987) and thus, the fluid would

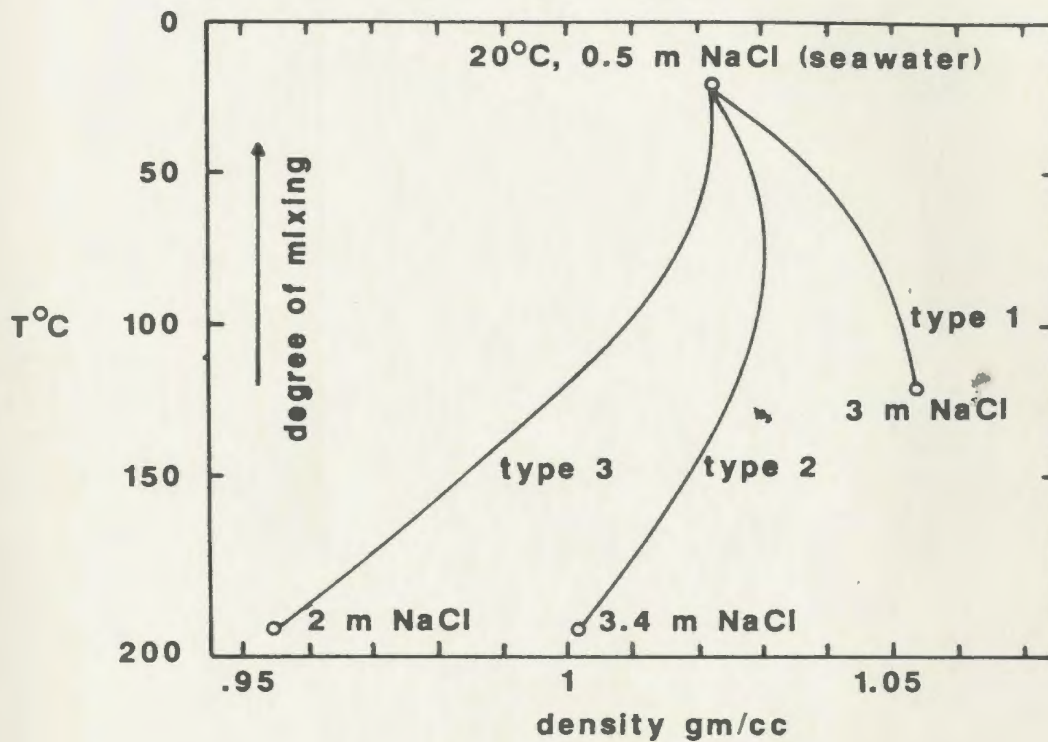


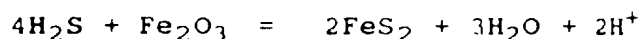
Fig. 5.5 Temperature, density, and salinity of hydrothermal fluids, after Sato (1972). Warren Creek Formation fluids were probably type 1, note that mixing is inhibited by the formation of a stable dense bottom layer.

naturally move downslope to settle in topographic lows, or if the basin was restricted, it would have formed the bottom anoxic layer of a stratified water column (Goodfellow, 1987). The metal chloride complexes reacted with H_2S^+ to form metal sulphides in a manner analogous to the following simplified reaction for sphalerite:



Metal sulphides precipitate out of solution as finely laminated sulphide beds. The finely laminated nature of the sulphide beds in the Warren Creek Formation suggests that this mineralization occurred in stable brine pools. The lack of any recognizable footwall alteration or metal zonation indicates that the sulphide beds were deposited distally from their discharge vents.

4: The reaction of $MeCl$ with H_2S may also occur in the surface layers of highly reduced pelagic sediments. The presence of decomposing organic material (preserved as graphite) greatly enhances the production of H_2S from pore water sulphate in pelagic sediments. The reaction of iron-bearing detrital minerals with H_2S in this environment results in the formation of diagenetic sedimentary pyrite (Hallberg, 1972; Berner, 1984; and Dexter-Dyer *et al.*, 1984) and is probably the source of the ubiquitous disseminated pyrite in the shales of the Upper Member of the Warren Creek Formation. The reaction may have proceeded according to the simplified equation for pyrite:



Thus, with active normal faults in place, there would be suitable topography for the deposition of dense brines in stable pools, sufficient reductant (H_2S) for the metal-bearing chloride complexes to react with and form sulphides, and massive sulphide deposition in the Upper Member of the Warren Creek Formation. The Warren and Date Grid sulphide horizons were deposited at this stage of basin evolution. These deposits are extremely iron-rich, and contain anomalous Zn (up to 4,702 ppm) and Cu (up to 612 ppm).

Stage 3: The middle dolostone bed is deposited at this stage (Fig. 5.6). The lateral extent of this bed is not known since it does not crop out west of Heart Pond. The presence of a chemical precipitate bed within the black shale sequence indicates that waters in the basin became hypersaline. This was probably caused by the shallowing of the basin by the protracted influx of detritus from the Archean highland. The detrital influx must have exceeded the rate of subsidence, indicating that the crustal heat flow was relatively low at this stage.

Stage 4: Rapid subsidence of the basin is reactivated with the return to the hydrologic and lithostatic conditions of Stage 2 (Fig. 5.7). Reactions 1 to 4 are again contributing a volumetrically significant sulphide component to the stratigraphy. The brine density and metal

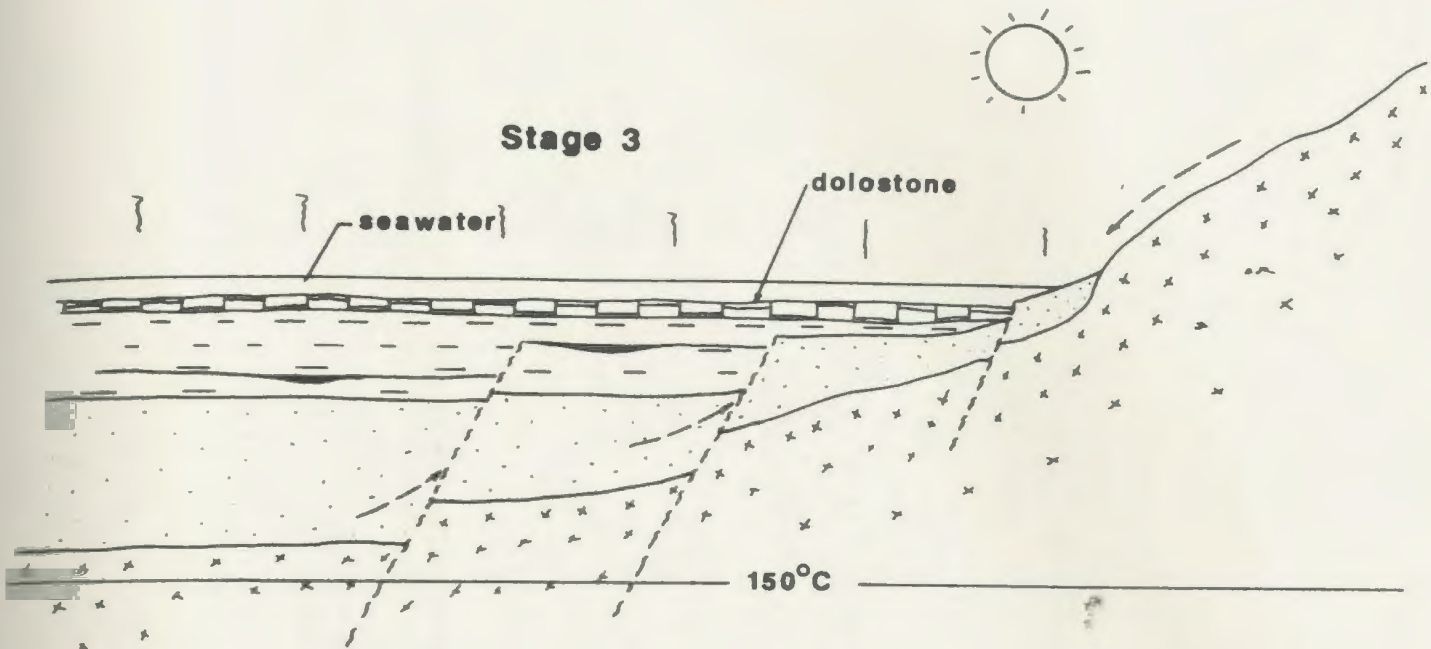


Fig. 5.6 Stage 3 of basin evolution, looking west.

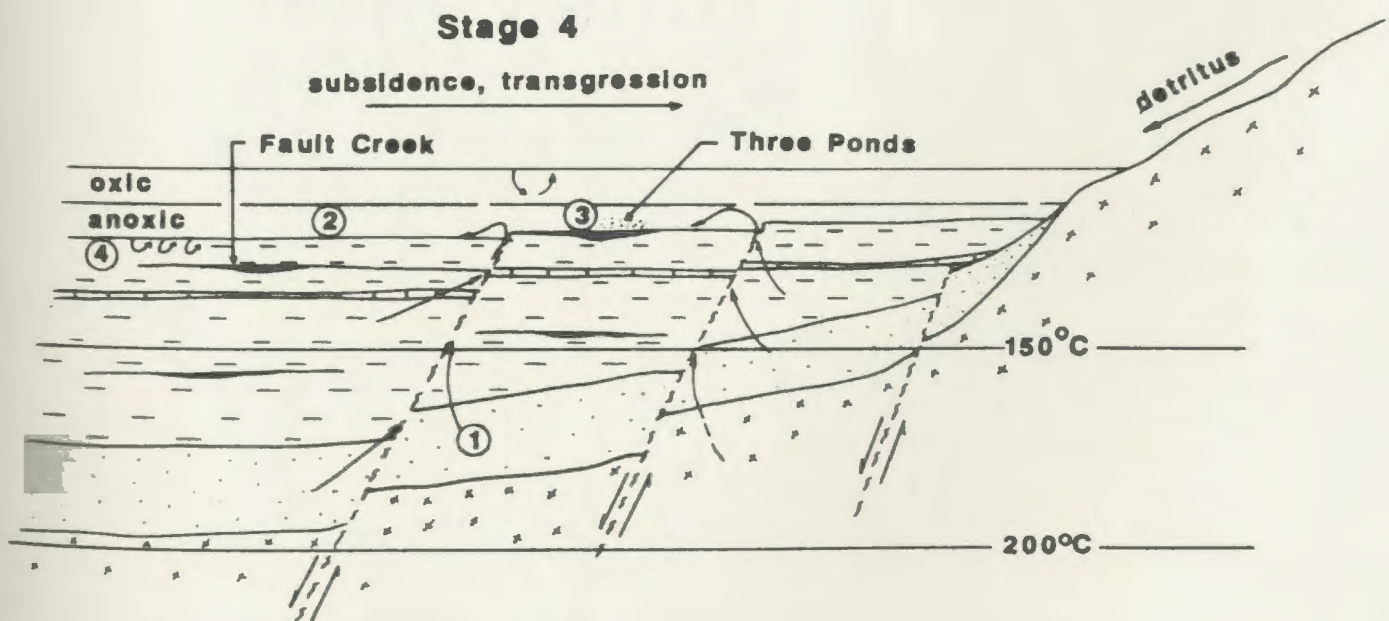


Fig. 5.7 Stage 4 of basin evolution, looking west.

content of the brines may have increased above the middle dolostone due to the contribution of chloride from this unit. The rate of fluid ascent is continually enhanced by the increasing thickness of sediments in the basin, and more efficient expulsion of pore water from basal sediments by advection and/or seismic pumping up normal faults. The Three Ponds and Fault Creek sulphide beds were deposited at this stage. Again, these contain anomalous concentrations of Zn (up to 2,865 ppm) and Cu (up to 759 ppm).

Stage 5: The Zn-rich Teuva showing is deposited at this stage (Fig. 5.8). The geochemistry and stratigraphic position of this mineral occurrence have important implications for the basinal heat flow and tectonic model of the basin. The Zn content of these rocks reaches 2.69%, but the Cu content is very low (max. 162 ppm). This metal fractionation and Zn enrichment trend is caused by an abrupt change in fluid chemistry resulting from a change in fluid flow from slow brine seepage and advective ascent in Stage 2 to 4, to rapid downward penetrating hydrothermal convection in this stage.

The Teuva mineralization is hosted in a clastic sedimentary horizon which was deposited immediately below a sequence of rocks which include vesicular basalt, arkose, and ironstone. These units were deposited in a stage of active tensional tectonics and uplift as described in Section 2.6. The deposition of these rocks, especially

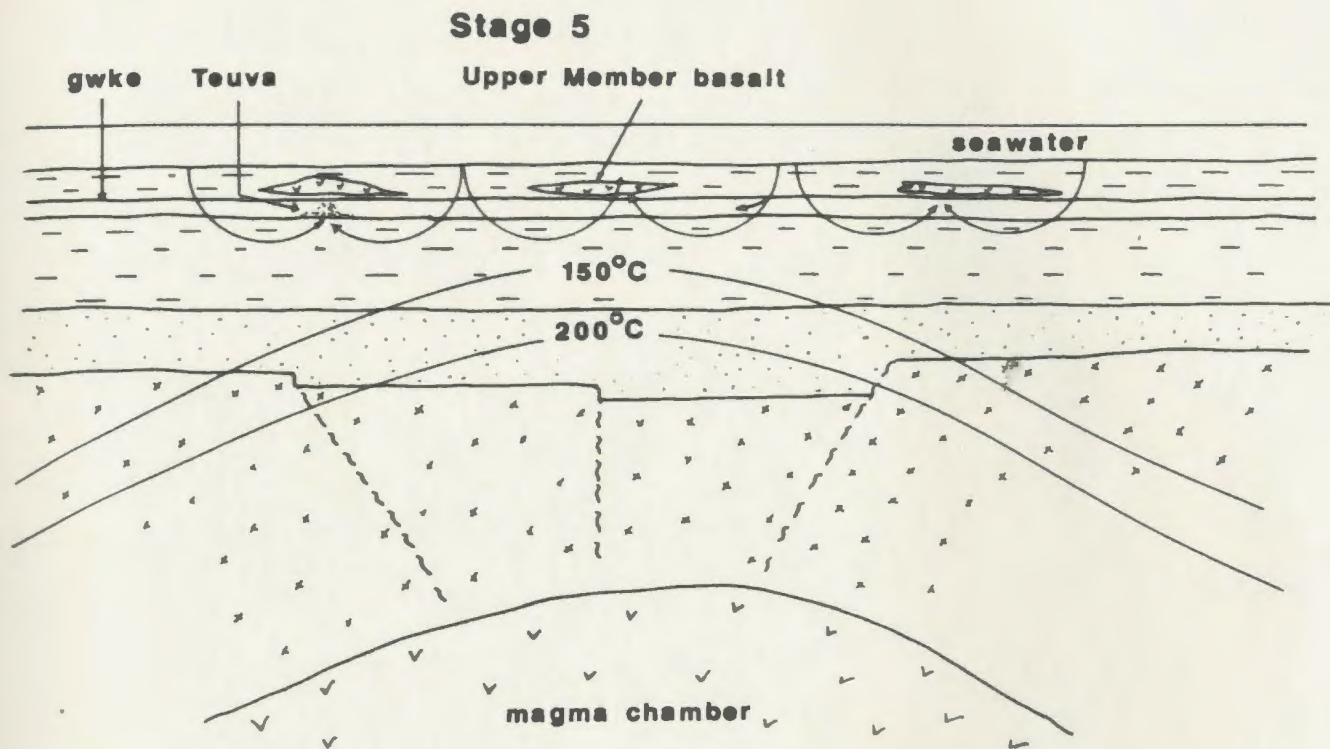


Fig. 5.8 Stage 5 of basin evolution, looking west.

the arkose which was deposited nearshore, requires significant crustal expansion and uplift from Stage 4. This would be facilitated by an increase in the geothermal gradient of the basin. This is indicated by the presence of vesicular and massive basalt flows in the upper portions of the Upper Member which appear directly above the Teuva Zn mineralization. These basalt flows are primitive (high Mg, Ti, Cr) relative to the succeeding Joe Pond Formation basalts, and represent the precursor magma to this later volcanism. These primitive lavas ascended along normal faults and tensional fractures which developed as the crust expanded under increased basinal heat flow.

Since the fluids which mineralized the Teuva showing did not contain a significant amount of Cu, they are interpreted to have been cooler than 200°C. Formation brines ascending from lower parts of the Upper Member at this stage would have probably been heated to at least 200°C as crustal isotherms were upwarped. Copper chloride complexes become much more soluble above this temperature (Lydon, 1983), however no significant Cu enrichment is present in the Teuva showing, in fact this mineralization is characterized by a depletion in Cu. This suggests that the mineralizing fluids were probably not heated formation waters derived from deep crustal levels, since the Teuva showing would probably contain at least as much copper as the stratiform sulphide mineral occurrences, and does not.

It is therefore proposed that the direction of fluid flow in the basin changed from upward seepage of Zn/Cu rich brines, to downward convection of seawater as crustal isotherms were upwarped prior to incipient Joe Pond volcanism. These fluids leached mobile Zn from shallow crustal levels by downward seawater penetration in a "conventional" circulating hydrothermal cell. The paucity of Cu in the Teuya showing indicates that these convection cells did not penetrate as deep as the 200°C isotherm. This also suggests that the newly initiated convective fluid flow was shortlived, since convection cells tend to progressively penetrate deeper crustal levels in active rifting environments (Russell et al., 1981; Russell, 1983). This interpretation is further supported by the observation that this stratabound sphalerite mineralization does not extend into the overlying porous arkose bed (see section 4.3), which it would have, if the hydrothermal regime had been active longer (subsequent to the deposition of this bed).

Stage 6: The Joe Pond Formation basalts ascend along an extensive network of normal faults and tensional fractures which developed in stages 1 to 5 and are upgraded in this stage by active tension and subsidence (Fig. 5.9). These basalts are fractionated relative to the underlying vesicular basalts in the Warren Creek Formation, reflecting the development of a stable a magma chamber

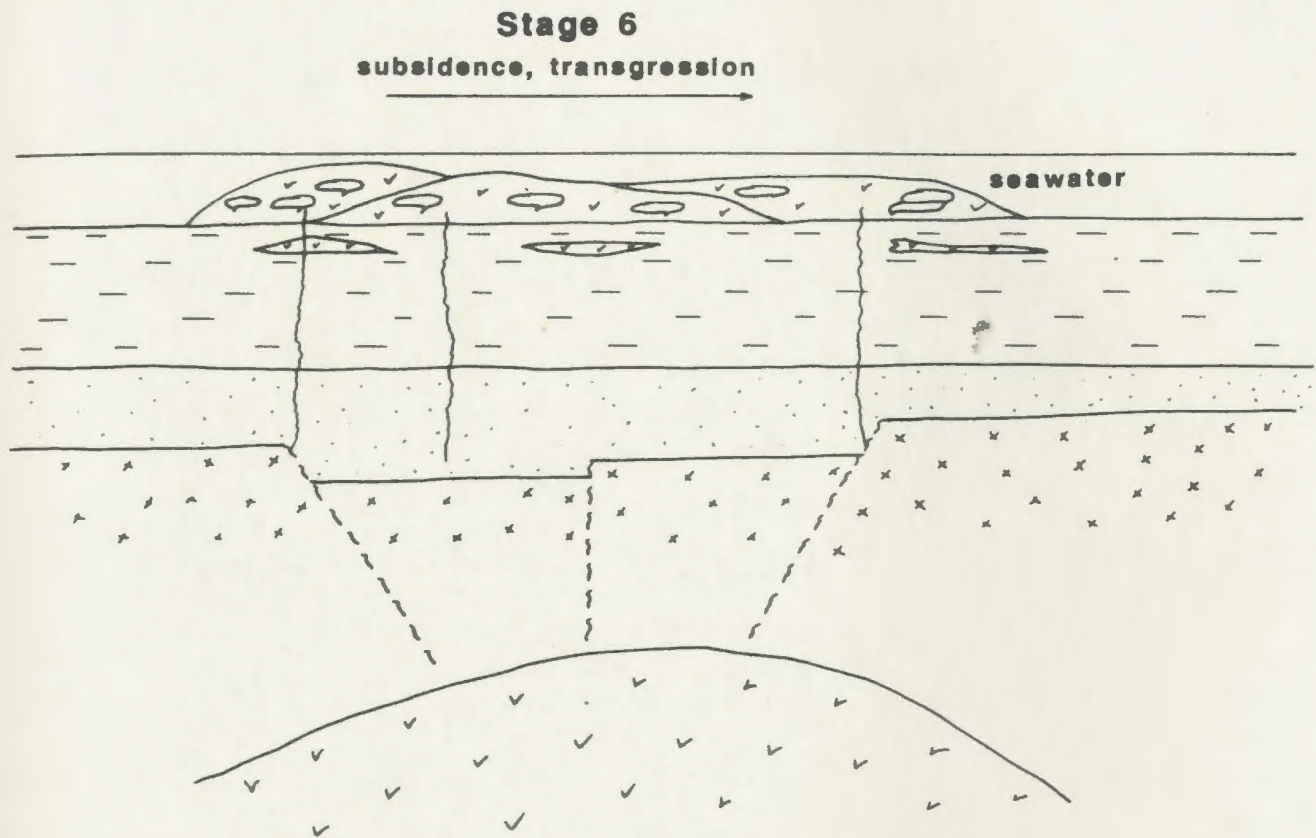


Fig. 5.9 Stage 6 of basin evolution, looking west.

below the basin.

5.3 Discussion and metallogenic model

Field mapping of the Moran Lake Group stratigraphy elucidated numerous common features between these rocks and typical marine transgressive sequences described in classic sedimentary exhalative Zn-Pb-Cu (Ag) deposit models (e.g. Morganti, 1981; Gustafson and Williams, 1981; Russell *et al.*, 1981, 1983; Carne and Cathro, 1982; Large, 1983; Lydon, 1983; Eugster, 1984). The combination of a porous basal sequence of sandstone and siltstone (Lower Member of the Warren Creek Formation) and an overlying black shale-siltstone sequence (Upper Member of the Warren Creek Formation) is of particular metallogenic significance. The hydrology of sedex deposits is such that, regardless of the sources for the metals and sulphur which form base metal sulphides, metalliferous brines must form and encounter H_2S to form stable sulphide ores. The combination of porous basal stratigraphy and tensional tectonics resulting in deep water shale deposition, are essential for the production and advection of metalliferous brines, and their expulsion and reaction with H_2S at, or near the sediment-seawater interface. The stratigraphy of the Moran Lake Group indicates that physical conditions for these reactions could have existed in this basin.

Geochemical study of sulphide mineralization in the

Moran Lake Group provided insight into less tangible aspects of basin evolution such as; degree of seismic activity from observation of the cyclic nature of massive sulphide deposition, basinal heat flow based on the development of chemically differentiated and texturally distinct sulphide mineralization (shown to vary from the base to the top of the Warren Creek Formation), and nature of formation brines based on metal content, degree of metal zonation within sulphide beds, and presence or absence of wall rock alteration. The results of this study indicate that none of the above features related to sulphide mineralization in the Moran Lake Group, are more than remotely similar to typical sedex orebody models, thus the Moran Lake Group does not represent an attractive exploration target. The reasons for this are described in greater detail below.

Metallogenic models for basin evolution near sedex orebodies climax with the deposition of a zoned exhalative Zn-Pb-Cu (Ag) orebody. The model for the evolution of the Moran Lake Group (above) does not climax with the deposition of a Zn-Pb-Cu (Ag) orebody. The geology and geochemistry of the Moran Lake Group suggest that such a climax is very unlikely since none of the geochemically analyzed samples contained significant amounts of Zn, Cu, Pb, or Ag (i.e. none of the "mineral occurrences" defined by the present work would constitute ore-grade

mineralization in a typical sedex orebody). At best there is potential for a clastic-hosted graphitic Zn-Cu deposit which might be developed by upgrading the Zn-Cu content of a typical stratiform graphitic pyrite bed such as the Three Ponds or Fault Creek mineral occurrences. There is also a possibility of forming a stratabound Zn deposit near the top of the Upper Member of the Warren Creek Formation similar in character to the Teuva mineral occurrence.

The lack of metal zonation within individual sulphide horizons, and absence of footwall alteration indicates that the sulphides were deposited under low temperatures from highly saline brines which were expelled from sediments undergoing compaction under the influence of a moderate geothermal gradient, ultimately to settle in topographic lows and deposit their metal load under reducing conditions. The fact that the solutions were very saline (3 m NaCl), and probably too dense to diffuse through pore spaces to any large degree (Lydon, 1983), indicates that these fluids were probably focused, and discharged from vents somewhere in the basin.

The chemistry of the lower mineral occurrences; Warren Grid, Date Grid, Fault Creek, and Three Ponds showings indicate, by their lack of metal fractionation, that pore fluids had a relatively long residency period with which to dissolve Zn and Cu from the hosting sediments. The base metal ratios of typical shale, showings, mineral

occurrences, and Archean basement are similar, indicating that no fractionation occurred from the leaching to depositional stages as sulphide-rich beds, thus the acquisition of these metals probably occurred over a protracted period, but the deposition was probably rapid, since no metal fractionation occurred after acquisition of these metals into the brines. In the Zambian, Kupferscheifer, and Angolan sedimentary copper belts, relatively oxidized grits and sandstone substrates act as a depository for Cu in ascending brines. The Cu is concentrated in oxidized zones proximal to the discharge vent, while mobile Zn is flushed through the sediments to distal sites of deposition (Van Eden, 1974; 1978).

Gustafson and Williams (1981) and Lydon (1983) advocate that the fractionation of Zn from Cu in sedex deposits is an inherent property of sedex mineralization. This can occur either by "filtering" through basal oxidized stratigraphy as discussed above, or simply by brine temperature and salinity (Carne and Cathro, 1982; Sato, 1977; Russell et al., 1981), or by deposition of Cu in footwall stockwork mineralization below finely bedded Zn-Pb-Ag ore as is the case at the giant Sullivan (Hamilton et al., 1983) McArthur River (Murray, 1975) and Rammelsberg (Hannak, 1981) orebodies.

The massive pyritic beds in the Moran Lake Group have none of these features, rather the brines implicated in the

deposition of the sulphide beds were low in overall base metal content, and are not selectively depleted in Cu by either; deposition of Cu in the Lower Member oxidized sandstones (since no Cu-rich Zn-poor mineral occurrences have ever been described in the Lower Member rocks), or deposition of Cu-rich stockworks below Zn-rich stratiform mineralization since no stockwork mineralization was discovered anywhere in this part of the Moran Lake Group.

Most of the sulphide mineralization in the Warren Creek Formation formed by slow seepage of brines through basal sandstones and shales with no abrupt redox changes, or temperature variation.

The Teuva showing is associated with significantly enriched Zn mineralization which is also fractionated with respect to Cu, reflecting uplift in the last stages of Upper Member deposition, and shallow penetration of ephemeral hydrothermal convection cells which did not penetrate to the 200°C isotherm. Zn was leached rapidly from the upper part of the Upper Member and deposited as podiform stratabound disseminated sphalerite in a porous sedimentary host. Copper is not enriched in the Teuva showing due to the short-lived downward penetrating convection and early saturation of fluids with the more mobile zinc chloride, and the shallow penetration of the convection cells. Obviously the Teuva mineralization does not fit the typical sedex Zn-Pb-Cu (Ag) model either, even

though "conventional" seawater convection did develop as suggested in the model of Russell et al. (1981).

5.4 Conclusions and recommendations

Known base metal mineralization in this part of the Moran Lake Group occurs as very low grade Fe-Zn-Cu stratiform sulphide beds and as small, Zn-rich, stratabound pods of disseminated sphalerite mineralization. Neither of these types of mineralization bear much similarity with the large sedex orebodies of the world such as Sullivan, Rammelsberg, Mt. Isa, or McArthur River. It is very unlikely that economic grade stratiform sediment-hosted Zn-Pb-Cu (Ag) ore occurs anywhere in this area. The style of mineralization in the Teuva however, should not be taken for granted since it may represent the incipient stages of classic "sedex" mineralization which was extinguished by effusive mafic volcanism.

From an economic perspective, the sphalerite mineralization similar to the type found at the Teuva showing represents the most attractive exploration target. The search for more of this type of mineralization would be most effective if directed in the Warren Creek Formation near the contact with the Joe Pond Formation, since this is where hydrologic and tectonic conditions were most favourable in the Moran Lake Group. The arkose bed in the core of the Mushroom Pond anticline would also be a

good place to look, should the hydrothermal system which mineralized the Teuva showing have existed subsequent to the deposition of this porous unit.

BIBLIOGRAPHY

- Andrew, A., Godwin, C.I., and Sinclair, A.J., 1984. Mixing line isochrons: a new interpretation of galena-lead isotope data from southeastern British Columbia. *Econ. Geol.*, vol. 79, p. 919-932.
- Arth, J.G., 1976. Behavior of trace elements during magmatic processes - a summary of theoretical models and their applications. *Journ. Research, U.S.G.S.*, vol. 4, no. 1, p. 41-47.
- Barrett, T.J. and Anderson, G.M., 1982. The solubility of sphalerite and galena in NaCl brines. *Econ. Geol.*, vol. 77, p. 1923-1933.
- Beavan, A.P., 1958. The Labrador uranium area. *G.A.C., Proceedings*, vol. 10, p. 137-145.
- Bell, T.H. and Etheridge, M.A., 1973. Microstructure of mylonites and their descriptive terminology. *Lithos*, vol. 6, p. 337-348.
- Berner, R.A., 1984. Sedimentary pyrite formation: an update. *Geochim. Cosmochim. Acta*, vol. 48, p. 605-615.
- Bonatti, E., 1975. Metallogenesis at oceanic spreading centers. *Ann. Rev. of Earth Plan. Sci.*, vol. 3, p. 401-431.
- Boucier, W.L., and Barnes, H.L., 1987. Ore solution chemistry - VII. Stabilities of chloride and bisulphide complexes of zinc to 350°C. *Econ. Geol.*, vol. 82, no. 7, p. 1839-1863.
- Cameron, E.M., and Garrels, R.M., 1980. Geochemical compositions of some Precambrian shales from the Canadian Shield. *Chemical Geology*, vol. 28, p. 181-197.
- Carne, R.C. and Cathro, R.J., 1982. Sedimentary exhalative (sedex) zinc-lead-silver deposits, northern Canadian Cordillera. *CIM Bull.* vol. 75, no. 840, p. 66-78.
- Corriveau, C.R., 1958. Report on the Montague No. 2 uranium prospect, Silas Lake area, Kaipokok Concession. Unpublished BRINEX report on file with Newfoundland Department of Mines.

- DeGrace, J.R., 1969. The geology of the Pocket Knife Lake area, Labrador. Unpublished BRINEX report on file with Newfoundland Department of Mines.
- Dexter-Dyer, B., Kretzschmar, M. and Krumbein, W.E., 1984. Possible microbial pathways in the formation of Precambrian ore deposits. *Jl. Geol. Soc. London*, vol. 141, p. 251-262.
- Dieterich, J.H., 1969. Computer experiments on mechanics of finite amplitude folds., *Can. Journ. Earth Sci.*, vol. 7, p. 467-476.
- Ellingwood, S.G., 1958. Report on geology of the Moran Lake area, Kaipokok concession. Unpublished BRINEX report on file with Newfoundland Department of Mines.
- Ermanovics, I.F. and Raudsepp, M., 1979a. Geology of the Hopedale block of eastern Nain Province, Labrador, NTS 13K and N: Report 1. In *Current Research, Part B, G.S.C., Pap. 79-1B*, p. 341-348.
- Etheridge, M.A., Wall, V.J., and Cox, S.F., 1984. High fluid pressures during regional metamorphism and deformation: implications for mass transport and deformation mechanisms., *Journ. Geophys. Research*, vol. 89, no. B6, p. 4344-4358.
- Eugster, H.P., 1985. Oil shales, evaporites and ore deposits. *Geochim. Cosmochim. Acta*, vol. 49, p. 619-635.
- Evans, E.L., 1950. Exploration in the Seal Lake area, Labrador. Unpublished Frobisher Exploration Limited report on file with Newfoundland Department of Mines and Energy, Mineral Development Division.
- Fahrig, W.F., 1959. Snegamook Lake, west half. *G.S.C., Map 1079A*.
- Fahrig, W.F. and Larochelle, A., 1972. Paleomagnetism of the Michael Gabbro and possible evidence of the rotation of Makkovik Subprovince. *C.J.E.S.*, vol. 9, p. 1287-1296.
- Fehn, U., 1986. The evolution of low temperature convection cells near spreading centers: a mechanism for the formation of the Galapagos mounds and similar manganese deposits. *Econ. Geol.*, vol. 81, no. 6, p. 1396-1407.

Finlow-Bates, T., 1979. Cyclicity in the lead-zinc-silver-bearing sediments at Mount Isa Mine, Queensland, Australia, and rates of sulfide accumulation. *Econ. Geol.*, vol. 74, p. 1408-1419.

Fulton, R.J., Hodgson, D.A., Minning, G.V., and Thomas, R.D., 1970. Surficial geology, Labrador (13K). G.S.C., Open File 81.

Goodfellow, W.D., 1987. Anoxic stratified oceans as a source of sulphur in sediment-hosted stratiform Zn-Pb deposits (Selwyn Basin, Yukon, Canada). *Chem. Geol. (Isotope Geoscience Section)*, vol. 65, p. 359-382.

Gower, C.F., Flanagan, M.J., Kerr, A., and Bailey, D.G., 1982. Geology of the Kapikok Bay - Big River area, Central Mineral Belt, Labrador. *Nfld Dept. of Mines and Energy Rept.* 82-7, 77 p.

Grant, N.K., Voner, F.R., Marzono, M.S., Hickman, M.H., and Ermanovics, I.F., 1983. A summary of Rb-Sr isotope studies in the Archean Hopedale Block and the adjacent Proterozoic Makkovik Subprovince, Labrador; Report 5, in *Current Research, Part B*, G.S.C. Pap. 83-1B, p. 127-134.

Graves, M.C. and Zentilli, M., 1988. The lithochemistry of metal-enriched cotecules in the Goldenville-Halifax transition zone of the Meguma Group, Nova Scotia. In *Current Research, Part B*, G.S.C., Paper 88-1B, p. 251-261.

Graybeal, A.L. and Heath, G.R., 1984. Remobilization of transition metals in surficial pelagic sediments from the eastern Pacific. *Geochim. Cosmochim. Acta*, vol. 48, p. 965-975.

Green, J., 1959. Geochemical table of the elements for 1959. *Geol. Soc. Am. Bull.*, vol. 70, no. 9, p. 1127-1183.

Gromet, L.P., Dyrek, R.F., Haskin, L.A., and Korotev, R.I., 1984. The "North American shale composite": It's compilation, major and trace element characteristics. *Geochim. Cosmochim. Acta*, vol. 48, p. 2469-2482.

Gustafson, L.B., and Williams, N., 1981. Sediment-hosted stratiform deposits of copper, lead, and zinc. *Econ. Geol. 75th Anniversary Volume*, p. 139-178.

- Haack, U., Heinrichs, H., Boness, M. and Schneider, A., 1984. Loss of metals from pelites during regional metamorphism. *Contrib. Mineral. Petrol.*, vol. 85, p. 116-132.
- Halet, R.A., 1946. Geological reconnaissance of the Naskaupi Mountains and adjoining regions, Newfoundland-Labrador. Unpublished Dome Exploration report on file with Newfoundland Department of Mines.
- Hallberg, R.O., 1972. Sedimentary sulfide mineral formation - an energy circuit system approach: *Mineral. Deposita*, vol. 7, p. 189-201.
- Hamilton, J.M., Delaney, G.D., Hauser, R.L., and Ransom, P.W., 1983. Geology of the Sullivan deposit, Kimberly B.C., Canada. in M.A.C. short course in sediment-hosted stratiform lead-zinc deposits, Victoria, May, 1983, ed. D.F. Sangster, p. 31-84.
- Hannak, W.G., 1981. Genesis of the Rammelsberg ore deposit near Goslar/Upper Hartz, Federal Republic of Germany, in Wolfe, K.H., ed., *Handbook of stratiform and stratabound ore deposits*, Elsevier Pub. Co. Amsterdam, vol. 9, p. 551-642.
- Hansuld, J.A., 1958. Exploration in Croteau Lake area, Block A, Frobisher Concession, Labrador, 1958. Unpublished BRINEX report on file with Newfoundland Department of Mines.
- Haynes, D.W., and Bloom, M.S., 1987. Stratiform copper deposits hosted by low energy sediments: IV. Aspects of sulphide precipitation. *Econ. Geol.*, vol. 82, no. 4, p. 875-893.
- Haynes, D.W., and Bloom, M.S., 1987. Stratiform copper deposits hosted by low energy sediments: III. Aspects of metal transport. *Econ. Geol.*, vol. 82, no. 3, p. 635-648.
- Hobbs, B.E., Means, W.D., and Williams, P.F., 1976. An outline of structural geology. John Wiley and Sons, Inc., 571 p.
- Hodgson, C.J., and Lydon, J.W., 1977. Geological setting of some volcanogenic massive sulphide deposits and active hydrothermal systems: some implications for exploration. *CIM Bull.*, vol. 70, no. 786, p. 95-106.

- Huston, D.L., and Large, R.R., 1987. Genetic and exploration significance of the zinc ratio ($100 \text{ Zn}/\text{Zn} + \text{Pb}$) in massive sulphide systems. *Econ. Geol.*, vol. 82, no. 6, p. 1521-1539.
- Irvine, T.N. and Baragar, W.R.A., 1971. A guide to the chemical classification of the common volcanic rocks. *C.J.E.S.*, vol. 8, p. 523-548.
- Jenner, G.A., Cawood, P.A., Rautenschlein, M., and White, W.M., 1987. Composition of back-arc basin volcanics, Valu Fa Ridge, Lau Basin., *J. Volc. Geochem. Res.* vol. 32, p. 209-222.
- Jowett, C.E., 1987. Genesis of Kupferschiefer Cu-Ag deposits by convective flow of Rotliegendes brines during Triassic rifting. *Econ. Geol.*, vol. 81, no. 8, p. 1823-1837.
- Krishnan, T.K., and Oertel, G., 1980. Aspects of strain history in folded sediments from the Schefferville mining district, Labrador Trough, Canada. *Tectonophysics*, vol. 64, p. 33-46.
- Lambert, I.B., 1983. The major stratiform lead-zinc deposits of the Proterozoic. *Geol. Soc. Am., Memoir* 161, p. 209-224.
- Landergrén, S., 1964. On the geochemistry of deep sea sediments. *Rep. Swed. Deep Sea Exped.*, vol. 10, p. 57-70.
- Large, D.E., 1983. Sediment-hosted massive sulphide lead-zinc deposits: an empirical model, in M.A.C. short course in sediment-hosted stratiform lead-zinc deposits, Victoria, May 1983, ed. D.F. Sangster, p. 1-30.
- Longerich, H.P., and Veinott, G., 1986. Study of precision and accuracy of XRF data obtained in the Department of Earth Sciences and Centre for Earth Resources Research at Memorial University of Newfoundland. Unpublished internal circular, 23 p.
- Lydon, J.W., 1983. Chemical parameters controlling the origin and deposition of sediment-hosted stratiform lead-zinc deposits, in M.A.C. short course in sediment-hosted stratiform lead-zinc deposits, Victoria, May 1983, ed. D.F. Sangster, p. 175-250.

- Mako, D.A. and Shanks, W.C., III, 1984. Stratiform sulfide and barite - fluorite mineralization of the Vulcan prospect, Northwest Territories: exhalation of basinal brines along a faulted continental margin. C.J.E.S., vol. 21, p. 78-91.
- Mathias, B.V., and Clarke, G.J., 1975. Mount Isa copper and silver-lead-zinc orebodies - Isa and Hilton mines. in Economic Geology of Australia and New Guinea, ed. C.L. Knight, Austral. Inst. Min. Metall., Mon., vol. 5, no. 1, p. 351-372.
- Middlemost, E.A.K., 1980. A contribution to the nomenclature and classification of volcanic rocks. Geol. Mag., vol. 117, p. 51-57.
- Miyashiro, A., 1974. Volcanic rock series in island arcs and active continental margins. Am. Journ. Sci., vol. 274, p. 321-355.
- Moore, D.W., Young, L.E., Modene, J.S., and Plahuta, J.T., 1987. Geologic setting and genesis of the Red Dog zinc-lead-silver deposit, Western Brooks Range, Alaska. Econ. Geol., vol. 81, no. 7, p. 1696-1727.
- Morganti, J.M., 1981. Ore deposit models-4. Sedimentary-type stratiform ore deposits, some models and a new classification, Geoscience Canada, vol. 8, p. 65-75.
- Murray, W.J., 1975. McArthur River H.Y.C. lead-zinc and related deposits, N.T. in Knight, C.L. ed., Economic Geology of Australia and Papua New Guinea, vol. 1 Metals, p. 329-339. Australas. Inst. Min. Metall., Melbourne.
- North, J.W. and Wilton, D.H.C., 1987a. Sediment-hosted stratiform zinc mineralization in the Moran Lake Group, Central Mineral Belt, Labrador. Newfoundland Department of Mines and Energy, Open File Report 13K/6 (171), 8 p.
- North, J.W. and Wilton, D.H.C., 1987b. Proterozoic sediment-hosted Fe-Cu-Zn massive sulphide horizons in the Warren Creek Formation of the Moran Lake Group, Labrador Central Mineral Belt. CIM Bull., vol. 80, p. 85.
- North, J.W., and Wilton, D.H.C., 1988. Stratigraphy of the Warren Creek Formation, Moran Lake Group, Central Mineral Belt of Labrador. in Current Research, Part C, G.S.C., Paper 88-1C, p. 123-128.

- O'Connor, J.T., 1965. A classification for quartz-rich igneous rocks based on feldspar ratios. USGS. Prof. Pap. 525B, p. 1379-1384.
- Pearce, J.A., 1975. Basalt geochemistry used to investigate past tectonic environments on Cyprus. Tectonophysics, vol. 25, p. 41-67.
- Pearce, J.A., and Cann, J.R., 1973. Tectonic setting of basic volcanic rocks determined using trace element analyses. E.P.S.L., vol. 19, p. 290-300.
- Perry, J., 1979. Annual exploration report, 1978, CANICO-BRINEX joint venture, Moran and Seal Lake areas, Labrador, NTS 13J, 13K, 13L. Unpublished CANICO report on file with Newfoundland Department of Mines.
- Perry, J., 1980. Annual exploration report, 1979, CANICO-BRINEX joint venture, Moran and Seal Lake areas, Labrador, NTS 13J, 13K, 13L. Unpublished CANICO report on file with Newfoundland Department of Mines.
- Perry, J., 1981. Annual exploration report, 1980, June 23-August 25, CANICO-BRINEX joint venture, Moran Lake area, Labrador, NTS 13J, 13K. Unpublished CANICO report on file with Newfoundland Department of Mines.
- Piloski, M.J., 1955. Geological report on the Aillik-Shoal Lake area. Unpublished BRINEX Ltd. report on file with Newfoundland Department of Mines.
- Piloski, M.J., 1958. Report on the Moran Lake lead-zinc occurrence, Moran Lake, Kaipokok concession. Unpublished BRINEX report on file with Newfoundland Department of Mines.
- Ramberg, H., 1963a. Fluid dynamics of viscous buckling applicable to folding of layered rocks., Am. Assoc. Petrol. Geol., vol. 47, p. 484-505.
- Ramberg, H., 1967. Gravity, deformation and the Earth's crust. Academic Press, New York, 214 p.
- Ramsay, J.G., 1967. Folding and fracturing of rocks. McGraw-Hill, New York, 568 p.
- Ramsay, J.G., 1976. Displacement and strain. Phil. Trans. R. Soc. Lond. A., vol. 283, p. 3-25.

- Robertson, A.H.F., 1981. Metallogenesis on a Mesozoic passive continental margin, Antalya Complex, southwest Turkey. *E.P.S.L.*, vol. 54, p. 323-345.
- Robertson, A.H.F., and Boyle, J.F., 1983. Tectonic setting and origin of metalliferous sediments in the Mesozoic Tethys ocean., in *Hydrothermal processes at sea floor spreading centers*, ed. P.A. Rona, K. Bostrom, L. Laubier, and K.L. Smith Jr., NATO conference series, Plenum Press, New York, p. 595-663.
- Russell, M.J., Solomon, M., and Walshe, J.L., 1981. The genesis of sediment hosted zinc-lead deposits, *Mineral. Deposita.*, vol. 16, p.113-127.
- Russell, M.J., 1983. Major sediment-hosted exhalative zinc + lead deposits: formation from hydrothermal convection cells that deepen during crustal extension. in *M.A.C. short course in sediment-hosted stratiform lead-zinc deposits*, Victoria, May 1983, ed. D.F. Sangster, p. 251-282.
- Ryan, A.B., 1984. Regional geology of the central part of the Central Mineral Belt, Labrador. Newfoundland Department of Mines and Energy, Mem. 3, 185 p.
- Sander, G.W., 1971. Report on the helicopter borne geophysical survey on behalf of BRINEX in the Ten Mile Lake, Seal Lake and Moran Lake areas of Labrador. Unpublished BRINEX report on file with Newfoundland Department of Mines.
- Sato, T., 1972. Behaviors of ore-forming solutions in seawater, *Mining Geology (Japan)*, vol. 22, p. 31-42.
- Sato, T., 1977. Los sulfuros masivos volcanogeneticos, su metalogenia y clasificacion. Dept. Geologia, Univ. Sonora, Publ. No. 1, 54 p.
- Sawkins, F.J., 1984. Ore genesis by episodic dewatering of sedimentary basins: application to giant Proterozoic lead-zinc deposits. *Geology*, vol. 12, p. 451-454.
- Scharer, U., Wardle, R.J., Ryan, A.B., and Gandhi, S.S. In prep. Uranium and lead ages of Lower to Middle Proterozoic volcanism and metamorphism in the Makkovik Province, Labrador.
- Scott, R.B., Rona, P.A., McGregor, B.A., and Scott, M.R., 1974. The TAG hydrothermal field. *Nature*, vol. 251, p. 301-302

- Shanks, W.C., Woodruff, L.G., Jilson, G.A., Jennings, D.S., Modene, J.S., Ryan, B.D., 1987. Sulphur and lead isotope studies of stratiform Zn-Pb-Ag deposits, Anvil Range, Yukon: basinal brine exhalation and anoxic bottom-water mixing., *Econ. Geol.*, vol. 82, p. 600-634.
- Shervais, J.W., 1982. Ti-V plots and the petrogenesis of modern and ophiolitic lavas. *E.P.S.L.*, vol. 59, p. 101-118.
- Sibson, R.H., Moore, J.McM. and Rankin, A.H., 1975. Seismic pumping - a hydrothermal fluid transport mechanism. *Jl. Geol. Soc. London*, vol. 131, p. 653-659.
- Smyth, W.R., Marten, B.E., and Ryan, A.B., 1975. Geological mapping in the Central Mineral Belt, Labrador: redefinition of the Croteau Group. In *Rept. of Activities 1974. Newfoundland Department of Mines and Energy*, Rept. 75-1, p. 51-74.
- Smyth, W.R., Marten, B.E., and Ryan, A.B., 1978. A major Aphebian-Helikian unconformity within the Central Mineral Belt of Labrador: definition of new groups and metallogenic implications. *C.J.E.S.*, vol. 15, p. 1954-1966.
- Smyth, W.R. and Ryan, A.B., 1977. Geological setting of the Moran Lake uranium showings, Central Mineral Belt, Labrador. In *Report of Activities for 1976, Newfoundland Department of Mines and Energy*, Rept. 77-1, p. 57-62.
- Smyth, W.R. and Ryan, A.B., 1978. Geological map of the Pocket Knife Lake area, NTS 13K/6. Newfoundland Department of Mines and Energy, Map 78-171.
- Stanton, R.L., 1976. Petrochemical studies of the ore environment at Broken Hill, New South Wales, 4 - environmental synthesis, *Trans. Instn. Min. Metall. (Sect. B: Appl. earth sci.)* vol. 85, p. 221-233.
- Streckeisen, A., 1976. Classification of the common igneous rocks by means of their chemical composition: a provisional attempt. *Neues Jahrbuch fuer Mineralogie, Monatshefte*, vol. 1, p. 1-15.

- Strens, M.R., Cann, D.L., and Cann, J.R., 1987. A thermal balance model of the formation of sedimentary-exhalative lead-zinc deposits. *Econ. Geol.*, vol. 82, no. 5, p. 1192-1203.
- Sun, S.S., 1980. Lead isotopic study of young volcanic rocks from mid-ocean ridges, ocean islands and island arcs. *Phil. Trans. R. Soc. Lond.*, A 297, p. 409-445.
- Sun, S.S., and Nesbitt, R.W., 1978. Geochemical regularities and genetic significance of ophiolitic basalts. *Geology*, vol. 6, p. 689-693.
- Sverjensky, D.A., 1987. The role of migrating oil-field brines in the formation of sediment-hosted Cu-rich deposits. *Econ. Geol.*, vol. 82, no. 5, 1130-1141.
- Sweeney, M., Turner, P., and Vaughan, D.J., 1987. Stable isotope and geochemical studies in the role of early diagenesis in ore formation, Konkola basin, Zambian Copper Belt. *Econ. Geol.*, vol. 81, no. 8. p. 1838-1852.
- Taylor, S.R., and McLennan, S.M., 1981. The composition and evolution of the continental crust: rare earth element evidence from sedimentary rocks. *Phil. Trans. R. Soc. Lond.*, A 301, p. 381-399.
- Thompson, F.J., and Klassen, R.A., 1986. Ice flow directions and drift composition, central Labrador; in *Current Research, Part A, G.S.C., Pap. 86-1A*, p. 713-717.
- Thompson, R.N., Morrison, M.A., Hendry, G.L., and Parry, S.J., 1984. An assessment of the relative roles of crust and mantle in magma genesis: an elemental approach. *Phil. Trans. R. Soc. Lond.* A 310, p. 549-590.
- Turekian, K.K., and Wedepohl, K.H., 1961. Distribution of the elements in some major units of the Earth's crust. *Geol. Soc. Am. Bull.*, vol. 72, no. 2, p. 175-191.
- Van Eden, J.G., 1974. Depositional and diagenetic environment related to sulphide mineralization, Mufulira, Zambia. *Econ. Geol.*, vol. 69, p. 59-79.
- Van Eden, J.G., 1978. Stratiform copper and zinc mineralization in the Cretaceous of Angola. *Econ. Geol.*, vol. 73, p. 1154-1161.

- Vine, J.D. and Tourtelot, E.B., 1970. Geochemistry of black shale deposits - a summary report. Econ. Geol., vol. 65, p. 253-272.
- Wardle, R.J. and Bailey, D.G., 1981. Early Proterozoic sequences in Labrador. In Proterozoic Basins of Canada, G.S.C., Pap. 81-10, p. 331-359.
- Wardle, R.J., Rivers, T., Gower, C.F., Nunn, G.A.G., and Thomas, A., 1986. The northeastern Grenville Province: new insights, in The Grenville Province, G.A.C., Spec. Pap. 33, p. 13-30.
- Wavra, C.S., Isaacson, P.E. and Hall, W.E., 1986. Studies of the Idaho black shale belt: stratigraphy, depositional environment, and economic geology of the Permian Dollarhide Formation. Geol. Soc. Am. Bull., vol. 97, p. 1504-1511.
- Westrich, J.T., 1983. The consequences and controls of bacterial sulphate reduction in marine sediments. Unpub. Ph.D. dissertation, Yale University, 530 p.
- Wilton, D.H.C., 1986. Pb isotope data from a reconnaissance galena sampling program in the Central Mineral Belt of Labrador. NFLD. Section G.A.C., Annual Spring Meeting, March 20-21, 1986, program with abstracts, 20 p.
- Wilton, D.H.C., MacDougall, C.S., and MacKenzie, L.M., 1986a. Final report on 1985 field work in the Central Mineral Belt, Labrador; ERDA Agreement II-2, Metallogeny of the Central Mineral Belt. Unpublished report submitted to Geological Survey of Canada, 149 p.
- Wilton, D.H.C., MacDougall, C.S., MacKenzie, L.M., and North, J.W. 1986b. Preliminary report on field work completed during 1986 in the Central Mineral Belt, Labrador; ERDA Agreement II-2, Metallogeny of the Central Mineral Belt. Unpublished report submitted to Geological Survey of Canada, 59 p.
- Wilton, D.H.C., MacDougall, C.S., MacKenzie, L.M., and North, J.W., 1987. Precious metal contents in samples from the eastern Central Mineral Belt, Labrador. Newfoundland Department of Mines and Energy, Open File Report Lab (724), 39 p.

- Wilton, D.H.C., and North, J.W., 1987. A comparison of stratigraphy between the Lower Aillik and Moran Lake Groups, Central Mineral Belt, Labrador. prog. with Abst., Newfoundland Sec. G.A.C., Annual Spring Meeting, "The Geology of Labrador", p. 7.
- Wilton, D.H.C., MacDougall, C.S., MacKenzie, L.M., and Pumphrey, C., 1988. Stratigraphic and metallogenic relationships along the unconformity between Archean granite basement and the early Proterozoic Moran Lake Group, central Labrador. in Current Research, Part C, G.S.C., Paper 88-1C, p. 277-282.
- Wilton, D.H.C., 1988. Copper occurrences in the Bruce River Group, Central Mineral Belt of Labrador. in Current Research, Part C, G.S.C., Paper 88-1C, p. 291-297.
- Wronkiewicz, D.J., and Condie, K.C., 1987. Geochemistry of Archean shales from the Witwatersrand Supergroup, South Africa: source-area weathering and provenance. Cosmochim. Geochim. Acta, vol. 51, p. 2401-2416.

APPENDIX 1
ANALYTICAL METHODS

Sample preparation

Grab samples weighing 2-4 kg. were collected for geochemical analysis. Oxide coatings and weathered rinds were removed using a rotary rock-cutting table saw. The rock slabs and chips were then crushed in a table top jaw crusher for up to two minutes before pulverizing in a tungsten-carbide puck mill. This produced a powder of at least -100 mesh. If a large quantity of chips were pulverized, the resultant powder was coned and split into halves until just enough powder remained to fill a 125 ml sample bottle.

Major element analyses

Loss on ignition (volatiles) was determined by weighing an aliquot of rock powder (weighed accurately to 10^{-4} g) into a porcelain crucible, heating the crucible to 1050° C for at least two hours, cooling in a dessicator, and then weighing the de-volatized sample for percent loss of volatiles.

P₂O₅ was analyzed with a Bausch and Lomb Spectronic 20 Colourimeter (ie. colourimetrically), based on a modification of the method outlined by Shapiro and Brannock (1962).

The other major element oxides were determined by atomic absorption spectrometry. Samples were prepared using the methods of Langmhyr and Paus (1968) and the elements were analyzed on a Perkin-Elmer Model 370 atomic absorption spectrometer with digital readout. Sulphide-rich samples from the Warren Creek formation required dissolution in aqua-regia. Precision of this method is indicated in Table 1.

Trace element analyses

The trace elements were determined by X-Ray fluorescence techniques on pressed whole rock powder pellets using a Phillips 1450 automatic X-Ray fluorescence spectrometer with a rhodium tube. The pellets were made from a mixed powder containing 10 g sample and 1-1.5 g binding material (Union Carbide Phenolic Resin TR-16933). The powder was pressed at 30 tons psi for a minute before being baked for 10 minutes at 150°C. Data reduction was computed with a Hewlett-Packard 9845B mini computer.

Precision and accuracy for the trace element analyses are given in Table 2 using the standards as listed. Published values are from Flanagan (1973).

Precious metal determinations

Seven prepared pulps were sent to Bondar-Clegg &

Company Ltd., Ottawa, Ont., for Au/Ag analysis by instrumental neutron activation analysis (I.N.A.A.). This method involves weighing and encapsulating 10 g of pulp into a vial, and analysis by neutron activation.

REE determinations

Rare earth elements (REE) were determined by the following method:

- 1- a standard HF/HNO₃ digestion of 0.1 gm sample
- 2- analysis of the solution by inductively coupled plasma mass spectrometry (ICP-MS) using the method of standard addition to correct for matrix effects.

Sample material insoluble in HF/HNO₃ was attacked with HCl/HNO₃. Some of the Warren Creek Formation massive sulphide/graphite samples required this, any residue after HCl/HNO₃ digestion was filtered off.

A reagent blank (RBK) and a sample of the CANMET geological reference standard SY-2 (syenite) were analyzed with the samples. The reagent blank concentrations are not subtracted from these analyses since this contamination is usually insignificant. At least one sample solution was analyzed in duplicate for each analytical run.

Scanning electron microscopy and ion probe analyses

Polished, carbon-coated thin sections were examined in

Table 1 Precision of Major Element Analyses

(based on four analyses of standard G-2. Published value from Flanagan (1970)).

<u>Element</u>	<u>Published</u>		<u>S.D.</u>	<u>Range</u>	
	<u>Value</u>	<u>Mean</u>		<u>Low</u>	<u>High</u>
SiO ₂	69.11	69.70	0.57	68.50	69.96
Al ₂ O ₃	15.40	15.10	0.24	14.75	15.60
Fe ₂ O ₃	2.65	2.60	0.02	2.64	2.74
MgO	0.76	0.80	0.005	0.75	0.82
CaO	1.94	2.00	0.10	1.92	2.14
Na ₂ O	4.07	4.30	0.02	4.07	4.21
K ₂ O	4.51	4.56	0.02	4.50	4.57
TiO ₂	0.50	0.50	0.01	0.47	0.51
MnO	0.03	0.03	0.00	-	-

Table 2 Precision and accuracy of trace element analyses

S.D. = standard deviation; N= no. of analyses; Pub. =
published value.

	<u>W-1</u>	<u>S.D.</u>	<u>N</u>	<u>Pub.</u>	<u>G-2</u>	<u>S.D.</u>	<u>N</u>	<u>Pub</u>
V	263	4.73	7	240	43	3	10	34
Cr	96.8	2.5	7	120	13	3	10	9
Cu	99.0	2.16	7	110	17	1	10	11
Zn	95.7	1.70	7	86	85	2	10	85
Rb	22.6	2.07	7	21	166	2	10	170
Sr	172	2.94	7	190	477	7	10	480
Y	25.1	3.08	7	25	11	2	11	12
Zr	87.3	1.70	7	105	292	3	10	300
Nb	7.29	1.50	7	9.5	10	1	10	14
Ba	183	10.2	7	160	1865	30	10	1850
Pb	9.86	3.33	7	8	27	2	10	29

a Hitachi S570 Scanning Electron Microscope at an accelerating voltage of 15-20 kv. Backscattered electron imaging utilized a GW Electronics Type 113 solid state Backscattered Electron Detector. X-ray analysis was performed on beam spot mode with a Tracor Northern 9500 Energy Dispersive X-ray analyzer equipped with a microtrace silicon X-ray spectrometer, Model 70152, with a spectral resolution of 145 eV. Detector-sample positioning gave an effective take-off angle of 30° .

Backscattered electron images were recorded on Polaroid Type 665 Positive/Negative film.

References cited in Appendix 1

Flanagan, F.J., 1970. Sources of geochemical standards-II. *Geochim. Cosmo. Acta*, v.34, p. 121-125.

Flanagan, F.J., 1973. 1972 values for internal geochemical reference standards. *Geochim. Cosmo. Acta*, v.37, p. 1189-1200.

Langmhyr, F.J., and Paus, P.E., 1968. The analysis of inorganic siliceous materials by atomic absorption spectrophotometry and the hydrofluoric acid decomposition technique. Pt.1. The analysis of silicate rocks. *Anal. Chimica Acta*, v.43, pp.397-408.

Shapiro, L. and Brannock, W.W., 1962. Rapid analysis of silicate, carbonate and phosphate rocks. *U.S. Geol. Surv. Bull.* 1144A, pp. 31-3.

APPENDIX 2

GEOCHEMICAL ANALYSES

Major and trace elements analyzed by A.A. and XRF respectively.

Archean basement

File Name : archean

Sample :	a-1	a-2	a-4	a-5	a-6	a-14	a-15	a-18
SiO ₂	81.70	72.00	70.80	68.00	69.90	70.60	71.20	60.10
TiO ₂	-	0.40	0.44	0.40	0.12	0.32	0.36	0.76
Al ₂ O ₃	9.62	13.90	14.60	14.70	11.60	13.90	12.50	14.40
FeO	0.11	2.27	2.92	2.60	2.23	2.54	4.03	6.88
MnO	0.01	0.03	0.02	0.04	0.09	0.03	0.03	0.08
MgO	0.10	1.08	1.66	1.49	1.63	1.00	0.92	3.51
CaO	0.36	0.80	1.24	1.76	3.66	2.42	1.14	2.92
Na ₂ O	3.39	5.20	4.05	4.38	4.58	5.02	1.83	4.35
K ₂ O	2.43	1.56	2.37	2.30	1.46	1.46	3.18	1.39
P ₂ O ₅	0.01	0.07	0.14	0.10	0.03	0.07	0.11	0.33
Total :	97.73	97.31	98.24	95.77	95.30	97.36	95.30	94.72
LOI	0.41	1.75	2.24	3.12	5.34	2.89	3.16	3.40
Mg #	62.00	46.00	50.00	51.00	57.00	41.00	29.00	48.00
Cr	-	-	-	1	-	3	13	23
Ni	-	-	-	4	-	-	-	5
V	-	36	35	42	18	28	48	125
Cu	-	3	1	1	2	3	34	-
Pb	-	-	-	-	-	5	866	-
Zn	-	36	50	53	8	34	191	106
Rb	-	56.00	94.00	82.00	50.00	43.00	109.00	52.00
Ba	-	312	674	1377	1164	684	-	338
Sr	-	197.0	193.0	159.0	193.0	239.0	106.0	239.0
Ga	-	19.00	18.00	18.00	12.00	15.00	25.00	20.00
Nb	-	4.00	5.00	6.00	4.00	5.00	2.00	10.00
Zr	-	112.0	138.0	162.0	74.0	104.0	160.0	193.0
Ti	-	2398	2638	2398	719	1918	2158	4556
Y	-	7.0	12.0	8.0	12.0	11.0	6.0	24.0
Th	-	-	-	-	3.000	-	10.000	-
U	-	-	-	-	3.00	-	3.00	-

Lower Member

File Name : lwrwarcr

Sample : vc-2 vc-3 vc-6

SiO ₂	91.20	67.40	64.20
TiO ₂	-	0.36	0.48
Al ₂ O ₃	0.56	15.80	16.70
FeO	2.76	3.91	4.63
MnO	0.49	0.01	0.04
MgO	0.56	1.77	2.23
CaO	1.16	0.26	1.26
Na ₂ O	0.01	2.40	2.80
K ₂ O	0.01	3.69	3.82
P ₂ O ₅	0.01	0.08	0.07
Total	: 96.76	95.68	96.23

LOI	2.27	2.65	3.45
-----	------	------	------

Mg #	27.00	45.00	46.00
------	-------	-------	-------

Cr	-	72	86
Ni	-	20	42
V	14	71	80
Cu	10	10	10
Pb	3	-	-
Zn	4	30	34

Rb	1.00	116.00	118.00
Ba	-	569	654
Sr	32.0	70.0	78.0
Ga	-	9.00	19.00

Zr	7.0	227.0	199.0
Ti	-	2158	2878
Y	6.0	70.0	18.0

Upper Member typical shale

File Name : wcshale

Sample	:	dg-2	dg-3	dg-4	wc-25	wc-35	wc-47	wc-49
SiO ₂		50.40	43.40	59.10	61.90	-	73.40	-
TiO ₂		1.96	1.36	0.44	0.36	-	0.12	-
Al ₂ O ₃		13.40	15.40	15.70	18.70	-	12.60	-
FeO		13.31	15.52	7.60	-	-	2.61	-
MnO		0.03	0.04	0.03	0.02	-	0.02	-
MgO		5.92	8.99	5.48	2.14	-	1.04	-
CaO		0.32	0.56	0.20	0.14	-	0.32	-
Na ₂ O		1.30	1.01	2.68	2.82	-	2.97	-
K ₂ O		2.30	1.19	2.02	3.97	-	2.65	-
P ₂ O ₅		0.16	0.39	0.10	0.05	-	0.07	-
Total	:	89.10	87.86	93.35	90.10	0.00	95.80	0.00
LOI		7.75	6.91	4.55	3.07	-	2.90	-
Mg #		44.00	51.00	56.00	100.00	0.00	42.00	0.00
Cr		169	26	110	83	83	43	1621
Ni		56	40	77	37	40	11	207
V		670	871	291	99	145	45	981
Cu		183	176	63	31	46	23	236
Pb		-	-	-	9	27	16	8
Zn		145	178	107	69	56	18	191
Rb		47.00	35.00	72.00	135.00	108.00	83.00	9.00
Ba		983	494	271	503	648	377	23
Sr		26.0	39.0	46.0	103.0	111.0	113.0	103.0
Ga		19.00	25.00	18.00	24.00	17.00	14.00	28.00
Nb		17.00	22.00	12.00	13.00	8.00	8.00	66.00
Zr		198.0	277.0	198.0	184.0	242.0	218.0	533.0
Y		37.0	61.0	21.0	20.0	18.0	17.0	42.0
Th		-	-	-	15.000	13.000	-	-
U		7.00	-	-	9.00	15.00	-	10.00

File Name : wcshale			
Sample	: wc-50	wc-55	wc-61
SiO ₂	-	-	61.10
TiO ₂	-	-	0.40
Al ₂ O ₃	-	-	18.10
FeO	-	-	4.34
MnO	-	-	-
MgO	-	-	1.60
CaO	-	-	0.20
Na ₂ O	-	-	3.85
K ₂ O	-	-	3.82
P ₂ O ₅	-	-	0.07
Total	0.00	0.00	93.48
LOI	-	-	5.27
Mg #	0.00	0.00	40.00
Cr	7	3	106
Ni	4	5	34
V	64	30	233
Cu	4	33	26
Pb	-	13	3
Zn	110	224	45
Rb	149.00	42.00	113.00
Ba	759	210	674
Sr	86.0	21.0	84.0
Ga	39.00	16.00	24.00
Nb	128.00	46.00	11.00
Zr	868.0	378.0	269.0
Y	65.0	29.0	24.0
Th	3.000	17.000	-
U	5.00	17.00	-

File Name : wcshale

Sample :	wc-110	wc-165	wc-195	wc-215	wc-224	wc-206	wc-200	wc-205	wc-115
Cr	849	222	155	73	933	99	146	103	141
Ni	47	53	43	28	304	40	48	22	1
Co	45	-	27	-	40	-	-	-	-
Sc	-	-	-	-	-	24	54	25	29
V	315	423	424	106	307	222	329	215	215
Cu	60	63	65	35	189	82	61	17	19
Pb	-	-	5	10	-	-	3	5	2
Zn	94	98	73	98	667	335	123	43	55
Rb	4.00	85.00	95.00	88.00	-	112.00	74.00	131.00	133.00
Ba	91	355	647	835	-	851	239	666	721
Sr	7.0	39.0	106.0	76.0	20.0	132.0	40.0	93.0	88.0
Ga	10.00	22.00	23.00	19.00	13.00	23.00	22.00	25.00	25.00
Nb	24.00	23.00	8.00	5.00	33.00	-	-	-	-
Zr	199.0	206.0	138.0	135.0	216.0	196.0	99.0	186.0	130.0
Y	13.0	28.0	21.0	13.0	24.0	19.0	15.0	18.0	19.0
Th	1.000	11.000	-	9.000	3.000	-	1.000	13.000	6.000
U	10.00	9.00	7.00	11.00	7.00	4.00	9.00	10.00	13.00

Showings

File Name : showings

Sample	:	trc-2	trc-3	trc-4	trc-5	trc-6	tre-1	uc-66
SiO ₂		48.60	51.80	45.30	50.70	62.30	20.00	-
TiO ₂		1.20	1.96	1.32	0.56	0.48	0.08	-
Al ₂ O ₃		12.50	18.40	15.50	9.50	10.40	5.33	-
FeO		19.69	11.10	17.95	20.12	15.23	50.95	-
MnO		0.04	0.04	0.05	0.31	0.04	0.04	-
MgO		8.05	4.22	4.62	5.72	2.21	3.41	-
CaO		0.52	0.46	0.38	2.88	1.58	0.06	-
Na ₂ O		0.67	1.60	1.84	0.22	1.12	0.55	-
K ₂ O		0.78	3.94	2.52	0.43	2.33	0.10	-
P ₂ O ₅		0.24	0.27	0.27	0.30	0.04	-	-
Total	:	92.29	93.79	89.75	90.74	95.73	80.52	0.00
LOI		7.49	5.37	9.30	7.78	3.42	19.43	-
Mg #		42.00	40.00	31.00	34.00	21.00	11.00	0.00
Cr		91	249	198	129	62	30	43
Ni		47	60	42	41	11	474	54
Co		-	-	-	-	-	80	-
Sc		-	-	-	-	-	-	-
V		706	641	621	338	65	291	338
Cu		229	320	126	150	-	191	361
Pb		9	-	-	-	-	31	-
Zn		214	772	275	207	46	658	664
Au		-	-	-	-	-	28.0	-
Rb		19.00	101.00	69.00	12.00	69.00	5.00	7.00
Ba		291	1419	933	168	655	94	54
Sr		19.0	38.0	43.0	73.0	49.0	4.0	50.0
Ga		17.00	21.00	17.00	7.00	9.00	-	8.00
Nb		15.00	16.00	15.00	8.00	8.00	11.00	-
Zr		190.0	209.0	174.0	101.0	179.0	59.0	76.0
Ti		7194	11750	7913	3357	2878	480	12000
Y		54.0	64.0	65.0	36.0	17.0	16.0	18.0
Th		-	-	-	-	-	-	-
U		5.00	2.00	1.00	-	2.00	-	16.00

File Name : showings

Sample	: wc-40b	wc-67	n-1	n-2	wc-94	wc-216	tra-1	tra-2
SiO ₂	39.30	28.90	26.40	46.10	-	17.60	91.60	96.70
TiO ₂	5.04	0.20	0.24	0.24	-	0.12	-	-
Al ₂ O ₃	12.40	5.95	3.02	5.67	-	1.04	-	-
FeO	21.76	38.84	36.38	20.34	-	55.80	2.91	0.23
MnO	0.15	0.02	-	-	-	0.03	0.04	-
MgO	6.27	1.85	0.40	0.70	-	1.11	0.22	-
CaO	1.38	0.04	-	0.02	-	-	0.74	0.06
Na ₂ O	0.02	1.41	0.42	1.11	-	0.01	-	-
K ₂ O	1.72	0.56	0.90	1.39	-	0.03	-	0.03
P ₂ O ₅	1.00	0.03	0.05	0.04	-	0.02	0.18	-
Total	: 89.04	77.80	67.81	75.61	0.00	75.76	95.69	97.02
LOI	7.37	22.27	32.41	23.83	-	22.95	2.85	2.22
Hg #	34.00	8.00	2.00	6.00	57.00	3.00	12.00	0.00
Cr	3049	70	79	92	359	-	-	4
Ni	1719	307	373	180	347	512	6	-
Co	-	-	72	280	79	-	-	94
V	836	501	838	941	281	250	-	4
Cu	266	533	347	612	486	759	40	7
Pb	26	15	69	42	-	26	-	7
Zn	859	4702	353	383	2865	2126	-	-
Au	-	-	78.0	70.0	19.0	-	-	-
Rb	44.00	15.00	30.00	50.00	-	8.00	3.00	1.00
Ba	342	144	165	309	-	-	5	14
Sr	27.0	8.0	3.0	12.0	245.0	-	29.0	4.0
Ga	6.00	-	4.00	11.00	-	-	-	-
Nb	46.00	8.00	7.00	9.00	15.00	16.00	2.00	3.00
Zr	504.0	65.0	71.0	109.0	122.0	55.0	5.0	6.0
Ti	30215	1199	1439	1439	6115	719	-	-
Y	45.0	18.0	19.0	39.0	28.0	-	7.0	6.0
Th	-	2.000	-	4.000	-	-	-	-
U	-	31.00	37.00	27.00	12.00	-	-	-

File Name : showings

Sample	: trb-1	trc-1		vc-224	vc-21	vc-206		vc-218
SiO ₂	45.10	48.80	SiO ₂	-	37.30	-	SiO ₂	51.30
TiO ₂	1.40	1.32	TiO ₂	-	4.68	-	TiO ₂	0.56
Al ₂ O ₃	13.30	8.76	Al ₂ O ₃	-	12.00	-	Al ₂ O ₃	12.20
FeO	20.90	22.33	FeO	-	19.55	-	FeO	11.52
MnO	0.02	0.16	MnO	-	0.16	-	MnO	0.09
MgO	8.17	3.88	MgO	-	10.79	-	MgO	7.09
CaO	0.28	1.68	CaO	-	1.70	-	CaO	0.38
Na ₂ O	0.74	0.25	Na ₂ O	-	0.05	-	Na ₂ O	3.28
K ₂ O	1.18	1.02	K ₂ O	-	1.05	-	K ₂ O	1.63
P ₂ O ₅	0.18	0.31	P ₂ O ₅	-	0.74	-	P ₂ O ₅	0.25
Total	91.27	88.51	Total	0.00	88.02	0.00	Total	: 88.30
LOI	8.05	10.23	LOI	-	7.95	-	LOI	8.47
Mg #	41.00	24.00	Mg #	0.00	50.00	0.00	Mg #	52.00
Cr	135	72	Cr	933	58	99	Cr	85
Ni	88	60	Ni	304	90	40	Ni	54
Co	61	53	Co	40	91	-	Co	91
V	706	404	Sc	18	-	-	V	537
Cu	210	516	V	307	906	222	Cu	155
Pb	8	-	Cu	189	85	82	Zn	127
Zn	173	184	Pb	-	-	-		
			Zn	667	200	335	Rb	32.00
Au	-	-					Sr	110.0
			Au	-	-	-	Ga	20.00
Rb	29.00	29.00						
Ba	463	396	Rb	-	15.00	112.00	Zr	200.0
Sr	17.0	40.0	Ba	-	2787	851	Y	37.0
Ga	17.00	8.00	Sr	20.0	60.0	132.0	Th	5.000
			Ga	13.00	32.00	23.00	U	2.00
Nb	13.00	13.00						
Zr	155.0	142.0	Nb	-	-	-		
Ti	8393	7913	Zr	216.0	466.0	196.0		
Y	36.0	45.0	Ti	34100	-	-		
Th	-	-	Y	24.0	49.0	19.0		
U	-	-	Th	3.000	-	-		
			U	7.00	-	4.00		

Teuva showing

File Name : teuva

Sample :	hp-1.1	hp-1.2	hp-1.3	hp-1.4	hp-7	hp-8
SiO ₂	42.50	49.10	48.60	45.10	46.70	35.50
TiO ₂	2.68	3.84	4.04	1.40	3.44	2.56
Al ₂ O ₃	10.60	9.10	9.10	9.85	8.55	5.63
FeO	15.11	14.23	15.31	13.16	20.23	14.83
MnO	0.10	0.12	0.12	0.08	0.18	0.27
MgO	14.81	12.57	12.28	14.78	10.46	13.18
CaO	0.88	0.68	0.72	1.08	0.78	9.60
Na ₂ O	-	-	-	0.01	-	0.01
K ₂ O	-	-	-	0.01	0.02	0.02
P ₂ O ₅	0.66	0.56	0.60	0.80	0.53	0.20
Total :	87.34	90.20	90.77	86.27	90.89	81.80
LOI	7.22	5.67	5.43	7.00	6.75	15.68
Mg #	64.00	61.00	59.00	67.00	48.00	61.00
Cr	-	82	39	-	97	1220
Ni	95	62	75	90	114	848
Co	59	49	57	-	59	-
V	547	757	718	383	556	436
Cu	99	162	123	121	86	115
Pb	-	-	-	-	-	4
Zn	26900	20900	22200	37295	206	110
Rb	3.00	3.00	5.00	2.00	3.00	2.00
Ba	28	37	44	39	148	29
Sr	40.0	29.0	29.0	43.0	35.0	146.0
Ga	30.00	23.00	25.00	37.00	13.00	-
Zr	402.0	341.0	336.0	392.0	326.0	154.0
Ti	16067	23021	24220	8393	20623	15347
Y	47.0	42.0	35.0	52.0	43.0	23.0
Th	-	1.000	-	1.000	-	-
U	-	5.00	-	-	-	-

Gabbro

File Name : gabbro

Sample	:	vc-24	vc-27	vc-174	vc-184	vc-185	vc-194	vc-196
SiO ₂		50.20	50.30	45.90	-	45.20	52.80	49.80
TiO ₂		0.92	1.40	0.36	-	3.44	0.64	0.76
Al ₂ O ₃		9.95	16.20	12.00	-	5.76	13.30	13.70
FeO		11.67	11.21	9.34	-	15.65	8.29	11.60
MnO		0.18	0.15	0.15	-	0.20	0.13	0.16
MgO		13.15	5.14	6.81	-	12.73	7.74	11.58
CaO		8.74	4.90	7.56	-	13.16	7.76	7.38
Na ₂ O		1.88	2.96	1.72	-	0.95	2.63	2.68
K ₂ O		1.11	2.32	2.23	-	0.34	2.90	1.32
P ₂ O ₅		0.20	0.61	0.21	-	0.30	0.30	0.22
Total	:	98.00	95.19	86.28	0.00	97.73	96.49	99.20
LOI		2.76	4.05	12.70	-	2.66	2.63	1.73
Mg #		67.00	45.00	57.00	67.00	59.00	62.00	64.00
Cr		378	93	409	1627	1076	413	388
Ni		106	22	51	538	766	171	103
Sc		-	-	33	-	-	24	-
V		221	269	208	136	399	204	232
Cu		38	76	2	33	233	88	10
Pb		-	3	-	-	-	2	1
Zn		129	89	68	74	130	56	88
Rb		26.00	61.00	68.00	39.00	7.00	77.00	36.00
Ba		786	751	526	356	86	800	410
Sr		330.0	508.0	273.0	372.0	182.0	545.0	360.0
Ga		9.00	18.00	14.00	8.00	14.00	16.00	11.00
Nb		7.00	8.00	-	5.00	32.00	-	6.00
Zr		69.0	100.0	70.0	64.0	244.0	83.0	96.0
Ti		5515	8393	2158	5200	20623	3836	4556
Y		24.0	32.0	14.0	12.0	29.0	17.0	15.0
Th		-	-	6.000	-	-	-	-
U		-	2.00	7.00	-	1.00	9.00	10.00

File Name : gabbro

Sample	: wc-192	wc-186	wc-214	wc-84	wc-189
SiO ₂	58.20	-	49.00	48.00	49.40
TiO ₂	0.40	-	0.44	0.44	0.28
Al ₂ O ₃	13.70	-	14.90	13.40	14.90
FeO	12.08	-	8.16	8.41	9.08
MnO	0.05	-	0.13	0.13	0.13
MgO	4.35	-	7.12	7.21	7.38
CaO	0.92	-	7.34	7.70	5.62
Na ₂ O	1.92	-	3.11	1.91	0.28
K ₂ O	1.51	-	1.79	1.48	2.09
P ₂ O ₅	0.21	-	0.17	0.16	0.27
Total	: 93.34	0.00	92.16	88.84	89.43
LOI	4.93	-	7.27	9.32	8.84
Mg #	39.00	40.00	61.00	60.00	59.00
Cr	312	1082	-	205	364
Ni	86	152	64	19	38
Sc	-	44	-	-	35
V	450	242	239	192	244
Cu	79	82	8	23	21
Pb	15	-	11	-	-
Zn	137	85	75	47	119
Rb	47.00	31.00	42.00	46.00	78.00
Ba	388	380	540	373	349
Sr	40.0	297.0	407.0	348.0	118.0
Ga	17.00	14.00	14.00	10.00	18.00
Nb	22.00	-	5.00	7.00	-
Zr	183.0	99.0	68.0	59.0	81.0
Ti	2398	-	2638	2638	1678
Y	22.0	20.0	16.0	16.0	19.0
Th	11.000	-	11.000	-	6.000
U	11.00	3.00	10.00	1.00	6.00

Joe Pond Formation

File Name : joepond

Sample	:	jp-1	jp-10	jp-14	jp-15	jp-17	jp-2	jp-5
SiO ₂		43.70	47.10	49.30	44.40	35.40	47.60	44.80
TiO ₂		0.68	0.80	0.88	4.80	4.92	0.76	4.36
Al ₂ O ₃		13.70	13.60	12.20	10.80	13.40	12.90	9.33
FeO		11.41	12.00	11.91	20.80	24.08	14.15	14.29
MnO		0.19	0.18	0.20	0.19	0.35	0.16	0.18
MgO		9.70	8.74	9.60	8.09	8.24	12.03	7.96
CaO		7.52	10.90	9.08	4.80	3.70	3.74	9.32
Na ₂ O		2.03	3.20	3.11	0.02	0.02	1.19	0.33
K ₂ O		0.36	0.10	0.15	0.11	1.38	0.04	2.65
P ₂ O ₅		0.05	0.07	0.05	0.56	0.55	7.34	0.48
Total	:	89.34	96.69	96.48	94.57	92.05	99.91	93.70
LOI		9.82	3.01	2.63	5.06	6.10	7.34	5.04
Mg #		60.00	56.00	59.00	41.00	38.00	60.00	50.00
Cr		370	211	177	69	136	142	81
Ni		180	107	91	74	124	68	73
Co		66	-	-	-	-	-	-
Sc		49	-	-	-	-	-	-
V		324	287	300	677	822	395	522
Cu		942	105	101	-	100	317	152
Pb		-	-	-	-	12	-	-
Zn		79	60	62	159	253	76	103
Rb		12.00	-	5.00	-	11.00	5.00	47.00
Cs		2.00	-	-	-	-	-	-
Ba		111	79	78	493	2311	50	4620
Sr		69.0	109.0	96.0	81.0	208.0	33.0	313.0
Ga		9.00	15.00	2.00	27.00	31.00	-	21.00
Nb		7.00	5.00	6.00	57.00	63.00	7.00	52.00
Zr		45.0	48.0	47.0	367.0	424.0	48.0	345.0
Ti		4077	4796	5276	28776	29495	4556	26138
Y		18.0	20.0	26.0	37.0	37.0	23.0	40.0
Th		-	1.000	-	5.000	6.000	-	-
U		1.00	4.00	-	8.00	16.00	-	7.00

File Name : joepond

Sample	: wc-13	wc-130	wc-16		wc-201	wc-23
SiO ₂	46.10	48.70	48.40	SiO ₂	53.90	41.10
TiO ₂	0.68	0.76	0.88	TiO ₂	1.32	5.60
Al ₂ O ₃	13.50	13.40	17.20	Al ₂ O ₃	13.40	10.30
FeO	11.26	9.69	8.80	FeO	16.00	17.36
MnO	0.17	0.17	0.13	MnO	0.17	0.20
MgO	9.58	7.36	6.16	MgO	5.73	9.19
CaO	11.00	7.68	6.56	CaO	1.50	9.36
Na ₂ O	2.34	3.43	3.38	Na ₂ O	2.36	0.31
K ₂ O	0.36	0.16	2.42	K ₂ O	0.84 ^p	1.05
P ₂ O ₅	0.04	0.09	0.24	P ₂ O ₅	0.09	0.70
Total	95.03	91.44	94.17	Total	: 95.31	95.17
LOI	3.67	7.42	5.07	LOI	3.77	5.20
Mg #	60.00	58.00	56.00	Mg #	39.00	49.00
Cr	180	209	18	Cr	223	29
Ni	121	101	8	Ni	82	85
Co	-	-	-	Sc	70	-
Sc	-	43	-	V	500	633
V	268	300	177	Cu	-	112
Cu	82	57	19	Zn	206	129
Pb	-	-	-	Rb	23.00	27.00
Zn	59	48	7	Ba	270	929
Rb	4.00	1.00	45.00	Sr	61.0	176.0
Cs	-	-	-	Ga	18.00	20.00
Ba	184	36	682	Nb	-	60.00
Sr	44.0	85.0	420.0	Zr	90.0	397.0
Ga	10.00	9.00	12.00	Ti	7913	33572
Nb	8.00	-	6.00	Y	20.0	45.0
Zr	48.0	42.0	56.0	Th	8.000	-
Ti	4077	4556	5276	U	4.00	-
Y	23.0	16.0	17.0			
Th	-	-	-			
U	-	7.00	4.00			

Upper Member basalt

File Name : wcbasalt

Sample : wc-41 wc-82 hp-4

SiO ₂	37.30	46.10	42.10
TiO ₂	4.28	2.04	4.12
Al ₂ O ₃	8.18	13.90	9.74
FeO	19.11	13.33	19.93
MnO	0.21	0.14	0.16
MgO	9.43	9.45	9.42
CaO	9.98	5.56	6.36
Na ₂ O	0.02	2.03	0.21
K ₂ O	0.10	2.06	0.48
P ₂ O ₅	0.38	1.17	0.35
Total	: 88.99	95.78	92.87
LOI	11.12	4.71	7.99
Mg #	47.00	56.00	46.00
Cr	93	150	46
Ni	119	62	135
V	595	262	722
Cu	181	25	119
Zn	128	106	134
Rb	11.00	61.00	27.00
Ba	58	1286	89
Sr	272.0	577.0	238.0
Ga	16.00	13.00	15.00
Nb	39.00	10.00	28.00
Zr	266.0	99.0	225.0
Ti	25659	12230	24699
Y	34.0	33.0	37.0
U	15.00	-	4.00

Trace and rare earth elements determined by ICP-MS

Archean basement

File Name : archean					
Sample :	a-2	a-18	a-6	a-4	a-5
Sc	1	13	1	2	2
Rb	57.22	56.90	49.03	95.67	82.80
Cs	1.51	1.51	0.58	3.27	2.00
Ba	331	332	1188	652	1409
Sr	199.1	265.9	201.4	200.6	172.7
Tl	0.36	0.29	0.31	1.48	0.49
Li	12.77	43.86	2.36	18.68	16.84
Ta	0.54	0.40	0.39	0.12	0.55
Nb	1.35	3.05	0.31	0.21	1.31
Hf	1.23	1.08	0.61	0.93	1.02
Zr	40.5	40.1	15.4	31.7	34.1
Y	1.8	15.1	3.1	1.9	1.8
Th	2.104	4.135	1.357	5.600	0.380
U	0.23	0.64	0.14	1.33	0.17
La	14.2	47.4	6.6	20.8	7.1
Ce	27.7	96.5	13.5	37.2	13.2
Pr	2.8	10.8	1.6	4.0	1.4
Nd	9.4	38.2	6.2	12.1	4.9
Sm	1.4	6.2	1.2	2.1	0.8
Eu	0.4	1.4	0.4	0.4	0.3
Gd	1.0	4.7	3.1	1.3	1.9
Tb	0.1	0.6	0.1	0.1	0.1
Dy	0.4	3.5	0.6	0.5	0.4
Ho	0.1	0.6	0.1	0.1	0.1
Er	0.2	1.8	0.3	0.5	0.2
Tm	0.0	0.2	0.0	0.1	0.0
Yb	0.1	1.5	0.1	0.1	0.1
Lu	0.0	0.2	0.0	0.0	0.0

showings

typical shale

File Name : showings						wcshale		
Sample :	vc-67	m-1	vc-94	vc-216	trc-3	vc-35	vc-206	NASC
Sc	13	9	16	3	48	9	12	15
Rb	11.76	36.10	2.11	0.63	84.29	107.46	109.63	125.00
Cs	2.11	2.85	1.35	0.21	1.53	2.10	2.35	5.16
Ba	122	163	5	46	991	537	784	636
Sr	11.6	9.4	278.6	4.8	43.8	114.5	112.1	142.0
Tl	6.90	6.71	0.36	3.43	5.87	0.73	1.00	-
Li	28.53	17.24	7.21	15.98	96.76	24.16	38.44	-
Ta	0.64	1.30	3.93	0.20	1.75	0.16	0.60	1.12
Nb	5.83	13.09	30.43	1.54	19.03	3.13	6.16	-
Hf	1.74	1.19	3.02	0.41	5.51	3.89	3.74	6.30
Zr	60.7	48.1	109.0	16.1	180.0	121.2	113.2	200.0
Y	9.5	16.9	26.7	3.7	15.3	11.7	7.9	-
Th	1.337	1.510	1.760	0.764	1.072	5.255	4.706	12.300
U	12.19	15.53	6.66	6.38	0.77	2.47	3.57	2.66
La	4.1	10.3	20.4	2.7	9.5	5.5	6.1	10.4
Ce	6.9	17.8	41.0	5.0	23.1	14.0	12.9	67.0
Pr	1.2	2.5	5.5	0.7	3.7	1.8	1.8	-
Nd	4.8	9.6	22.7	2.9	17.7	7.3	6.7	30.4
Sm	1.1	1.9	5.2	0.7	4.6	2.1	1.6	6.0
Eu	0.3	0.5	1.8	0.2	1.1	0.7	0.4	1.3
Gd	1.1	1.8	5.0	0.6	4.3	1.8	1.6	3.7
Tb	0.2	0.3	0.8	0.1	0.6	0.3	0.3	0.3
Dy	1.4	2.1	4.4	0.7	3.7	2.1	1.7	3.7
Ho	0.3	0.5	0.9	0.1	0.8	0.4	0.3	-
Er	1.1	1.8	2.4	0.4	2.4	1.3	1.1	2.2
Tm	0.2	0.3	0.3	0.1	0.4	0.2	0.2	-
Yb	1.4	2.4	2.1	0.5	2.6	1.4	1.2	3.1
Lu	0.3	0.5	0.3	0.1	0.4	0.2	0.2	0.2

*NASC = North American Shale Composite.

Teuva showing

Upper Member basalt

File Name : teuva
 Sample : hp-1.1 hp-1.4

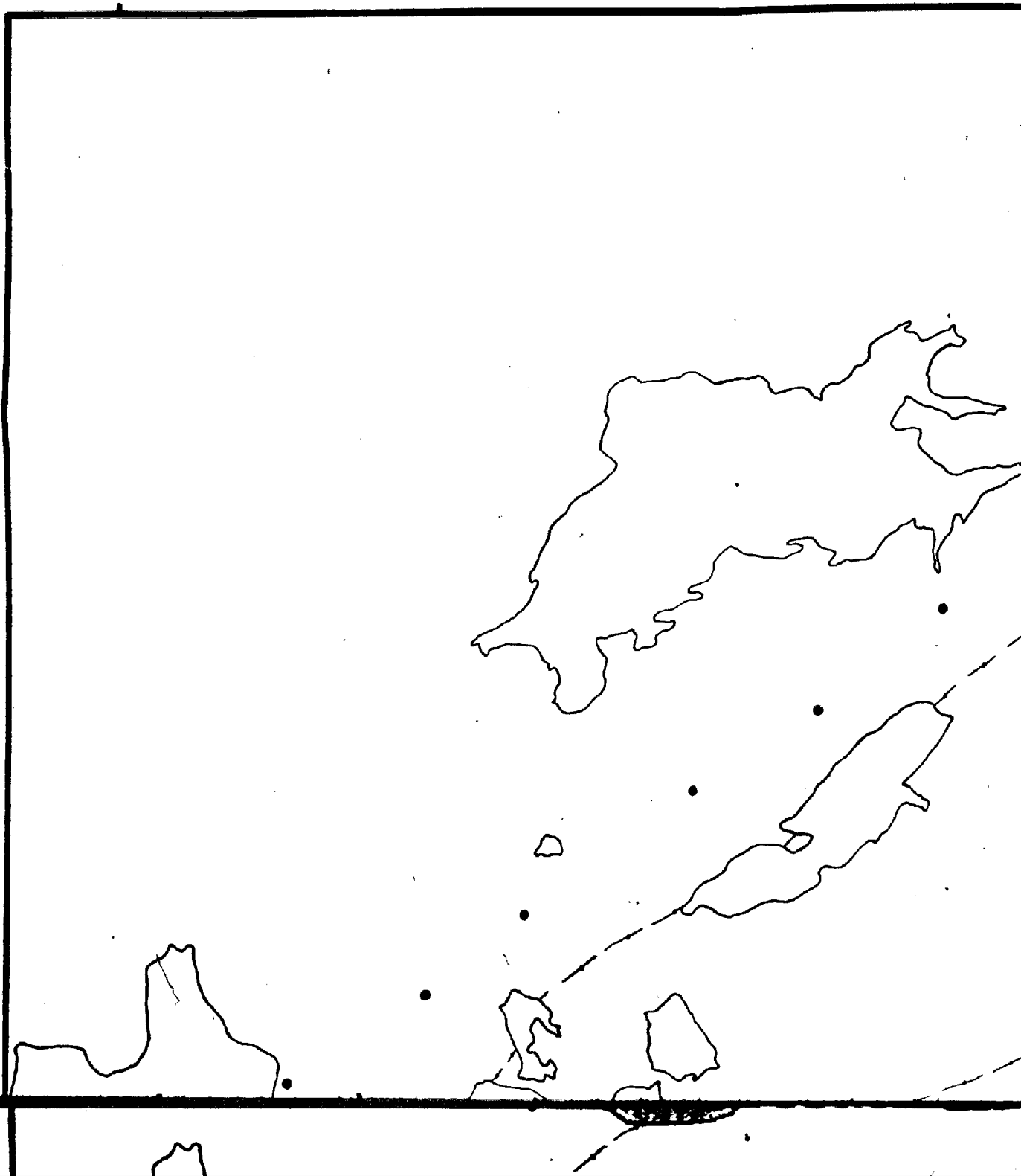
Sc	24	17
Rb	0.38	0.50
Cs	0.32	0.36
Ba	8	8
Sr	48.0	50.4
Tl	0.06	0.07
Li	27.56	23.65
Ta	1.13	0.12
Nb	18.18	2.21
Hf	8.75	5.22
Zr	339.7	261.3
Y	35.8	39.0
Th	3.757	4.008
U	1.04	1.25
La	47.1	53.1
Ce	116.6	134.7
Pr	16.4	18.2
Nd	68.9	78.9
Sm	15.1	17.1
Eu	4.5	4.9
Gd	12.8	13.3
Tb	1.8	1.9
Dy	8.6	9.0
Ho	1.5	1.6
Er	3.7	3.9
Tm	0.4	0.5
Yb	2.5	2.5
Lu	0.3	0.4

File Name : wcbasalt
 Sample : wc-41 wc-82

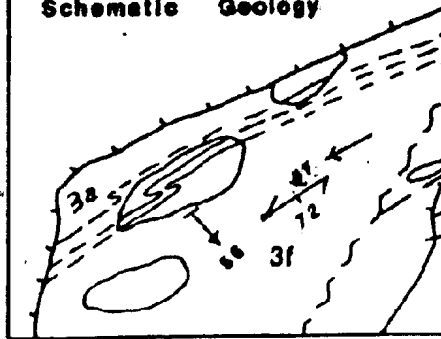
Sc	31	25
Rb	7.01	62.51
Cs	0.79	7.97
Ba	25	1326
Sr	285.9	602.5
Tl	0.17	0.59
Li	14.55	65.00
Ta	2.57	0.64
Nb	38.57	8.25
Hf	4.64	2.79
Zr	148.1	82.3
Y	22.4	23.0
Th	2.534	0.955
U	0.61	0.28
La	22.4	28.3
Ce	53.7	63.9
Pr	7.3	8.8
Nd	31.6	38.1
Sm	8.0	7.7
Eu	2.4	2.2
Gd	7.2	6.6
Tb	1.1	0.8
Dy	5.8	5.0
Ho	0.9	0.9
Er	2.3	2.6
Tm	0.3	0.3
Yb	1.5	2.1
Lu	0.2	0.3

Joe Pond Formation

File Name : joepond					
Sample :	jp-1	jp-10	jp-14	jp-15	jp-17
Sc	41	37	44	32	37
Rb	13.08	1.05	2.69	2.80	16.16
Cs	0.93	0.44	0.34	0.98	0.85
Ba	97	76	60	380	3130
Sr	73.8	109.2	94.8	88.8	224.8
Tl	0.14	0.09	0.11	0.04	0.16
Li	75.64	31.75	25.48	45.29	87.74
Ta	0.30	0.16	0.17	2.85	1.44
Nb	2.13	1.27	1.22	36.62	26.85
Hf	0.95	1.23	1.12	8.53	10.77
Zr	23.5	33.8	28.2	273.7	396.3
Y	12.5	15.0	16.1	32.4	34.0
Th	0.172	0.147	0.135	4.197	5.020
U	0.05	0.05	0.04	0.94	1.43
La	1.5	1.8	2.1	43.8	48.8
Ce	4.5	5.2	5.6	106.9	111.7
Pr	0.7	0.9	0.9	14.5	14.5
Nd	3.7	4.4	4.8	61.1	59.8
Sm	1.3	1.7	1.7	13.9	12.7
Eu	0.4	0.6	0.6	3.8	3.6
Gd	1.8	2.3	2.4	11.9	13.4
Tb	0.3	0.4	0.5	1.6	1.6
Dy	2.4	2.7	3.0	7.7	8.4
Ho	0.5	0.6	0.7	1.3	1.5
Er	1.5	1.9	2.0	3.4	3.8
Tm	0.2	0.3	0.3	0.4	0.5
Yb	1.5	1.8	1.9	2.2	2.6
Lu	0.2	0.3	0.3	0.3	0.4



Heart Pond Zine Showing
Schematic Geology



N

2a,2b

2a

1a,b

unconformity section

MEATHOOK
LAKE

3a

Dragon
Pond

3a

Warren

Creek

Date Grid (inset)

Mo

3a,3c

3a,3c

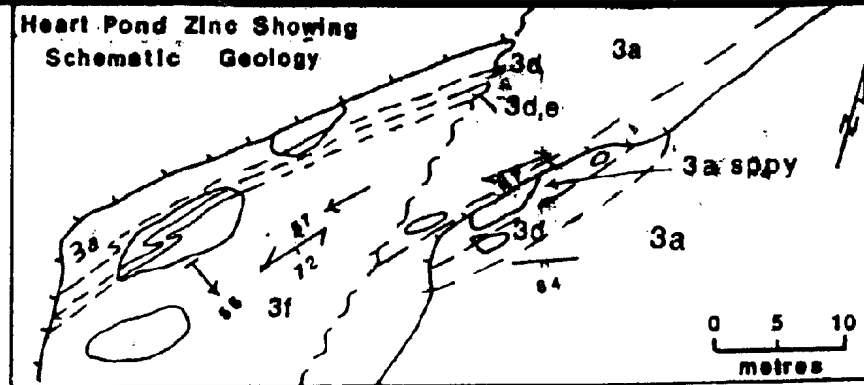
3a,3c

3a,3c

3a,3c

N

Heart Pond Zinc Showing
Schematic Geology



MEATHOOK
LAKE

2a,2b

1a,b

1a

unconformity section

unconformity section

Moon Pond

Warren

Creek

3a

3a,3c

3a,b

2b

Date Grid (inset)

LEGEND

6

Post Tectonic Gabbro: 6a, massive, fine to medium-grained, hornblende and biotite gabbro sills and dikes.

PALEOHELIKIAN

Bruce River Group

5

Brown Lake Formation: 5a, red polymictic conglomerate; 5b, spherulitic felsic volcanic; 5c, tuffaceous red sandstone.

APHEBIAN

Moran Lake Group

4

Joe Pond Formation: 4a, massive and pillowed basalt, minor clastic and chemical interflow sediments.

Warren Creek Formation

3

Upper Member: 3a, black fissile shale, argillite, and greywacke, abundant grey silt interbeds; 3b, arkose and quartz arenite; 3c, dolostone; 3d, chert; 3e, iron formation; 3f, vesicular basalt; 3g, green to beige siltstone.

2

Lower Member: 2a, green to beige, laminated, cross and graded bedded feldspathic sandstone and siltstone; 2b, dolostone, minor calcareous siltstone; 2c, black shale; 2d, chert; 2e, quartz arenite.

ARCHEAN

1

1a, foliated to massive iron/hematite, gneiss; 1b, pegmatite veins and dikes.

SYMBOLS / ABBREVIATIONS

bedding, tops known (inclined, vertical, overturned)	
bedding, tops unknown (inclined, vertical)	
pillowed volcanic, tops indicated (top known, unknown)	
S1 slaty cleavage (inclined, vertical)	
fracture cleavage (inclined, vertical)	
joint (inclined, vertical)	
plunge of L1 stretching lineation, slickenside in S1	
plunge of F1 axis, inclination of axial plane shown	
plunge of F2 axis	
plunge of F3 axis	
geologic contact (defined, assumed, covered)	

54°25'

61°20'

2a

3a

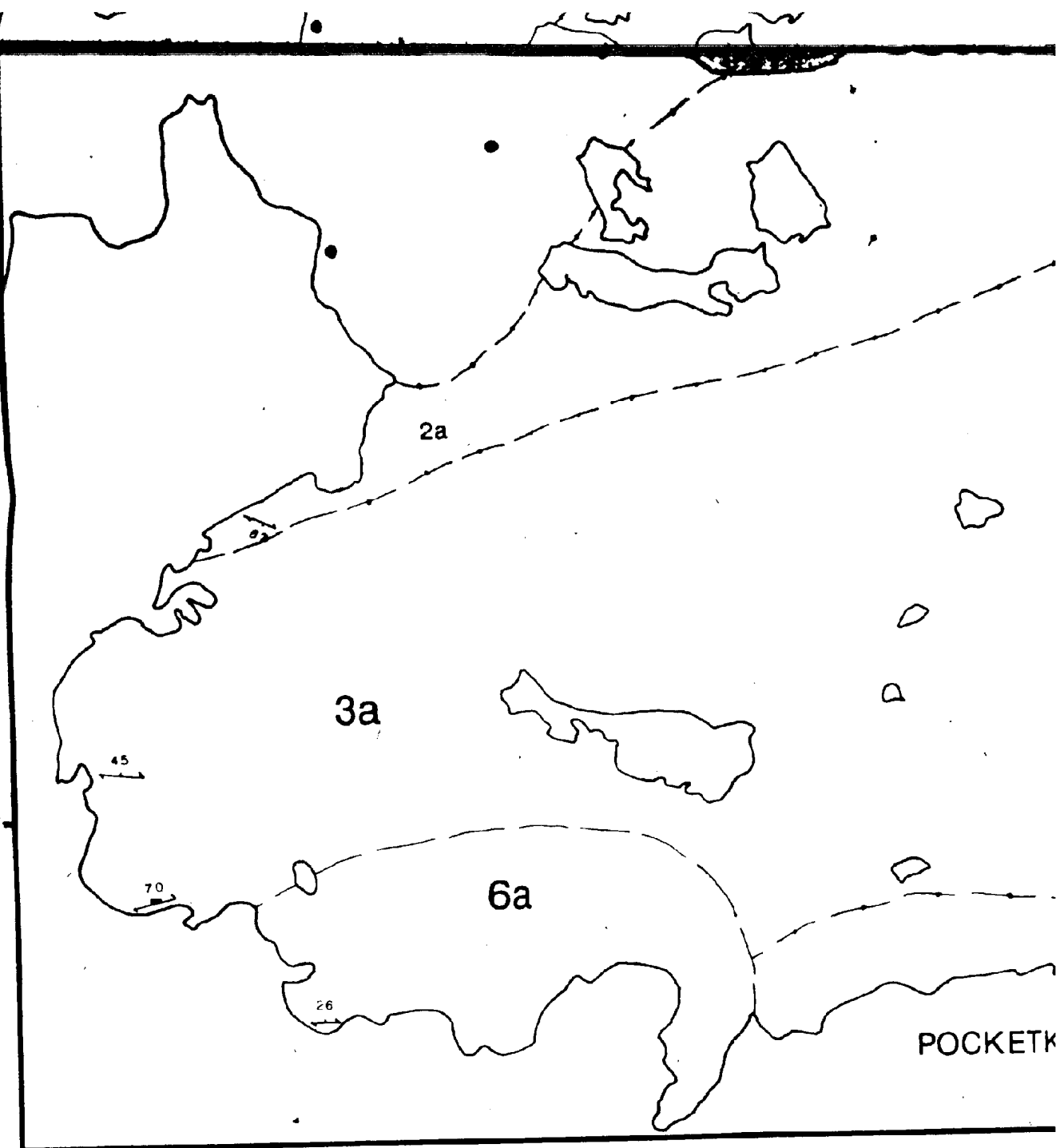
6a

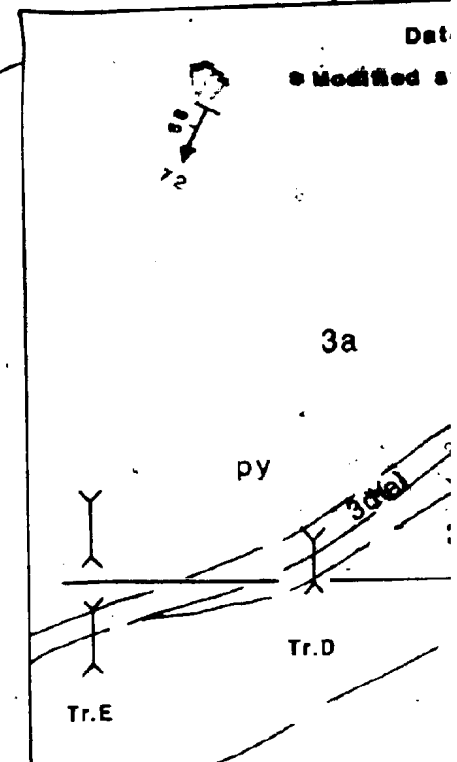
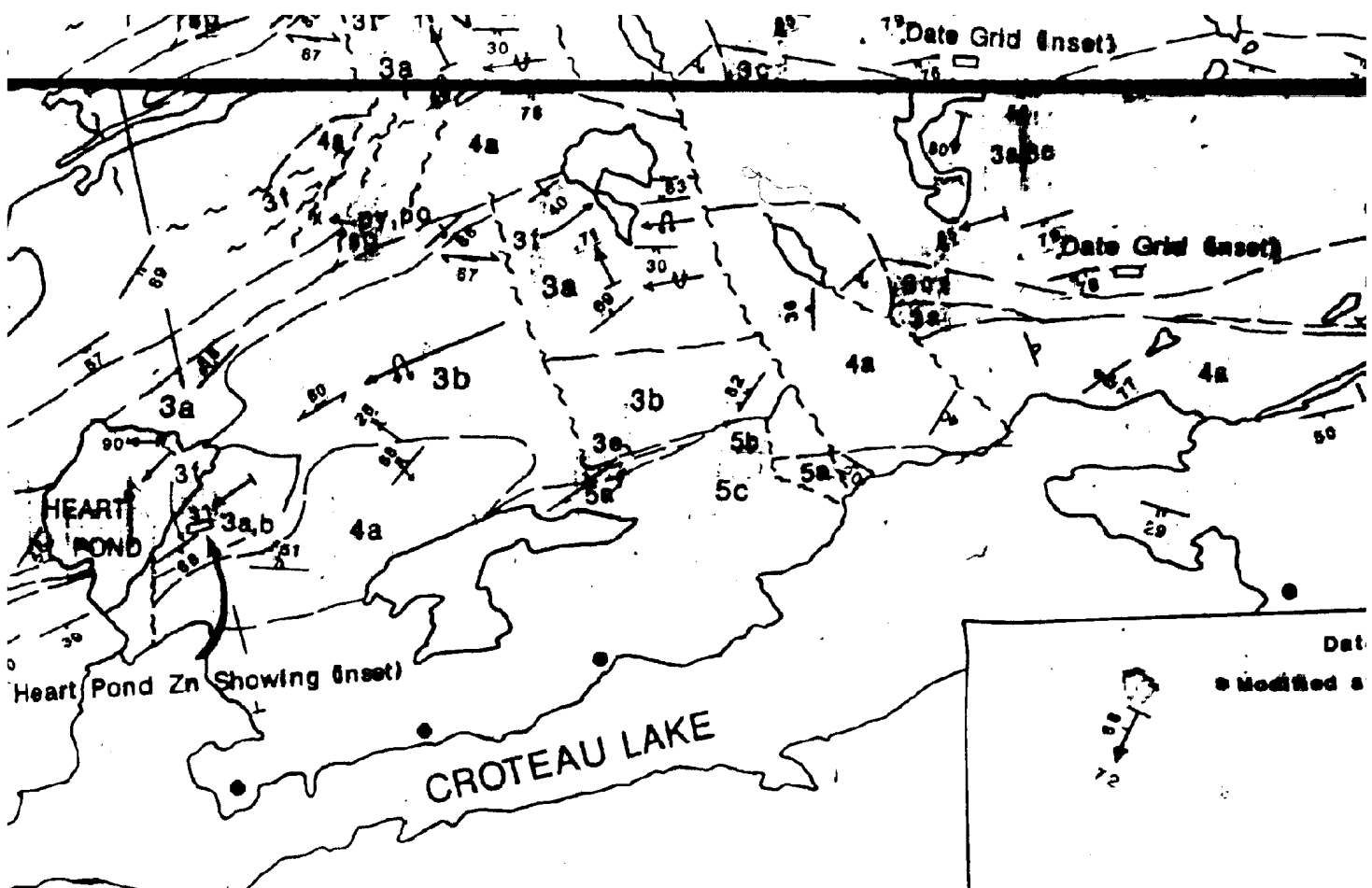
POCKETK

45

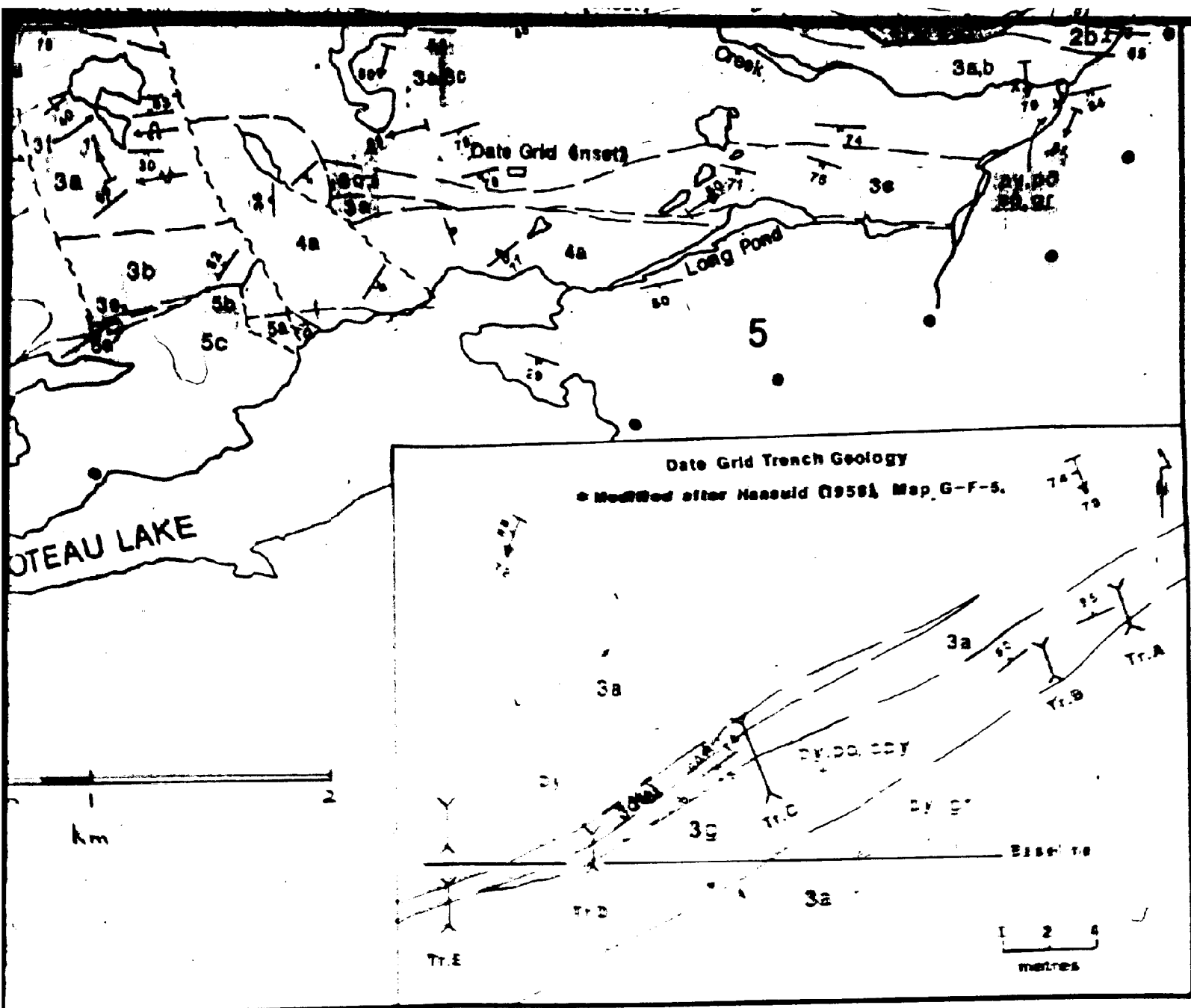
70

26





61°10'



plunge of F₁ direction, dip-slip, strike-slip
 plunge of F₂ direction, dip-slip, strike-slip
 plunge of F₃ direction, dip-slip, strike-slip
 regional contact defined, assumed, covered
 fault defined, assumed
 plunging anticline (upright, overturned)
 plunging syncline (upright, overturned)
 mineral occurrence
 limit of mapping

pyrite py
 pyrrhotite po
 sphalerite sp
 iron formation if
 graphite gr

chalcocite cc
 galena ga

MORAN LAKE GROUP GEOLOGY Central Mineral Belt, Labrador

Scale 1:20,000 or as shown on insets.

